From yeast to mammals: the exploration of a conserved, intrinsically disordered deubiquitinase that regulates ribosomal RNA synthesis.

Benjamin James Reed

A dissertation submitted in partial fulfillment of the requirements for the degree of

Doctor of Philosophy

University of Washington
2015

Reading Committee:
Richard Gardner, Chair
Sandra Bajjelieh
Dana Miller

Program Authorized to Offer Degree:
Pharmacology

University of Washington

Abstract

From yeast to mammals: the exploration of a conserved, intrinsically disordered deubiquitinase that regulates ribosomal RNA synthesis.

Benjamin James Reed

Chair of Supervisory Committee:
Associate Professor Richard Gardner
Department of Pharmacology

Ribosomes are a key component of cell cycle regulation and protein production. Proper control of ribosome synthesis is necessary for normal cellular functioning. Improper regulation can lead to cell death or uncontrolled growth. RNA Polymerase I is responsible for synthesizing three of the four ribosomal components of the ribosome. While the upstream signaling pathways required for initiation RNA Polymerase I are well understood, very little is understood about what systems regulate RNA Polymerase I elongation. This thesis explores new roles for the post-translational modification ubiquitin in regulating RNA Polymerase I. First, it identifies how the conserved yeast deubiquitinase Ubp10 is involved in removing ubiquitin from Rpa190, a required catalytic subunit of RNA Polymerase I. It presents evidence that Ubp10 regulates the ubiquitination of Rpa190, and that ubiquitination is used to regulate degradation of chromatin bound Rpa190. Second, it highlights how Ubp10 uses intrinsic disorder to interact with the network of ribosome processing proteins. Ribosomal RNA recruits up to 200 different proteins, most of which are required for ribosome biosynthesis, and this work highlights how Ubp10 uses linear motifs within its intrinsic disorder to interact with them during ribosomal RNA transcription. Finally, this work demonstrates that both the function and intrinsic disorder of Ubp10 are conserved up to human deubiquitinase USP36. It shows that USP36 is able to functionally rescue *ubp10*Δ yeast and is capable of interacting with ribosomal processing proteins via conserved binding modules.

ACKNOWLEDGEMENTS

My journey to become a scientist has led me through many different work environments filled with the advice and support of so many, many different people. I feel very lucky to have had the wide variety of experiences I've had, and do not believe I would have made it here today without everyone's support.

To Richard Gardner, my mentor at the University of Washington, thank you for giving me the creativity to explore, succeed, and fail during my time working on my Ph.D. The process of learning how to apply myself successfully as a scientist is largely due to the trust you place in all of your students. Thank you as well for always being available to answer questions, and supportive of where we want to take our lives, and making work a place I was always excited to come to, each day.

To my family, especially my Mother and Father, and always supporting and encouraging me regardless of how many times I changed my mind about what I wanted to do with my life, from directing, to marketing, to psychology, and finally biology. You always helped me get where I was going and offered whatever advice you could find along the way. My love for research comes from my Dad, who is an expert-in-a-day at everything he applies himself to. My love for sharing ideas, working with others and communicating ideas comes from my Mom, who can make friends with anyone, at any place and any time. Thank you so much.

To Jen, my wife, who has been a constant source of support and love. Thank you for always asking and being interested in what I do, regardless of how complicated it may seem. You always ask questions and try to learn about everything, and I love the interest you find in the world around you. Thank you as well for always supporting whatever hair brain schemes I come up with. I look forward to you being my best friend in life's coming adventures.

To all of the past and present Gardner Lab members, thank you for making work fun and supportive. Be it either planning experiments or going out for a beer, everyone always came together as a team.

To Ian Sweet, thank you for taking on a recently graduated psychology student and teaching him the world of molecular biology. You gave me a much enjoyed ‘crash course’ in the world of biological research and I couldn’t have asked for a better place to learn the ropes.

To Edward Weaver and Kathryn James, thank you for my first opportunities to explore research science and to present my own data at a national conference. I’ll never forget losing my voice the night before due to over-practicing.

To my friends, each and everyone one of you, who helped form the person I am today. I was lucky to maintain such close relations with people from high school up through college and beyond, and the adventures we had together are the reason I am aim for the heights I do today.

TABLE OF CONTENTS

LIST OF FIGURES

LIST OF TABLES

LIST OF ABBREVIATIONS

5-FOA	5-fluorootic acid
BSA	bovine serum albumin
DAPI	4',6-diamidino-2-phenylindole
DHR2	DEAH-box RNA helicase 2
DUB	Deubiquitinase
GAD	Gal4 activation domain
GBD	Gal4 DNA-binding domain
GFP	Green Florescent Protein
H2B	histone H2B
NEM	n-ethylmaleimide
PGK1	3-PhosphoGlycerate Kinase
PTM	Post-translational modification
RENT	Complex (NET1, SIR2, CDC14) for nucleolar silencing and telophase exit
RPA190	Ribosomal Protein 190
SDS-PAGE	Sodium dodecyl sulfate polyacrylamide gel electrophoresis
SIR4	Silent Information Regulator 4
SUMEB	SDS, Urea, MOPES, EDTA and Bromophenol Blue
TBF	TATA-Binding Factor
TUBE	Tandem Ubiquitin Binding Entity
TOR	Target of Rapamycin
Ub-AMC	Ubiquitin conjugated 7-amido-4-methylcoumarin
UAF	Upstream activating Factor
UBP	UBiquitin Protease
USP36	Ubiquitin specific protease 36
URA3	Orotidine 5'-phosphate decarboxylase
Y2H	Yeast 2-hybrid

CHAPTER ONE:
BACKGROUND AND SIGNIFICANCE

Ribosomes and cell growth

Life is about propagation – the ability of a lifeform to adapt to its environment, survive and to create offspring. For single-celled organisms, such as bacteria or single-celled yeast, this means sensing the availability of nutrients and being able to respond appropriately: doubling when nutrients are plenty or restricting growth when nutrients are scarce. These signals become more complex in multi-cellular organisms where cell growth is not just about replication, but cell differentiation for the development and growth of a complex organism. However, whether it is for the duplication of a single-cell or the development of an entire organism, all cells rely on complex protein machines that are responsible transforming information encoded in DNA blue prints into protein components that allow them to grow and to thrive.

One of the most basic concepts of biology is that protein complexes convert our genetic code, or DNA, into functioning protein machines (van der Gulik and Speijer, 2015). To do this, RNA polymerases begin by transcribing that DNA into mRNA, or a genetic copy (Feklistov, 2013; Michaelis and Treutlein, 2013; Vannini and Cramer, 2012). This mRNA is transcribed by multi-protein complexes called ribosomes, which are responsible for translating that code into new functional protein machinery (Graifer and Karpova, 2014; Ramakrishnan, 2014). While this process at its core sounds simple, the regulation required to maintain this process is provided by the orchestration of hundreds of different proteins. These proteins are responsible for the hundreds of thousands of mRNA that are produced in growing cells (Moore and Proudfoot, 2009). Cells are thought to contain an staggering number of ribosomes in order to efficiently translate these mRNA blueprints into functional proteins; yeast, for example, contain 200,000 ribosomes during rapid phase growth, which requires them to produce 2,000 ribosomes per minute for normal growth. This is estimated to make up 80% of the total RNA produced by yeast, with the remaining 15% being tRNA and only 5% being mRNA (Warner, 1999). This means that cells face a huge economic burden, needing to tightly regulate their ribosomal production so that ribosomes are produced only when cell division and growth is required. This, of course, is not a problem faced solely by yeast. All organisms from *E.coli* to humans face this

problem and must regulate ribosome production to correctly match their need for protein production and cell growth.

The synthesis of a single ribosome is no simple matter, as ribosomes are one the most complex cellular machine. Ribosomes in eukaryotes are made up of four ribosomal RNAs, which compose its catalytic core, as well as seventy-eight supportive ribosomal proteins. The production of all of these components requires all three RNA Polymerase (I, II and III). Synthesis of three of the four ribosomal RNAs is carried out by RNA Polymerase I, which synthesizes the 35S ribosomal RNA (rRNA), which is then processed into the 18S, 5.8S and 28S ribosomal subunits. RNA Polymerase III is responsible for the fourth rRNA components, 5S rRNA, as well as supportive small nucleolar RNAs. RNA Polymerase II is responsible for transcribing the ribosomal proteins, which act to support mRNA translation by ribosomes (Woolford and Baserga, 2013). The transcription activity by all three polymerases is regulated primarily by RNA Polymerase I, which has been demonstrated to be a key integrating factor in the rate of ribosome biogenesis (Lempiainen and Shore, 2009). The research in this thesis will work to explain and expand on the current mechanisms that regulate RNA Polymerase I function in order to better understand how the cell is able to maintain the complicated construction of such a complex molecular machine.

Regulation of Ribosome Biogenesis.

Ribosome biosynthesis is highly tuned to internal nitrogen, carbon, energy levels, and growth signals within the cell (Lempiainen and Shore, 2009). Current understanding of ribosome biogenesis has identified both long-term and short-term mechanisms of regulation that respond to these regulatory signals. Long-term regulation of ribosome biogenesis is controlled primarily through silencing of ribosomal DNA (rDNA). Short-term regulation is done through the regulation of recruitment of RNA Polymerase I to active rDNA. Both of these mechanisms of regulation will be reviewed below.

Long-term regulation: rDNA silencing. RNA Polymerase I is responsible for transcribing rDNA into the large precursor rRNA, known as the 35S rRNA This is then processed into the

18S, 5.8S and 28S rRNA subunits that compose most of a mature ribosome. In order to meet demands of ribosome biosynthesis, yeast have up to 200 tandem repeats of rDNA in a single locus per haploid genome. In mammals, this increases up to 600 tandem repeats throughout five separate chromosomes per haploid genome. Only a fraction of these are required for normal growth, with 50% of the rDNA repeats actively transcribing rRNA during interphase (Drygin et al., 2010).

These rDNA repeats are necessary to meet the ribosome production requirements of the cell; however, the highly repetitive nature of rDNA makes them very susceptible to DNA damage and unwanted recombination (Ganley and Kobayashi, 2014). As such, one of the major regulatory roles for rDNA silencing is to maintain genomic integrity. This is regulated primarily by the RENT complex, whose core components are Sir2, Net1 and Cdc14 (Ha et al., 2012; Straight et al., 1999). The RENT complex associates with histones within the rDNA to propagate silent chromatin and the association of RENT is positively correlated with cell cycle progression (Shou et al., 2001). Loss of the RENT complex, due to mutation or inactivation, leads to higher rates of rDNA recombination and shortened life span in yeast.

The RENT complex has also been found to be recruited to silence rDNA in response to low nutrients. (Ha and Huh, 2010). Studies using Psoralen, a DNA-crosslinking agent able to identify active versus silenced rDNA, show that yeast grown in low nutrients (low carbon or nitrogen sources) contain a larger number of silenced rDNA genes (Oliver, 1992). This response to nutrient stress has been shown to be mediated by the kinase Target of Rapamycin (TOR), which recruits RENT to the yeast rDNA to propagate chromatin silencing (Tsang et al., 2003).

Short-term regulation: RNA Polymerase I initiation. To meet the needs of ribosome production required by the cell, rRNA synthesis has taken on another unique trait: the ability to recruit multiple polymerases to each rDNA gene. Electron micrographs of unraveled rDNA repeats (Miller Chromatin Spreads) of organisms from *E.coli* to humans have demonstrated a "Christmas tree" like phenomena, with each rDNA loci recruiting as many as 150 actively transcribing RNA Polymerase I complexes (Ra≈°ka et al., 2006). The total number of recruited and actively transcribing polymerases changes in response to increases or decreases internal nutrient, energy, and stress signals (Lempiainen and Shore, 2009; Neuman-Silberberg et al.,

1995; Wu et al., 2004). As such, recruitment of RNA Polymerase I recruitment to the rDNA is tightly regulated, and used to quickly tune the synthesis of ribosomes to the requirements of the cell. Thus, regulating RNA Polymerase I binding is a way of regulating ribosome biogenesis.

There are four essential components which comprise the pre-initiation complex required for RNA Polymerase I recruitment in yeast. They are upstream activating factor (UAF) (Keys et al., 1996), core factor (Bedwell et al., 2012), TATA-binding factor (TBF) (Schultz et al., 1992), and Rrn3 (Yamamoto et al., 1996). These components are responsible for both tuning the consistent recruitment of RNA Polymerase I, as well as excluding RNA Polymerase II and III. The DNA bound pre-initiation complex is composed of upstream activating factor, core factor, and TATA-binding factor. UAF primes the pre-initiation complex as one of its six components contains sequence specificity to target it to the rDNA promoter, whereas its association with histone H3 and H4 provide affinity for the rDNA (Vu et al., 1999). Core factor associates with both the rDNA, as well as UAF, and is required for promoter specific recruitment of RNA Polymerase I. TBF is not required for promoter specific recruitment of RNA Polymerase I, but it has been shown to enhance recruitment (Choe et al., 1992; Kulkens et al., 1991; Schneider, 2012). While the regulation of recruitment by these factors is not as well understood in yeast, their regulation in vertebrates has been shown to be controlled by several growth factors, such as ERK or c-MYC, and play an important role titering RNA Polymerase I recruitment and therefore the rate of ribosome biogenesis (Ruggero and Pandolfi, 2003).

The best-understood mechanism for regulating initiation of RNA Polymerase I is through Rrn3 (yeast)/TIF-IA (vertebrates). Rrn3 associates with nucleoplasmic RNA Polymerase I, forming an Rrn3-RNA Polymerase I complex that is initiation competent and capable of binding the pre-initiation complex at active rDNA (Beckouet et al., 2008; Yamamoto et al., 1996). While RNA Polymerase I unassociated with Rrn3/TIF-IA has been shown to be capable of transcription in several in vitro experiments (Keener et al., 1998), such is not the case *in vivo*.

There are several post-translational modifications that are capable of inhibiting the formation of the Rrn3-RNA Polymerase I complex. The best studied of these is through the TOR-kinase, which is responsible for linking cellular growth to intracellular nitrogen and amino acid levels (Philippi et al., 2010a). In conditions of low nutrients, or when yeast begin to reach stationary phase, TOR-kinase initiates a kinase cascade that leads to the phosphorylation of

Rrn3, which inhibits its ability to complex with RNA Polymerase I (Mayer et al., 2004). More recent work has suggested that TOR may also operate through an Rrn3-independent mechanism as well, as a TOR-insensitive Rrn3 does not completely separate TOR inhibition from a substantial decrease in ribosomal biosynthesis (Philippi et al., 2010b).

The phosphorylating protein AMP kinase has also been shown to have a similar function to TOR but instead responds to internal cellular energy levels, sensing internal ratios of ATP:ADP (Neuman-Silberberg et al., 1995). When this ratio drops, AMP kinase phosphorylates TIF-IA/Rrn3, blocking its ability to bind the pre-initiation complex (Hoppe et al., 2009). This causes a halt in ribosome production until ATP:ADP are recovered to the cellular norm. The inhibition of RNA Polymerase I recruitment to the pre-initiation complex is therefore thought to allow recovery of internal energy levels.

The mechanisms responsible for regulating recruitment of RNA Polymerase I work together with rDNA silencing pathways. Combined, these mechanisms titer RNA Polymerase I on rDNA as needed for the protein production and growth of a cell. However, these mechanisms do no monitor the quality control of transcription once RNA Polymerase I is recruited. Given that hundreds of polymerases can be actively transcribing up to eighty genes, there must be mechanisms that are responsible for maintaining quality control once transcription begins.

The need for quality control mechanisms during RNA Polymerase I elongation.

While rDNA silencing and initiation of RNA Polymerase I has been studied extensively, much less research has been conducted to understand quality control during RNA Polymerase I elongation, a term used to describe the rate of transcription activity. This is surprising, due to two features of RNA Polymerase I elongation that make it unique compared to RNA Polymerase II and III. First, the formation of ribosomes occurs actively during transcription. As each RNA Polymerase I complex transcribes ribosomal RNA, it recruits over 200 proteins onto the synthesized rRNA, building a large pre-RNA associated protein complex called the SSU Processome (For a review of this process, see (Henras et al., 2008; Woolford and Baserga, 2013)) (Fig 1.1). The SSU Processome is responsible for the folding, processing, and cleavage of rRNA into mature ribosomal subunits. Failure of this complex to form properly leads to delayed and often severely reduced ribosomal levels. Second, up to 150 RNA Polymerase I complexes

can transcribe a single rDNA gene at a time. This means that each rDNA is a packed assembly line of transcribing polymerases, each actively forming a new ribosome. As such, it would seem necessary for quality control mechanisms to oversee the quality control and processivity of each rDNA highway to ensure ribosome production occurs successfully.

RNA Polymerase I processivity therefore provides a complex point of regulation for the cell. With each active rDNA containing hundreds of active RNA Polymerase I complexes, failure of one polymerase could provide a kinetic block that disrupts progression of any other polymerases past it (Schneider, 2012). Several proof reading mechanisms have been described (Rpa49/43 (Albert et al., 2012), Rpa12.2 (Prescott et al., 2004), Rpa135 (Beckouet et al., 2008)), all of which maintain elongation in the face of minor DNA damage or minor internal/external kinetic barriers. However, these internal proofreading and rescue mechanisms have been shown to fail. Given the possibility they may not be able to overcome a large kinetic barrier or internal failure, it would be expected the failed RNA Polymerase I would need to be extracted in order to let the remaining RNA Polymerase I complexes progress.

Currently, no such mechanism for extracting failed RNA Polymerase I is known. Such mechanisms have instead been described for other polymerases, such as RNA Polymerase II (Verma et al., 2011; Wilson et al., 2013). In cases of DNA damage, the C-terminal tail of RNA Polymerase II is post-translationally modified by the protein ubiquitin(Reid and Svejstrup, 2004; Ribar et al., 2006, 2007). This modification leads to its extraction from chromatin by chaperone CDC48 and degradation by the proteasome (Verma et al., 2011). Given the sheer number of active RNA Polymerase I complexes per rDNA, it seems very likely similar mechanism of extraction would be necessary if catastrophic failure of an RNA Polymerase I complex occurred.

Ubiquitination as a post-translational regulator of RNA Polymerase I elongation.

Post-translational modifications (PTMs) are key regulators of protein function after protein translation. Though proteins are often built with an intrinsic function, the addition of PTMs is able to alter their functional role through activation/inactivation, directing or redirecting cellular localization, building protein complexes or targeting misfolded proteins to be refolded or degraded. Many of these PTMS are small molecules such as phosphorylation, acetylation, methylation, or lipid modification. However, proteins themselves can be used to modify other

proteins. One such protein PTM, ubiquitination, is used to regulate every cellular process, and is an incredibly well conserved protein with 96% conservation from yeast to humans (Varshavsky, 2006).

What is Ubiquitination? Ubiquitination is the post-translational modification of a protein by ubiquitin, an 8kDa protein, and is catalyzed by a three-enzyme cascade. First, a ubiquitin activase (or E1) activates ubiquitin in an ATP-dependent manner. Next, this activated ubiquitin is transferred to an ubiquitin conjugase (or E2). Finally, the ubiquitin conjugase interacts with a ubiquitin ligase (or E3), which covalently attaches ubiquitin to the target lysine of a substrate (Ciechanover, 2006). This process is also dynamic, with the removal of ubiquitin facilitated by a deubiquitinase (Amerik and Hochstrasser, 2004; Baek, 2003). The level of a given ubiquitinated substrate can therefore be precisely controlled: both through the rate of ubiquitination of a substrate, as well as through the rate of deubiquitination.

The vast degree of roles ubiquitin plays in regulating cellular function is likely in part due to the complexity of different signals it alone is able to communicate. Proteins are capable of being modified by ubiquitin both by the addition of a single ubiquitin, and by the building of ubiquitin chains (Emmerich et al., 2011; Kirisako et al., 2006). These ubiquitin chains can be built through the conjugation of additional ubiquitin onto already existing ubiquitin moieties; there are seven different lysines on ubiquitin from which chains can be built, all of which have very different cellular roles. While mono- and poly- ubiquitination has been shown to play important roles in regulating a number of different important cellular functions (a few are DNA repair, transcription, autophagy, and intracellular trafficking) (Hochstrasser, 1996; Varshavsky, 2006), it is best known for the roles of in protein quality control, which is mediated through poly-ubiquitination chain built off lysine 48 (K48) on ubiquitin (Hochstrasser, 1996; Varshavsky, 2006). A protein that is poly-ubiquitinated by a K48 ubiquitin chain is recognized by either the proteasome or protein chaperones (Esser et al., 2004), which localize it to the proteasome for degradation. This form of ubiquitination is regulate protein function by maintaining high or low steady states (Kirisako et al., 2006; Thrower et al., 2000), as well as degrade aberrant proteins to maintain overall cellular protein quality (Fredrickson and Gardner,

2012). K48 ubiquitin chains are also the primary cellular modification used to extract proteins from protein complexes or off chromatin (Mogk and Bukau, 2004; Wickner et al., 1999).

Known roles of ubiquitination in RNA Polymerase regulation. While these qualities alone would make ubiquitination a key candidate for regulating turnover of aberrant RNA Polymerase I, ubiquitin has always been intimately involved with ribosome biogenesis as well. Of the four ubiquitin genes in yeast, three of those genes are ubiquitin fused to a ribosomal protein (UBI1: Ubiquitin-RPL40A; UBI2: Ubiquitin-RPL40B; UBI3: Ubiquitin-RPS31) (Lacombe et al., 2009). Expression of UBI3, and one of UBI1 or UBI2, is required for cell viability (Finley et al., 1987; Ozkaynak et al., 1987). Mono-ubiquitination of many ribosomal proteins is also required for their efficient integration during the building of the ribosomal subunits (Kressler et al., 2010). Ubiquitin also plays an important role in eukaryotes in regulating ribophagy as well, by ubiquitinating ribosomes and targeting them for lyzosomal breakdown (Kraft et al., 2008).

This thesis expands the roles for ubiquitin's relationship in regulating ribosome production by identifying new mechanisms for regulating RNA Polymerase I. I first discuss how new roles for the yeast deubiquitinase Ubp10 lead us to identify ubiquitin as a key modifier in RNA Polymerase I turnover. I then expand on this to show how Ubp10's intrinsic disorder plays an important structural role with its interactions with a number of different ribosome processing proteins. Finally, I prevent evidence for the conservation of Ubp10's function and intrinsic disorder from yeast to humans through the characterization of its human ortholog, USP36. My conclusions provide new insight into the importance of both protein ubiquitination and intrinsic disorder for coordinating RNA Polymerase I function.

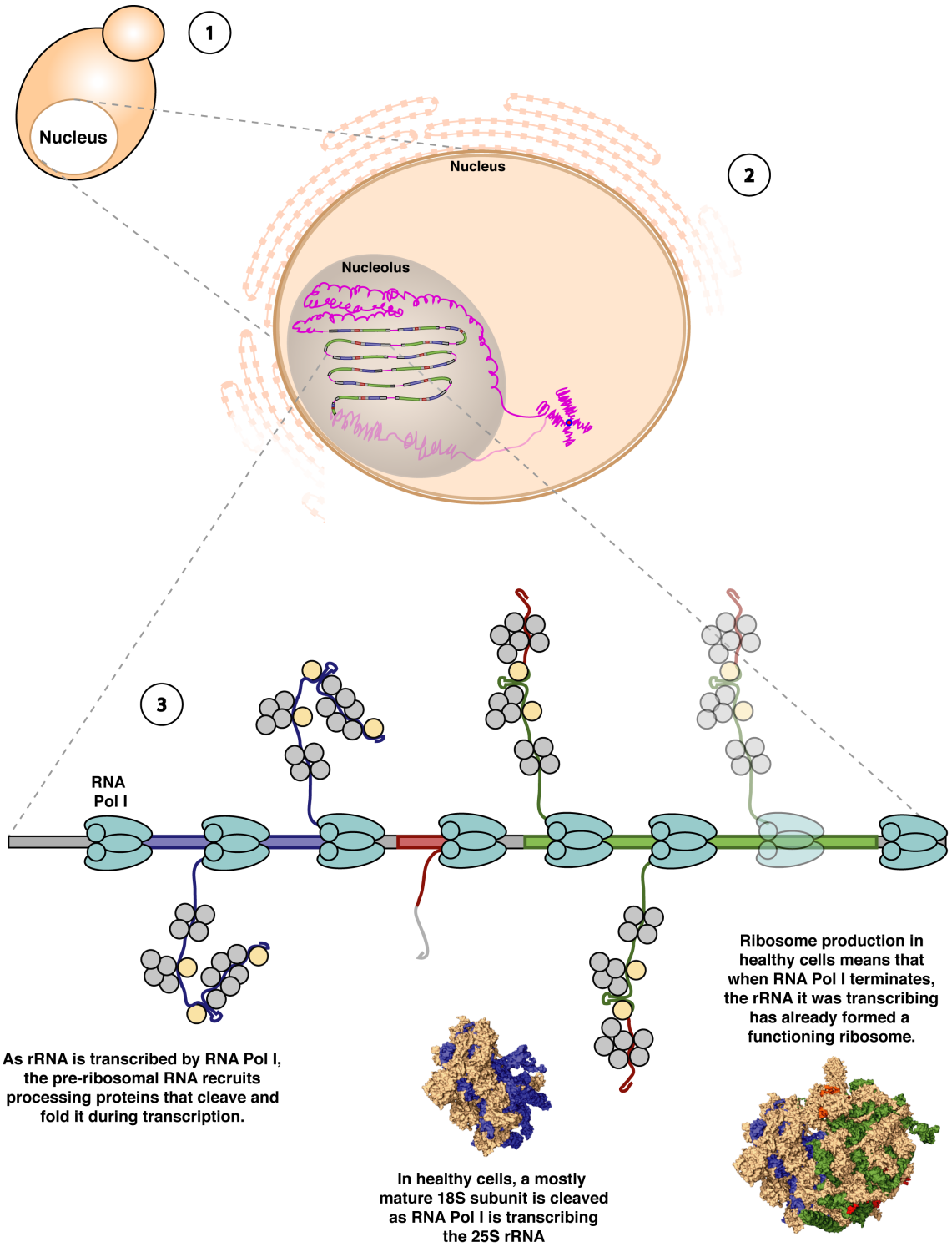

Figure 1.1 – Cartoon representation of ribosome biogenesis. 1, a representative yeast cell; 2, active and inactive tandem repeats of rDNA are segregated to the nucleolus, the largest sub-cellular compartment of the nucleus; 3, Up to 150 RNA Polymerase I (RNA Pol I) complexes are recruited to each rDNA to transcribe it into the 35S pre-ribosomal RNA, which is cleaved and processed into the 18S, 58S and 25S subunits.

CHAPTER TWO:

UBIQUITINATION-DEPENDENT DEGRADATION OF RPA190, A LARGE SUBUNIT OF RNA POLYMERASE I, IS REGULATED BY DEUBIQUITINASE UBP10

History of Ubp10: Identifying new roles outside of chromatin silencing

The eventual identification of ubiquitin as a regulator of RNA Polymerase I began with the identification and characterization of the yeast gene UBiquitin Protease 10 (*UBP10*). Initially named *DOT4* (Disruptor of telomere silencing 4), *UBP10* was first identified as a deubiquitinase that associated with the yeast chromatin silencing complex required for telomere and mating-type silencing. This protein complex, called the SIR protein complex, is composed primarily of three proteins (Sir2, Sir3 and Sir4), which are recruited to nucleosomes in yeast in order to propagate silent chromatin. Work by Kahana and Gottschling (Kahana and Gottschling, 1999) identified that Ubp10 directly interacted with Sir4, and that deletion or overexpression of Ubp10 was associated with a partial loss of silencing at the telomere and mating type loci. The deletion of Ubp10 was also found to lead to a slow growth phenotype associated with a delay in the G1 phase of the cell cycle. This work concluded that Ubp10 likely regulated chromatin silencing through interaction with Sir4 and ubiquitin-dependent degradation of members of the SIR complex.

It was then identified in 2005 that Ubp10 was recruited to nucleosomes by Sir4 in order to regulate histone H2B ubiquitination. In work first published by (Emre et al., 2005) and later expanded on by (Gardner et al., 2005), *ubp10*Δ yeast were shown to contain a 3-fold increase in histone H2B ubiquitination when compared to wild-type cells. This increased ubiquitination was associated with higher rates of K4 and K79 methylation, both of which had been previously shown to be markers of heterochromatin in yeast (Feng et al., 2002; Osley, 2004; Strahl et al., 1999). To support this, transcript array analyses were performed that showed an increase in gene expression at both telomeric genes, as well as genes in the mating-type loci. When the cells expressed reporters at either the telomere or mating type loci that were required for growth on minimal media, *ubp10*Δ showed higher rates of growth when compared to their wild-type counterparts. Although work on Ubp10's actions let to the conclusions that Ubp10 regulated chromatin silencing through recruitment by Sir4 for histone deubiquitination, this did not explain

why *ubp10*Δ yeast had the slow growth phenotype originally observed in the (Kahana and Gottschling, 1999) paper.

This confounding observation led to the conclusion that Ubp10 had a second action. A clear distinction of this effect from silencing related actions was supported by observations that the slow growth was not linked to Ubp10's interaction with the SIR complex. Previous work in the Gottshling lab had identified a region of Ubp10, amino acids 94-250, that was required for Ubp10 to interact with Sir4 (Gardner et al., 2005). The ubp10$^{\Delta 94\text{-}250}$ mutant was unable to be recruited to nucleosomes by Sir4, and thus *ubp10*$^{\Delta 94\text{-}250}$ yeast showed similar levels of histone H2B ubiquitination as *ubp10*Δ yeast. However, serial dilutions of *ubp10*$^{\Delta 94\text{-}250}$ yeast grown on rich media revealed that *ubp10*$^{\Delta 94\text{-}250}$ yeast had growth rates similar to wild-type *UBP10* yeast, while *ubp10*Δ yeast showed a much slower rate of growth (Fig 2.1). A catalytic mutant of Ubp10 incapable of deubiquitination (Ubp10^{C371S}) also showed similar growth rates compared to *ubp10*Δ yeast (Fig 2.1). Finally, *sir2*Δ*, sir3*Δ and *sir4*Δ yeast strains showed growth rates similar to wild-type *UBP10*. These data suggested that the small colony size was not due to defects in the SIR complex chromatin silencing function, and was the result of a different enzymatic target of Ubp10.

Re-evaluation of Ubp10's nuclear localization identified that it is primarily localized to the nucleolus (Fig 2.2), the sub-nucleolar site of ribosome biogenesis. Yeast in which a GFP tag had been incorporated into the endogenous Ubp10 gene revealed co-localization with the protein Nop58, a ribosome processing protein localized primarily to the nucleolus (Grandi et al., 2002). Yeast were grown to log phase, fixed and stained with DAPI, then imagined with florescent microscopy. The resulting microscopy demonstrates that Ubp10 co-localizes with Nop58, implying it is localized to the nucleolus. As the nucleolus's primary role is in ribosomal RNA transcription, these results implied that Ubp10 likely had an enzymatic target associated with ribosome biosynthesis.

To explore a potential new role for Ubp10's role in regulating ribosome biosynthesis, we worked with Susan Baserga's lab at Yale to determine if yeast depleted in Ubp10 had fewer ribosomes. We looked for changes 18S and 25S RNA ribosomal subunits, the two largest subunits of a mature ribosome. Yeast strains were engineered in which the expression of *UBP10*, *UTP16*, or *UTP26* were placed under control by the Galactose 1 (GAL1) promoter. Yeast strains

were grown for 72 hours in either galactose or glucose at 16°c, were then lysed, and the RNA was purified. The purified RNA was separated on agarose gel by electrophoresis and probed for 28S and 18S ribosomal RNA content using methylene blue. In the yeast grown in galactose, *UBP10*, *UTP16* and *UTP26* are all expressed. In each case, both 28S and 18S levels remain consistent between each condition (Fig 2.3). However, when yeast are grown in glucose, the strains depleted for Ubp10 show a decrease in both 28S and 18S ribosomal RNA subunits. This is contrast to depletion of Utp16 and Utp26, which are known to regulate processing of only the 18S ribosomal RNA (Bernstein et al., 2004; Dragon et al., 2002; Perez-Fernandez et al., 2007), and as such only show defects 18S ribosomal RNA levels. These results demonstrate that expression of *UBP10* is required for normal ribosome biogenesis to occur.

These data support a new enzymatic role for Ubp10. Ubp10's localization to the nucleolus and requirement for normal levels of 18S and 28S ribosomal subunits both heavily imply a role in regulating the synthesis of ribosomes. These also both provide possible explanations the slow growth seen in *ubp10*Δ cells, as malfunctioning ribosome biogenesis is tied to slow cell growth.

Ubp10 interacts with ribosomal RNA processing proteins.

Having determined that the slow growth phenotype seen in *ubp10*Δ yeast was associated with ribosome biogenesis, we next sought to link Ubp10's deubiquitination action to its effects on this process. To look for Ubp10 substrates, a previous student named Lauren Richardson used an unbiased crosslinking mass spectrometry approach to identify new potential interactors of Ubp10. A yeast strain was developed that expressed 3HA-epitope tagged Ubp10. Yeast with or without epitope tagged Ubp10 were grown to log phase after which the proteins in the cells were covalently crosslinked by treatment with formaldehyde. Ubp10 and associated proteins were purified from cell lysates using anti-HA affinity resin, and the resulting eluate processed for mass spectrometry analysis.

This analysis revealed that Ubp10 interacts with a very large number of proteins required for either ribosomal processing or ribosomal transcription (Richardson et al., 2012). These proteins and their relation to Ubp10 are shown schematically in Figure 2.4. Bold lines represent interactors of Ubp10 identified from the screen. Many of these interactors are part of complexes

required for ribosomal RNA processing and transcription, and these protein complexes are represented by thin lines. (Bernstein et al., 2004; Dragon et al., 2002; Gallagher et al., 2004).

Of the ribosome processing proteins that were identified as potential interactors of Ubp10, a large percentage were known proteins necessary for processing the 18S ribosomal subunit (Richardson et al., 2012). During ribosomal RNA synthesis by RNA Polymerase I, protein complexes begin to associate with the pre-ribosomal RNA to aid in processing and folding. The mass spectrometry data identified interactions between Ubp10 and several of the protein complexes that first associate with ribosomal RNA, and are required for efficient elongation and ribosome synthesis (Bernstein et al., 2004). Ubp10 was also found to interact with Rpa190, one of the two large catalytic subunits of RNA Polymerase I (Kuhn et al., 2007). A functional cartoon of these interactions is shown on the bottom of Figure 2.4

We next wanted to confirm that Ubp10 was capable of directly interacting with ribosomal synthesis and processing proteins *in vivo*. This analysis was carried out through two different approaches, the yeast 2-hybrid assay and co-immunoprecitation. Two different approaches were used to maximize identification of protein-protein interactions within nucleolus, as opposed to one method alone. Using the yeast 2-hybrid assay (Young, 1998), Ubp10 interacted with both Dhr2 (a DEAD-box RNA helicase) (Colley et al., 2000), as well as Utp22 (an 18S ribosomal RNA processing proteins) (Bernstein et al., 2004) (Figure 2.5*B*). Both proteins are required for normal ribosome biogenesis, as well as cell growth, and are indicated in the cartoon in figure 2.4. Ubp10 was also found to interact with ribosome processing proteins using co-immunoprecitation. Ubp10 was C-terminally HSV tagged and several potential interactors were C-terminally HA tagged. Yeast were grown to log phase, lysed, and Ubp10 was immunoprecitated using beads conjugated with anti-HSV. Lysates and eluate were separated on SDS-PAGE by electrophoresis and the identification of either HSV or HA was probed via western. The results in figure 2.5*A* identified several other *in vivo* interactors of Ubp10, which are represented in the model figure 2.4. Ubp10 was found to interact with Pwp2, Cbf5, Nop56, and Nop58, all of which play important roles in 18S rRNA processing (Bernstein et al., 2004).

These data together confirm that Ubp10 is interacting with several ribosomal processing proteins. Our data up until now has shown that both *ubp10*Δ yeast, as well as catalytic dead *ubp10*^{C371S} mutant, have a slow growth/small colony size defect. We are therefore lead to believe

that Ubp10 is interacting with ribosomal synthesis and processing proteins. This interaction is directing its deubiquitinating function, which is required for normal biogenesis. Therefore, our next step was to identify potential enzymatic targets for Ubp10 to deubiquitinate.

Rpa190 of RNA Polymerase I is ubiquitinated, and deubiquitinated by Ubp10.

The next step was to identify potential Ubp10 targets from the identified ribosome processing components. To do this we sought to identify proteins that were more highly ubiquitinated in *ubp10*Δ yeast. Our strategy was to isolate ubiquitinated proteins from *UBP10* and *ubp10*Δ yeast, and then compare them using proteomic techniques. To do this, I utilized a yeast strain developed in the Gardner Lab in which all endogenous ubiquitin genes encode 8-histidines at the amino terminus. This epitope sequence allows metal affinity purification of ubiquitinated proteins. Using this approach for proteomic analyses of ubiquitinated proteins, I identified twenty candidate proteins to study as potential targets of Ubp10 action. Yeast strains in were engineered to contain 3HA epitope tag on the carboxyl terminus of target proteins. *UBP10* was genetically knocked out from these strains, allowing the comparison of ubiquitinated substrate levels between *UBP10* and *ubp10*Δ yeast.

UBP10 versus *ubp10*Δ yeast containing 8HIS-ubiquitin and the tagged substrate were grown to log phase, lysed in denaturing lysis buffer, flowed across a metal affinity column, and eluted for the ubiquitinated proteome. Lysate, flow and eluate fractions were separated on SDS-PAGE by electrophoresis for western blot analysis. The results found Rpa190 of RNA Polymerase I as the sole target of Ubp10, out of the entire pool of twenty screened proteins. Rpa190 is one of the fourteen protein components that comprise RNA Polymerase I. It is one of the two large catalytic components, and is required for the transcription of rDNA into rRNA (Memet et al., 1988; Russell and Zomerdijk, 2006). Rpa190 showed increased levels of ubiquitination in *ubp10*Δ yeast compared to wild-type *UBP10* (Fig. 2.6). These results were reconfirmed through tandem ubiquitin binding entites (TUBEs); TUBEs (Life Sensors) are agarose bound moieties capable of binding ubiquitin for purification with a high affinity for poly-ubiquitinated versus mono-ubiquitinated substrates (Fig 2.6). When looking at the protein levels Rpa190 in *UBP10* versus *ubp10*Δ yeast, *ubp10*Δ yeast show a much lower steady state of Rpa190 than their wild type counterparts. These data suggests that not only is Ubp10 required for

normal levels of ubiquitinated Rpa190, but that Rpa190's ubiquitination may be used to target it for degradation as well.

To confirm that Ubp10 was directly capable of deubiquitinating Rpa190, I next performed an *in vitro* deubiquitination experiment. Ubiquitinated Rpa190 was purified from yeast, and exposed to recombinant Ubp10 purified from *E. coli.* Results in Figure 2.8 show that after 40 minutes of exposure to purified Ubp10, the ladder of ubiquitinated Rpa190 is reduced down to a single band, previously associated with unmodified Rpa190 (Richardson et al., 2012). This is in comparison to when Rpa190 is not exposed to Ubp10, wherein no loss of ubiquitinated Rpa190 is seen. These results confirm that Ubp10 is capable of directly deubiquitinating ubiquitinated Rpa190 *in vitro*.

*Ubp10*Δ yeast have a lower Rpa190 steady state than *UBP10* yeast. One possible explanation for this decrease in steady state is that increased ubiquitination of Rpa190 targets it for degradation. To confirm that the increased ubiquitination of Rpa190 is resulting its degradation, I next determined if Rpa190 was degraded more quickly in *ubp10*Δ yeast than *UBP10* yeast. *UBP10* or *ubp10*Δ yeast were grown to log phase, then cycloheximide was added, which chemically blocks protein synthesis. Fractions of the yeast cultured removed and lysed throughout a three-hour time-course. These lysates were separated on an SDS-Page gel by electrophoresis and assayed by western blot. The results (Fig 2.7) show that Rpa190 is degraded quickly in *ubp10*Δ yeast, in comparison to *UBP10* yeast. Degradation rates of Rpa190 can be rescued back to wild-type rates by the re-introduction of *UBP10* in *ubp10*Δ yeast. The catalytic mutant $ubp10^{C371S}$ has similar rates of degradation of Rpa190 in *ubp10*Δ yeast as well, implying that Ubp10's catalytic function is required for normal protein levels of Rpa190.

As Rpa190 is required for RNA Polymerase I to function, decreased steady state of Rpa190 in a *ubp10*Δ mutant is a plausible explanation for the slow growth and decreased ribosomal subunits observed earlier. Therefore, I would expect that if we overexpress Rpa190 in *ubp10*Δ yeast, I could recover the slow growth associated with decrease ribosomal production. *UBP10* and *ubp10*Δ yeast were transformed with an over-expression plasmid containing either empty vector or Rpa190. Yeast were then plated in 10-fold dilutions and grown on minimal media to assay colony size and growth. As seen in Figure 2.9, *ubp10*Δ yeast over-expressing

Rpa190 show growth similar to *UBP10* yeast. This data supports that the slow growth of *ubp10*Δ yeast is the direct result of low steady state levels of Rpa190.

Ubp10 dependent ubiquitination occurs on lysine 410 of Rpa190.

With the discovery that *ubp10*Δ yeast shows increased Rpa190 ubiquitination and decreased Rpa190 steady state compared to *UBP10* yeast, a major question that arose was whether this is a direct, secondary, or tertiary result of the *ubp10*Δ phenotype. The most direct method we have to confirm Ubp10's role in regulating Rpa190, as well as ubiquitin's role in regulating Rpa190, is by identification and elimination of the site of ubiquitination on Rpa190. As discussed earlier in this manuscript, the ubiquitin enzymatic cascade covalently targets ubiquitin to a lysine on a target substrate. By identifying and mutating the ubiquitinated lysine on Rpa190 to an arginine, ubiquitination can be blocked while maintaining side chain charge and protein folding (Ciechanover, 2006).

The major drawback of using this mutagenesis approach is that one first needs to identify the ubiquitinated lysine(s) of interest. This was a particularly daunting task for Rpa190, as it contains a total of 133 lysines across 1664 total amino acids (Memet et al., 1988). My first approach was to purify the ubiquitinated proteome in *ubp10*Δ yeast, using a yeast strain that expressed 8HIS-tagged ubiquitin, followed by a second immunoprecipitation using an antibody against an epitope tagged Rpa190. Enriched ubiquitinated Rpa190 was then trypsin digested and mass spectrometry was used to identify the ubiquitination site. Unfortunately, this approach was unsuccessful, and several mass spectrometry attempts were only able to identify ~43% of the total predicted peptides from Rpa190's trypsin digest (data not shown). I include this information to emphasize that many trypsin-digest based assays are most likely insufficient for the identification of ubiquitin sites on a given protein and that secondary or tertiary approaches are often necessary.

During this time, Sam Entwisle (a rotation student working in Judit Villen's lab at the University of Washington) performed a similar mass spectrometry screen using the diglycine ubiquitin antibody (Udeshi et al., 2013) to identify ubiquitinated peptides across the entire yeast proteome. The diglycine ubiquitin antibody is designed to recognize a dual Glycine-Glycine overhang that occurs on the ubiquitinated lysine of a peptide that has been digest by the trypsin

protease. Their results turned up two unique potential ubiquitinated peptides in Rpa190 (Table 2.1). In order to identify if either or both of these sites were targeted for ubiquitination that was associated with our *ubp10*Δ phenotype, I created two over-expression plasmids that contained mutations in all local lysines (Table 2.1). UBP10 or *ubp10*Δ yeast expressing 8HIS-ubiquitin were transformed with Rpa190-3HA, Rpa190^{K410R}-3HA or Rpa190^{K1376}-3HA expression plasmids and assayed for ubiquitinated Rpa190 via purification of the ubiquitinated proteome and western analysis with anti-HA. The results (Fig 2.9) indicated that in *ubp10*Δ yeast, the Rpa190^{K410R}-3HA mutant shows no visible ubiquitination, as compared to the wild type Rpa190-3HA. This is in comparison to the Rpa190^{K1376R}-3HA mutant, which shows similar, if not greater Rpa190 ubiquitination compared to Rpa190-3HA. These results demonstrate that Ubp10 dependent ubiquitination of Rpa190 occurs at or around lysine 410.

Ubiquitination at lysine 410 on Rpa190 is not required for RNA Polymerase I function.

The identification of lysine 410 as the potential target lysine for regulating Ubp10 dependent ubiquitination raised two questions. First, is ubiquitination of lysine 410 essential for Rpa190/RNA Polymerase I function? Second, if it is not essential, does mutation of lysine 410 to an arginine rescue the slow growth phenotype in *ubp10*Δ yeast.

To answer these questions I first developed a yeast strain that was endogenously delete for *RPA190*, but instead relied on expression of Rpa190 from a plasmid. This strain was developed in order to easily switch from wild-type *RPA190* to *RPA190^{K410R}* and be able to confirm whether it was essential for RNA Polymerase I function (Picture diagram in Fig 2.10, *Top)*. To switch the Rpa190 expression reliance from endogenous to an extrachromosomal plasmid, diploid yeast strains were engineered that were heterologous for both *RPA190* and *UBP10* (*RPA190*/*rpa190*Δ*, UBP10*/*ubp10*Δ). A plasmid containing an epitope tagged Rpa190 (*RPA190-3HA::URA3*) was transformed into the strain. The strain was then sporulated, which causes gene duplication and separation into four haploid yeast spores. These spores were isolated by dissection onto rich media. The resulting strains were then replica plated onto selective minimal plates for each condition (*rpa190*Δ*::KanMX, ubp10*Δ*::LEU2*, Rpa190-3HA::URA3 2μ). Strains were chosen and verified for each mutation (data not shown).

Next, to switch wild-type Rpa190-3HA to the Rpa190^{K410R}-3HA mutant, I transformed in a second plasmid to the *UBP10* and *ubp10*Δ strains. This plasmid contained either empty vector, a wild type epitope tagged Rpa190 (Rpa190-3HA), or an epitope tagged mutant Rpa190^{K410R}-3HA. Finally, strains were plated onto minimal media with or without the drug 5-fluorootic acid (5-FOA), which in the presence of Orotidine 5'-phosphate decarboxylase (URA3) is actively converted into a toxic metabolite (5-fluorouracil). Yeast are thus forced to eject the wild type *RPA190-3HA*::URA3 plasmid, or die. The results of the 5-fluorouracil selection can be seen in Figure 2.10. Yeast transformed with the additional plasmid containing only vector show no growth, due to their reliance on the URA3 plasmid. However, both *RPA190-3HA* and *RPA190^{K410R}-3HA* strains grow normally. These data demonstrate that ubiquitination of lysine 410 on Rpa190 is not essential, as yeast strains carrying this mutation are capable of growing at similar rates to their wild-type counterpart.

Mutation of lysine 410 in Rpa190 is sufficient to block decreased steady state and slow growth in *ubp10*Δ yeast.

Our current understanding of *ubp10*Δ cells suggested that uncontrolled ubiquitination of Rpa190 results decreased steady state, which leads to a reduction in ribosomal biosynthesis and slow growth. I therefore hypothesized that yeast relying solely on the Rpa190^{K410R}-3HA mutation would not have the slow growth phenotype of *ubp10*Δ yeast. To confirm that ubiquitination and steady state levels of Rpa190^{K410R}-3HA were normal, I grew *UBP10* and *ubp10*Δ yeast strains expressing the Rpa190^{K410R}-3HA mutation. These cells were lysed in non-denaturing buffer and then the ubiquitinated proteome was purified using TUBE agarose beads. The lysate and eluate were separated on SDS-PAGE gel with electrophoresis and analyzed via western blot. The results (Fig 2.11) show that *ubp10*Δ yeast expressing Rpa190^{K410R}-3HA show no Rpa190 ubiquitination as compared to wild type Rpa190-3HA. The *ubp10*Δ Rpa190^{K410R}-3HA mutant also had Rpa190 steady state levels similar to our wild type yeast, demonstrating the requirement of lysine 410 for decreased steady states in *ubp10*Δ yeast. This is in comparison to yeast expressing wild-type Rpa190-3HA, which show increased ubiquitination and decreased steady state levels in *ubp10*Δ yeast. The Rpa190^{K410R} mutant does not show decreased steady

state levels in *ubp10*Δ yeast as well, and are similar to those in both strains with wild-type *UBP10*.

Having confirmed that the Rpa190^{K410R} mutation rescued the decreased Rpa190 steady state levels in *ubp10*Δ yeast, I next wanted to show that the mutation was capable of recovering the slow growth phenotype due to reduced RNA Polymerase I function in *ubp10*Δ yeast. Yeast containing iterations of *RPA190-3HA*, *RPA190^{K410R}*, *UBP10* and *ubp10*Δ were plated in 10-fold dilutions on rich media and allowed to grow for 3 days at 30°c. The results of this assay (Fig. 2.12) demonstrate that, while *RPA190*/*ubp10*Δ yeast show a slow growth phenotype compared to wild-type *RPA190*/*UBP10* yeast, the *RPA190^{K410R}*/*ubp10*Δ yeast mutant has similar rate of growth compared to *RPA190/UBP10*.

All together, these data confirm several functional mechanisms of Rpa190 ubiquitination. First, I have identified the Ubp10 dependent ubiquitination site on Rpa190 as lysine 410. I have demonstrated that this is the primary ubiquitination site regulated by Ubp10. I have demonstrated that ubiquitination of Rpa190 is not essential, but likely regulatory. Finally, I have shown that loss of this site is capable of blocking degradation of Rpa190 and rescuing slow growth in *ubp10*Δ yeast compared to *UBP10* yeast. This confirms the slow growth and loss of ribosome biogenesis seen in *ubp10*Δ yeast is the direct result of increased ubiquitination of Rpa190 caused by loss of *UBP10*.

Ubiquitinated Rpa190 is chromatin bound.

I have identified that ubiquitin is used to regulate Rpa190 degradation and RNA Polymerase I function and ribosome biogenesis. However, the regulatory purpose for this ubiquitination event is still unknown. One approach to narrow down the purpose of ubiquitination of Rpa190 would be to identify if it is ubiquitinated on or off chromatin. If Rpa190 is ubiquitinated off chromatin, then it is likely not used to regulate transcription, and most likely used to control total RNA Polymerase I levels. (Lempiainen and Shore, 2009). Conversely, if Rpa190 is ubiquitinated on chromatin, it would more likely be a regulatory mechanism associated with initiation, elongation or termination or Rpa190.

To identify where ubiquitinated Rpa190 was enriched, I separated out the soluble and chromatin fractions of yeast, then purified the ubiquitinated proteome from each and looked for levels of ubiquitinated Rpa190. To assay this, a yeast chromatin fraction was performed on yeast on *UBP10* versus *ubp10*Δ yeast. Cells were grown to an optical density (O.D.) of 0.5 and then spheroplasted (removal of outer cell wall using chemical digestion to all for a gentle lysis over 30 minutes. Fractionation was conducted as previously described (Keogh et al.) using sucrose fractionation. Lysate were taken out of the total, as well as soluble, and chromatin sub-cellular fractions. Then each fraction (Total, Soluble, Chromatin) was diluted in denaturing lysis buffer and the ubiquitinated proteome was purified with metal affinity resin, as previously described in this work. The resulting fractions (Lysates: Total, Soluble, Chromatin; Eluate: Total, Soluble, Chromatin) for both *UBP10* and *ubp10*Δ yeast were then separated on SDS-PAGE with electrophoresis and evaluated by western blotting.

The lysate and ubiquitin purification reveals that much of Rpa190 is localized to the chromatin (Fig 2.13). In the lysate fraction, *ubp10*Δ yeast have decreased steady state levels of Rpa190, most of which is located on chromatin. This is comparison to wild type *UBP10* yeast, which contain equal levels of Rpa190 between soluble and chromatin fraction. Our controls, histone H2B and Pgk1, indicate that the fractionation has correctly separated chromatin from the soluble proteins. When I analyzed the purified ubiquitinated proteome, I see that ubiquitinated Rpa190 is entirely chromatin localized in both *ubp10*Δ and *UBP10* yeast. This fractionation is confirmed through our enrichment for ubiquitinated histone H2B primarily in the chromatin fraction as well.

The identification of primarily ubiquitinated Rpa190 in our chromatin fraction supports the hypothesis that Rpa190 is ubiquitinated during elongation. I have shown earlier in this work that loss of ubiquitination of Rpa190 does not lead to a loss of function (Fig 2.10). We therefore would not expect that this ubiquitination event is required to direct initiation or recruitment of RNA Polymerase I. The depletion of the soluble pools of Rpa190 in *ubp10*Δ yeast also supports the hypothesis that ubiquitination is being used as a response, likely during a regulatory event, to tag Rpa190 for ubiquitination and degradation. To better understand the role of ubiquitination on chromatin, I next asked how Ubp10 is recruited to the chromatin and rDNA.

Ubp10 is recruited to the nucleolus to deubiquitinate Rpa190

The identification that Rpa190 is ubiquitinated on chromatin is highly suggestive that Ubp10 is recruited to rDNA as well. There are three models for recruitment of Ubp10 to deubiquitinate Rpa190. The first, and most obvious, is that Rpa190/RNA Polymerase I directly recruits Ubp10. Our lab has attempted multiple different methods in order to demonstrate this (data not shown), and to date the only method capable of showing a direct interaction between Ubp10 and Rpa190 is through formaldehyde cross-linking. Given the indirect nature associated with identifying interactions with cross-linking, and the crowded nature of the nucleolus (Raska et al., 2006), we believe that Ubp10 does not directly interact with Rpa190. The second model would predict that Ubp10 is instead recruited through one of the many ribosome-processing proteins that bind rRNA/protein scaffolds during ribosome biogenesis. This model is supported by the identification of several ribosome processing proteins that interact with Ubp10. The third model is that Ubp10 directly binds the rRNA itself. In this model Ubp10 instead is recruited to ribosomal RNA, and interacts to coordinate or scaffold its identified protein interactors.

To identify how Ubp10 might be recruited to the rDNA or rRNA, I first analyzed Ubp10's amino acid sequence for potential rDNA or rRNA recruiting motifs (Emmott and Hiscox, 2009; Zhang et al.). Analysis of Ubp10's domain structure indicates the only known domain, the cysteine protease domain responsible for its deubiquitinating capability, which is flanked by two arms with unknown function (Fig 2.14). A major canonical mechanism for rRNA/nucleolar recruitment is thought to be through a highly basic peptide sequence within the protein (Emmott and Hiscox, 2009; Zhang et al.). A short, basic sequence was found at the very end of Ubp10's C-terminal tail (Fig 2.14). Similar basic peptides sequences have been identified in many other nucleolar proteins that are recruited in as ribosome processing proteins, such as Nop58 and Nop56 (Grandi et al., 2002). To identify if this sequence was necessary for Ubp10's nucleolar localization, I created a Ubp10 mutant that lacked the C-terminal region following its catalytic domain, *UBP10*$^{\Delta 738\text{-}792}$. I expressed either a wild type Ubp10 with a C-terminal GFP tag, or Ubp10$^{\Delta 738\text{-}792}$ with a C-terminal GFP tag and used fluorescent imaging to identify localization of Ubp10. As seen in Figure 2.15, wild-type Ubp10-GFP is localized primarily to the nucleolus and overlaps with Nop58-mCherry. In stark contrast, Ubp10$^{\Delta 738\text{-}792}$-GFP has lost this nucleolar localization and is instead found diffuse throughout the nucleus. This imaging data

demonstrates the necessity of the short-basic identified region in Ubp10's C-terminal tail for its recruitment into the nucleolus.

I next wanted to show that this region of Ubp10 was not only necessary for recruitment to the nucleolus, but was sufficient as well. To test this, I fused Ubp10's C-terminal tail (amino acids 738-792) with or without the identified nucleolar localization signal to GFP. By fluorescent microscopy, NLS-GFP alone is diffuse throughout both the nucleus and the cytoplasm (Fig 2.16). However, the attachment of Ubp10's C-terminal tail results in GFP signal that overlaps well with mCherry, primarily in the nucleolus. This retention is completely lost in the NLS-GFP construct containing Ubp10's C-terminal lacking the lysine/arginine basic region. These data together demonstrate that Ubp10 contains a basic amino acid stretch within its C-terminal tail that targets it to the nucleolus.

Having identified that Ubp10 is recruited to the nucleolus, we wanted to ask whether Ubp10's recruitment was needed to maintain normal levels of ubiquitinated of Rpa190. I again analyzed steady state Rpa190 and ubiquitinated Rpa190 levels using the ubiquitin pull-down assay in cells expressing 8HIS-Ubiquitin. Yeast strains expressing *UBP10*, *Ubp10*Δ, or $Ubp10^{\Delta 738\text{-}792}$ were grown to log phase, lysed, and their ubiquitinated proteomes were purified. Each sample was separated on SDS-PAGE by electrophoresis and evaluated by western blot. Rpa190 steady states were compared between *UBP10*, *Ubp10*Δ, and $Ubp10^{\Delta 738\text{-}792}$ yeast strains. As seen in figure 2.17, while $Ubp10^{\Delta 738\text{-}792}$ yeast show an Rpa190 steady state similar to wild-type *UBP10*, they have levels of ubiquitinated Rpa190 similar to *ubp10*Δ yeast. These results demonstrate that localization of Ubp10 to the nucleolus is necessary to maintain wild-type levels of ubiquitinated Rpa190, though nuclear localized $Ubp10^{\Delta 738\text{-}792}$ is still capable of deubiquitinating Rpa190 to a lesser degree. My data confirms the initial hypothesis that Ubp10 is being recruited in to the nucleolus by it's basic C-terminal tail and this recruitment is a primary mechanism for maintaining normal ubiquitination of Rpa190.

Discussion

Prior to the work done here, the only known role for Ubp10 was to regulate chromatin silencing through the regulation of histone H2B (Emre et al., 2005; Gardner et al., 2005; Kahana and Gottschling, 1999). I have now demonstrated a role for Ubp10 to regulate ubiquitination of Rpa190/RNA Polymerase I, and that this ubiquitination event is used to regulate ribosome

biogenesis. While this ubiquitination event leads Rpa190 degradation, I have also demonstrated that a site mutation resulting in the loss of the lysine 410 ubiquitination on Rpa190 to be sufficient to rescue increased ubiquitination in *ubp10*Δ cells. Not only this, but *ubp10*Δ yeast expressing only an $RPA190^{K410R}$ mutant grow normally when compared to strains with wild-type *RPA190*. This implies that this ubiquitination of Rpa190 is not required for RNA Polymerase I transcription of rDNA, but most likely a regulatory event in response to cell stress or failure of RNA Polymerase I.

As discussed earlier in this work, there is only one other known role for ubiquitin in regulating the RNA Polymerases, which is the regulation of RNA Polymerase II (Harreman et al., 2009; Wilson et al., 2013). There are multiple mechanisms that may cause RNA Polymerase II to stall, including DNA damage (Verma et al., 2011), nucleotide depletion, chromatin impediment, and polymerase inhibition (Wilson et al., 2013). In these conditions, the large subunit of RNA Polymerase II, Rpb1, is subject to a multi-step ubiquitination process. Stalled RNA Polymerase II is first mono-ubiquitinated on Rpb1 by the ubiquitin ligase Rsp5 in response to DNA damage or a kinetic barrier (Huibregtse et al., 1997; Somesh et al., 2005). Mono-ubiquitination of Rpb1 on RNA Polymerase II is actively reversible by the deubiquitinase Ubp2 given repair or removal is successful. If unsuccessful, the Elc1-Cul3 complex is recruited to K48 poly-ubiquitinate Rpb1, which results in its degradation by the 26S proteasome (Anindya et al., 2007; Ribar et al., 2006).

Rpa190 contains a high degree of identity to Rpb1, and both proteins play a similar role in their respective RNA Polymerase (Kuhn et al., 2007). It would not be surprising to find that ubiquitin is used for a similar role in RNA Polymerase I, which is to extract it in response to some catastrophic failure. Ubiquitin plays a major role in both chromatin extraction and substrate degradation (Mogk and Bukau, 2004; Rumpf and Jentsch, 2006), and it therefore seems likely that it plays a similar role for RNA Polymerase I that it does for RNA Polymerase II. The implication that ubiquitin's role in regulating Rpa190/RNA Polymerase I is associated with its active transcription of ribosomal RNA largely suggests of a regulatory mechanism during elongation. Because ubiquitination of RNA Polymerase I is not required for ribosome biogenesis, it very possible that it is instead being used to regulate elongation of RNA Polymerase I.

Another indication that ubiquitination is used to regulate RNA Polymerase I elongation is suggested by Ubp10's recruitment to the nucleolus. Although there are no universal consensus sequences for nucleolar localization, many proteins are recruited to snoRNA or rRNA processing proteins or actively transcribed rRNA through short, basic amino acid sequences (Emmott and Hiscox, 2009; Zhang et al.). The predicted nucleolar signal identified in Ubp10's C-terminal tail is similar to other identified sequences, and was shown to be both necessary and sufficient for nucleolar recruitment. I have until now primarily discussed that Ubp10 deubiquitinates Rpa190/RNA Polymerase I. Our work has also shown that while Ubp10 deubiquitinates Rpa190, it is through interaction with other proteins that this occurs. Identification that Ubp10 interacts with multiple ribosomal processing proteins *in vivo* suggests that Ubp10 recruitment by ribosome processing proteins may be crucial for deubiquitinating Rpa190/RNA Polymerase I. If so, how and why is this regulation occuring?

In the next chapter, I will begin to explore the structure of Ubp10 to better explain how and why it interacts with ribosomal processing proteins. This work will help explain Ubp10's role in ribosome production, and give us hints as to how its deubiquitination of Rpa190 is regulated.

Acknowledgements

Much of this work was done through the teamwork and communication with colleagues, and as such, was a great lesson in working with a great group of people. Rich Gardner was responsible for the work and observation for the slow growth of *ubp10*Δ yeast being divergent from Ubp10's chromatin silencing function. The Northern blot work was done through by Susan Baserga's lab and conducted by Emily Freed. The predicted ubiquitination sites of Rpa190 were found as a result of work done by Sam Entwisle as a rotation student in Judit Villen's lab. Finally, much of this work could not have been done without the teamwork of Lauren Richardson, who was responsible for the initial mass spectrometry work that identified ribosomal interactors of Ubp10. She is also responsible for the co-immunoprecipitation that verified Ubp10's interactors, as well as the cycloheximide assays.

Figures 2.1, 2.3, 2.4, 2.5, 2.7, and 2.8 are derived from the following publication:

Richardson, L.A., Reed, B.J., Charette, J.M., Freed, E.F., Fredrickson, E.K., Locke, M.N., Baserga, S.J., and Gardner, R.G. (2012). A conserved deubiquitinating enzyme controls cell growth by regulating RNA polymerase I stability. Cell Rep 2, 372-385.

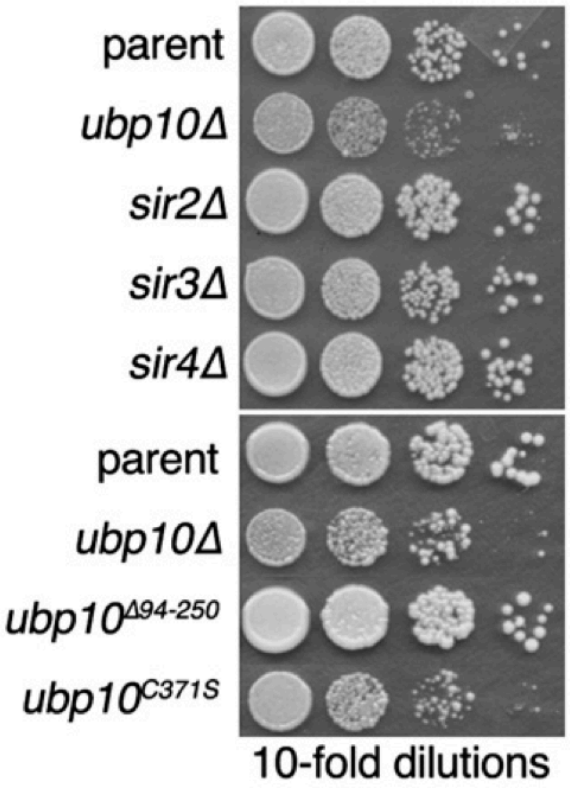

Figure 2.1 – *ubp10*Δ yeast have a slow growth phenotype not associated with chromatin silencing. Yeast spot tests of parent strain compared to *ubp10*Δ, *sir2*Δ, *sir3*Δ, *sir4*Δ, $ubp10^{\Delta 94\text{-}250}$ and $ubp10^{C371S}$ strains. Ten-fold serial dilutions of each strain were spotted onto rich media and incubated at 30° for 3 days.

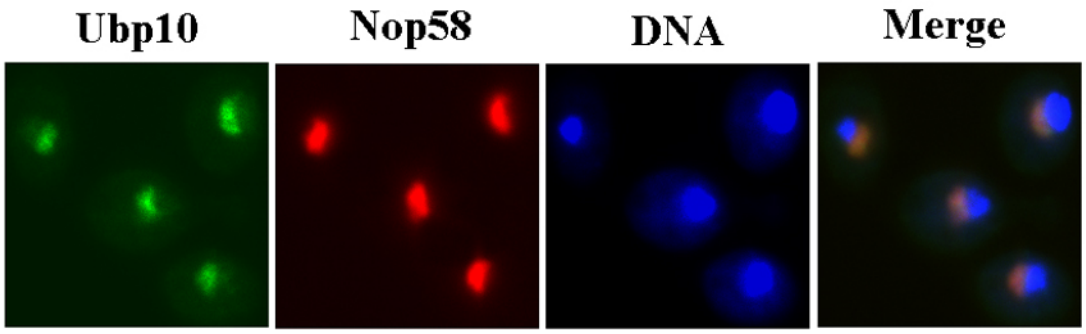

Figure 2.2 – Ubp10 is localized to the nucleolus. Florescence microscopy of exponentially growing cells co-expressing Nop58-mCherry and Ubp10-GFP. Nop58-mCherry marks the nucleolus and DAPI staining marks the nucleus.

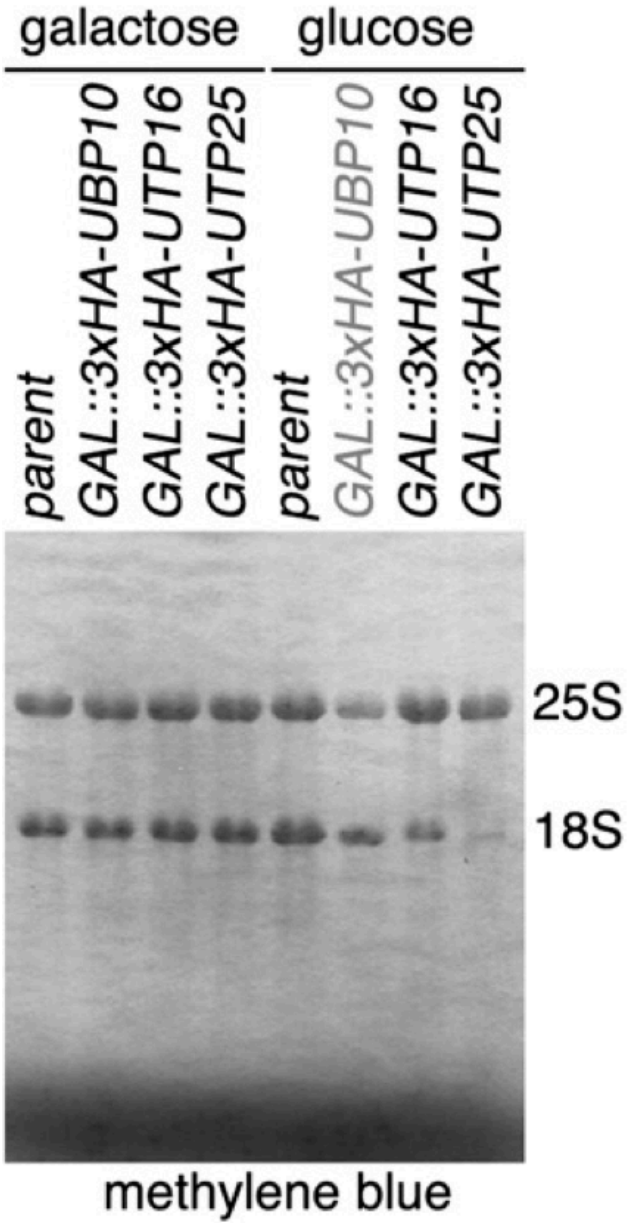

Figure 2.3 – Ribosome biogenesis is impaired in cells depleted for Ubp10. Genetic depletion of Ubp10 resulted in the decrease of mature 25S and 18S rRNA. Total RNA was extracted from yeast after genetic depletion of indicated protein for 72 hr at 17°C. Mature 18S and 25S rRNA was detected using methylene blue staining.

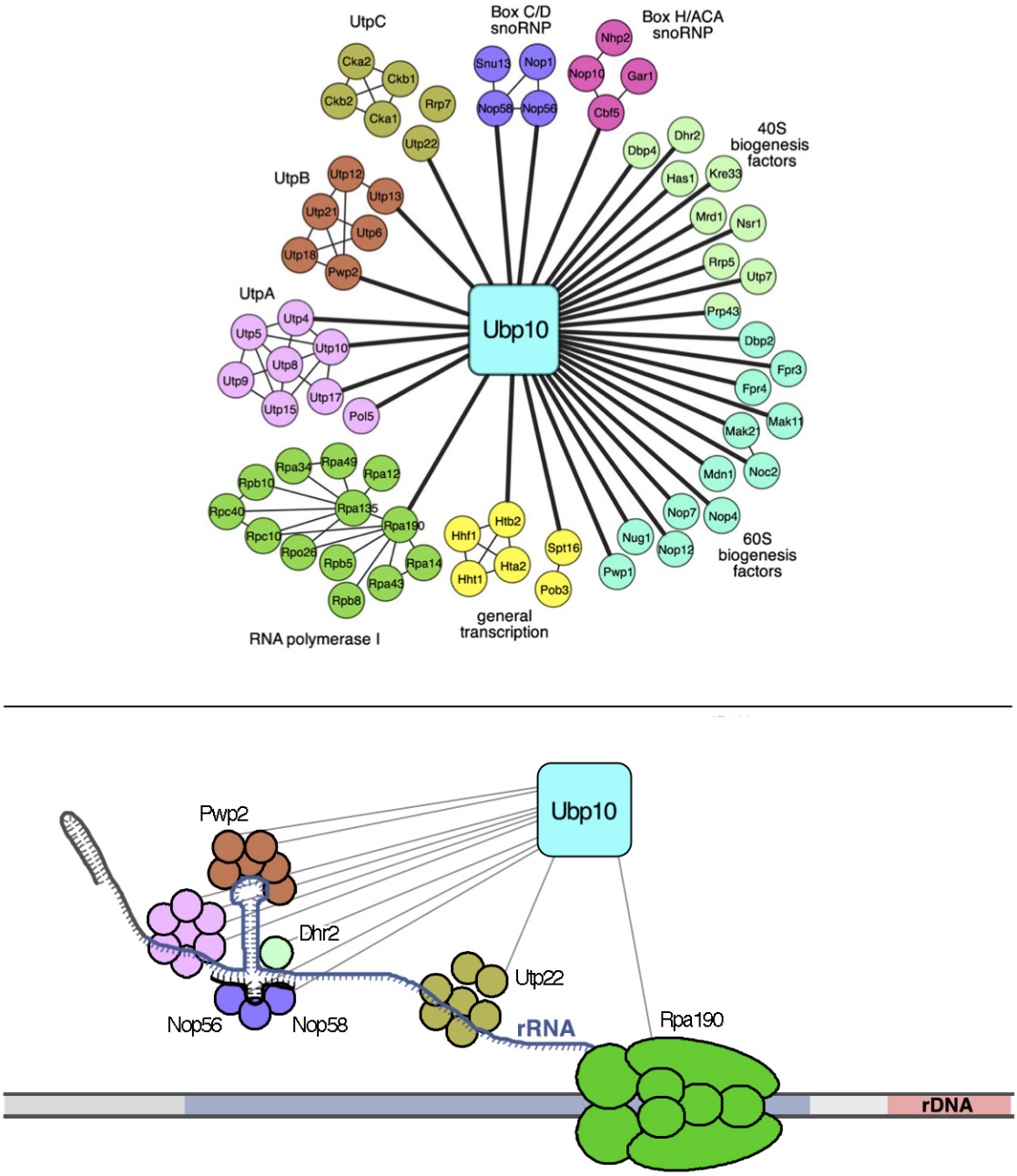

Figure 2.4 – Formaldehyde crosslinking MS/MS proteomic analysis of Ubp10 associated proteins indicates multiple Ubp10 interactions with ribosomal processing proteins. Top: Network diagram of the nucleolar-localized proteins identified by crosslinking co-immunoprecipitation MS/MS with Ubp10-3HSV. Diagram was generated using Cytoscape (http://www.cytoscape.org/). Bottom: Reorganization of network diagram into functional cartoon showing protein interactors and their complexes associated with 18S rRNA processing. Proteins verified to interact with Ubp10 through secondary methods (CoIP/Yeast 2-Hybrid) are labeled (except for Rpa190). Data for those interactions are in Figure 2.5.

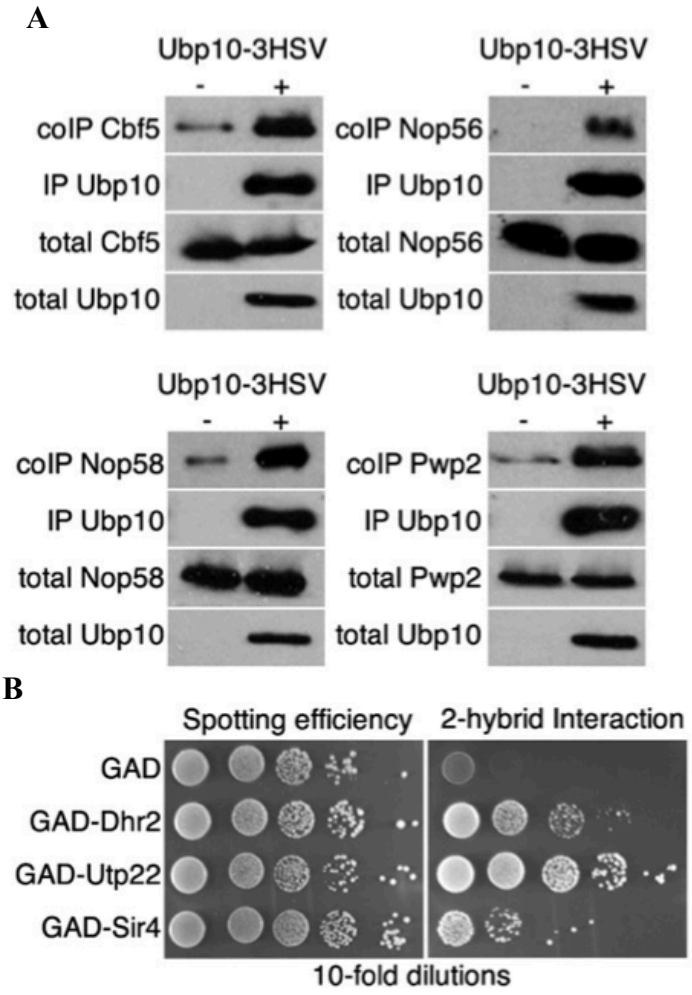

Figure 2.5 – Co-immunoprecipitation and Yeast 2-hybrid studies confirm Ubp10 interaction with multiple ribosome processing proteins. A, Co-immunoprecipitation between Ubp10-3HSV and the indicated 3-HA-tagged target proteins. Ubp10-3HSV was purified with its interacting proteins by immunoprecipitation using anti-HSV antibodies. Samples were run on SDS-PAGE and analyzed by anti-HSV and anti-HA western blotting. B, Yeast 2-Hybrid interactions between cells expressing GBD-Ubp10 and each indicated GAD fusion protein. Cells were spotted onto minimal media plus or minus histidine to measure spotting efficiency and Yeast 2-Hybrid interaction, respectively.

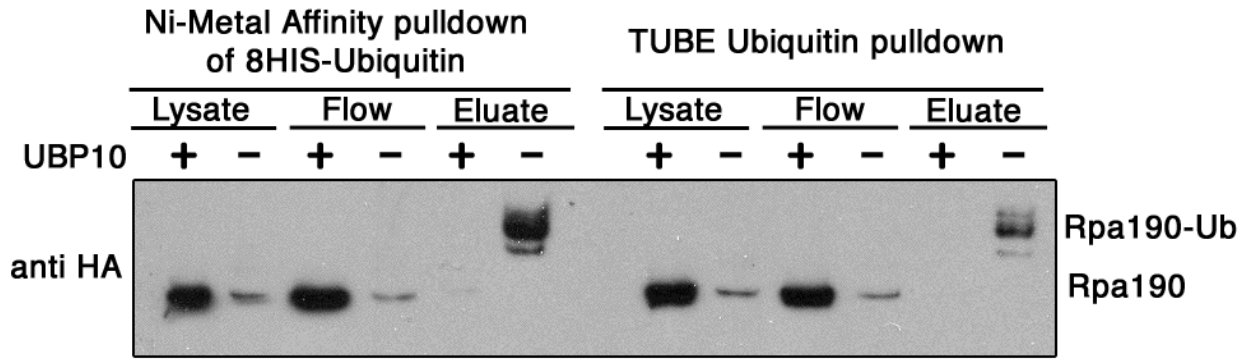

Figure 2.6 – Rpa190, a large subunit of RNA Polymerase I, is more highly ubiquitinated in *ubp10*Δ yeast. Ubiquitin proteomes from *UBP10* (wt) or *ubp10*Δ (Δ) cells were isolated by metal affinity purification (Lanes 1-6) or Tandem Ubiquitin Binding Entities (Lanes 7-12). Levels of Rpa190-3HA in lysates, flow or eluate were determined by western analysis using anti-HA antibodies. Lanes 1-2, and 7-8 indicate steady-state levels of Rpa190 in total lysates of *UBP10* and *ubp10*Δ cells. Lanes 5-6 and 11-12 indicate levels of ubiquitinated Rpa190 in the ubiquitinated proteome of UBP10 and *ubp10*Δ cells.

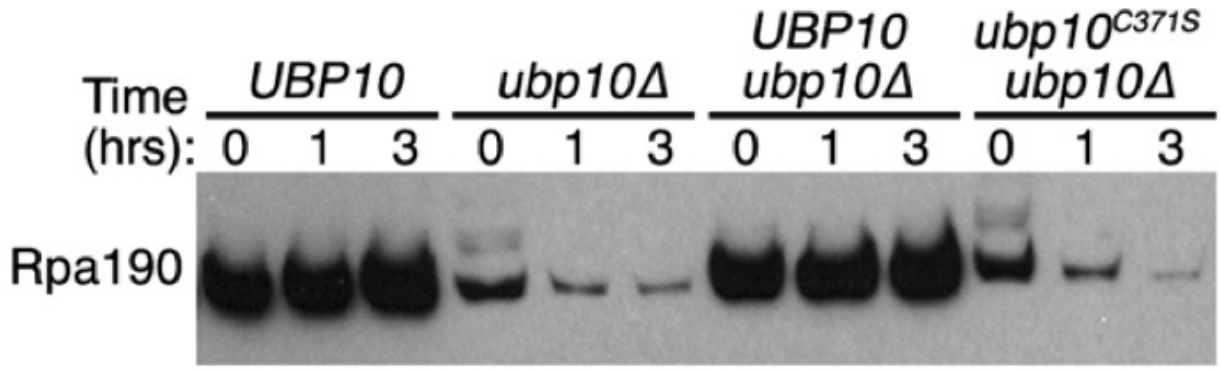

Figure 2.7 – Rpa190 is rapidly degraded in *ubp10*Δ yeast. Cycloheximide-chase degradation assays of *UBP10*, *ubp10*Δ, *ubp10*Δ*::UBP10-3HSV,* or *ubp10*Δ ::*ubp10*^{C371S}*-3HSV* cells expressing Rpa190-3HA. Time after cycloheximide addition is indicated above each lane. Western analysis of whole-cell extracts was performed using anti-HA antibodies.

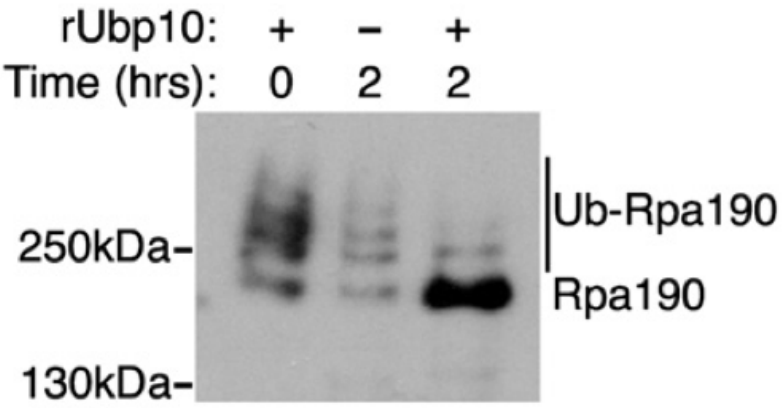

Figure 2.8 – Ubiquitinated Rpa190 is deubiquitinated *in-vitro* by **recombinant Ubp10**. *In vitro* Rpa190 deubiquitination assay. Recombinant Ubp10 was added to purified ubiquitinated Rpa190 for the indicated time. Western analysis of Rpa190 was performed using anti-HA antibodies.

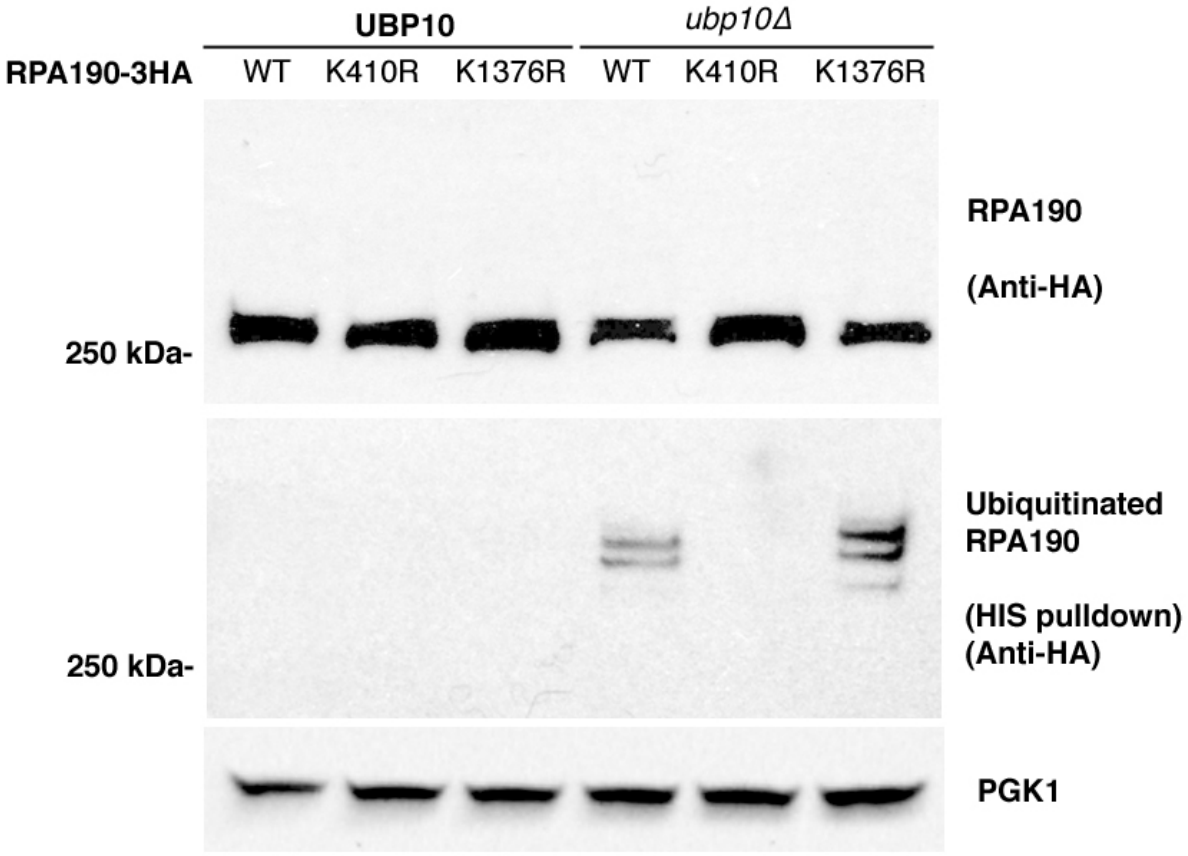

Figure 2.9 – A lysine to arginine mutation at lysine 410 on Rpa190 blocks ubiquitination in *ubp10*Δ yeast. Ubiquitinated proteomes from *UBP10* (wt) or *ubp10*Δ (Δ) cells over-expressing plasmids containing *RPA190-3HA*, *RPA190*^{K410R}*-3HA*, or *RPA190*^{K1376R}*-3HA* were isolated by metal affinity purification. Levels of Rpa190 in lysates (total protein) and eluates (ubiquitinated Rpa190) were determined by western analysis using anti-HA antibodies. Top panel indicates lysates, middle panel indicated eluates, and the bottom panel is loading control PGK1. A decrease in Rpa190-3HA steady states for *ubp10*Δ cells was not observed due to overexpression from plasmid.

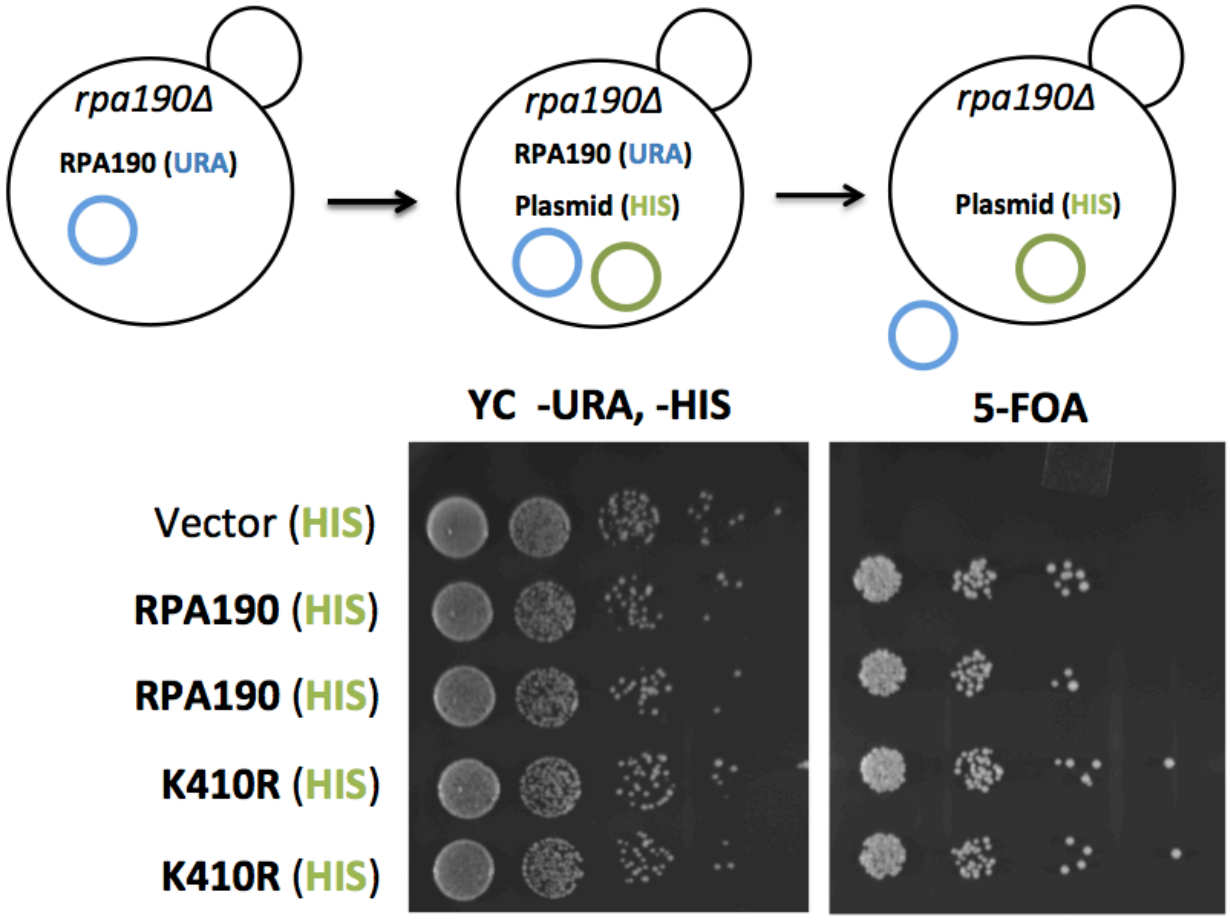

Figure 2.10 – Ubiquitination of lysine 410 on Rpa190 is not required for normal growth. *Rpa190*Δ yeast relying on expression of Rpa190 from extrachromosomal plasmid were transformed with a second plasmid containing empty vector, wild type *RPA190*, or *RPA190*^{K410R}. Yeast were plated onto either minimal media lacking URA and HIS, or minimal media with 5-Fluoroorotic acid (5-FOA). Cartoon (top) demonstrates that plating on to 5-FOA forces ejection of the URA3 plasmid (BLUE) and reliance on the HIS plasmid (GREEN). Yeast containing either wild-type *RPA190* or *RPA190-*^{K410R} were done in duplicate for confidence in results.

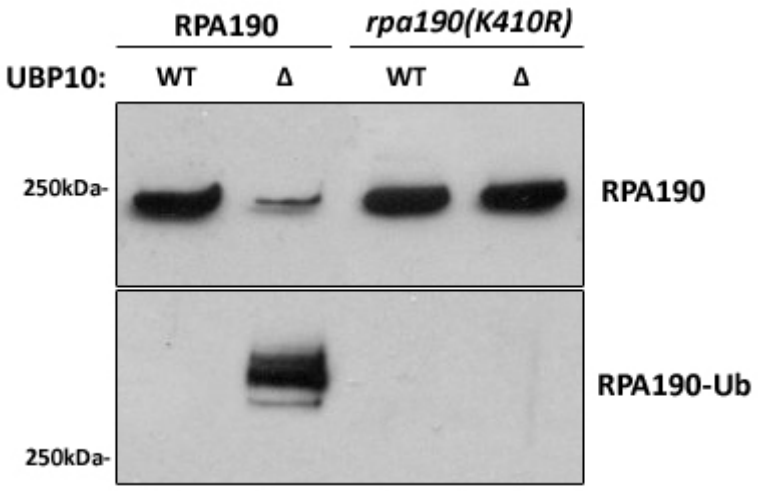

Figure 2.11 – *K410R* site mutation in *Rpa190* rescues its loss of steady state in *ubp10*Δ yeast. Ubiquitinated proteomes were isolated by metal affinity purification from *UBP10* (wt) or *ubp10*Δ (Δ) cells, both of which were *rpa190*Δ but instead expressed either *RPA190-3HA* or $RPA190^{K410R}$*-3HA* from an extrachromosomal plasmid. Levels of Rpa190 in lysates (total protein) and eluates (ubiquitinated Rpa190) were determined by western analysis using anti-HA antibodies. Top panel indicates lysates (total protein) and the bottom panel indicated eluates (ubiquitinated Rpa190).

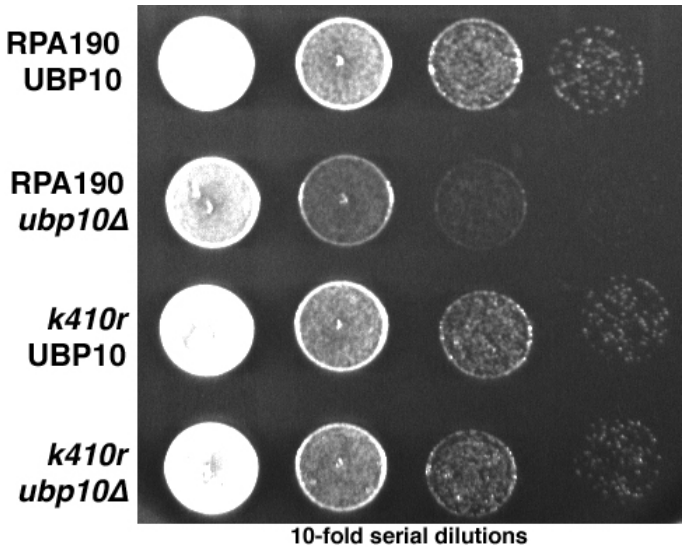

Figure 2.12 – *K410R* site mutation in *RPA190* rescues slow growth in *ubp10*Δ yeast. *UBP10* (wt) or *ubp10*Δ *(*Δ*)* cells that are delete for Rpa190 (*rpa190*Δ*)* but instead express either Rpa190 or Rpa190^{K410R} from an extrachromasomal plasmid were plated onto rich media and incubated for 3 days at 30°C.

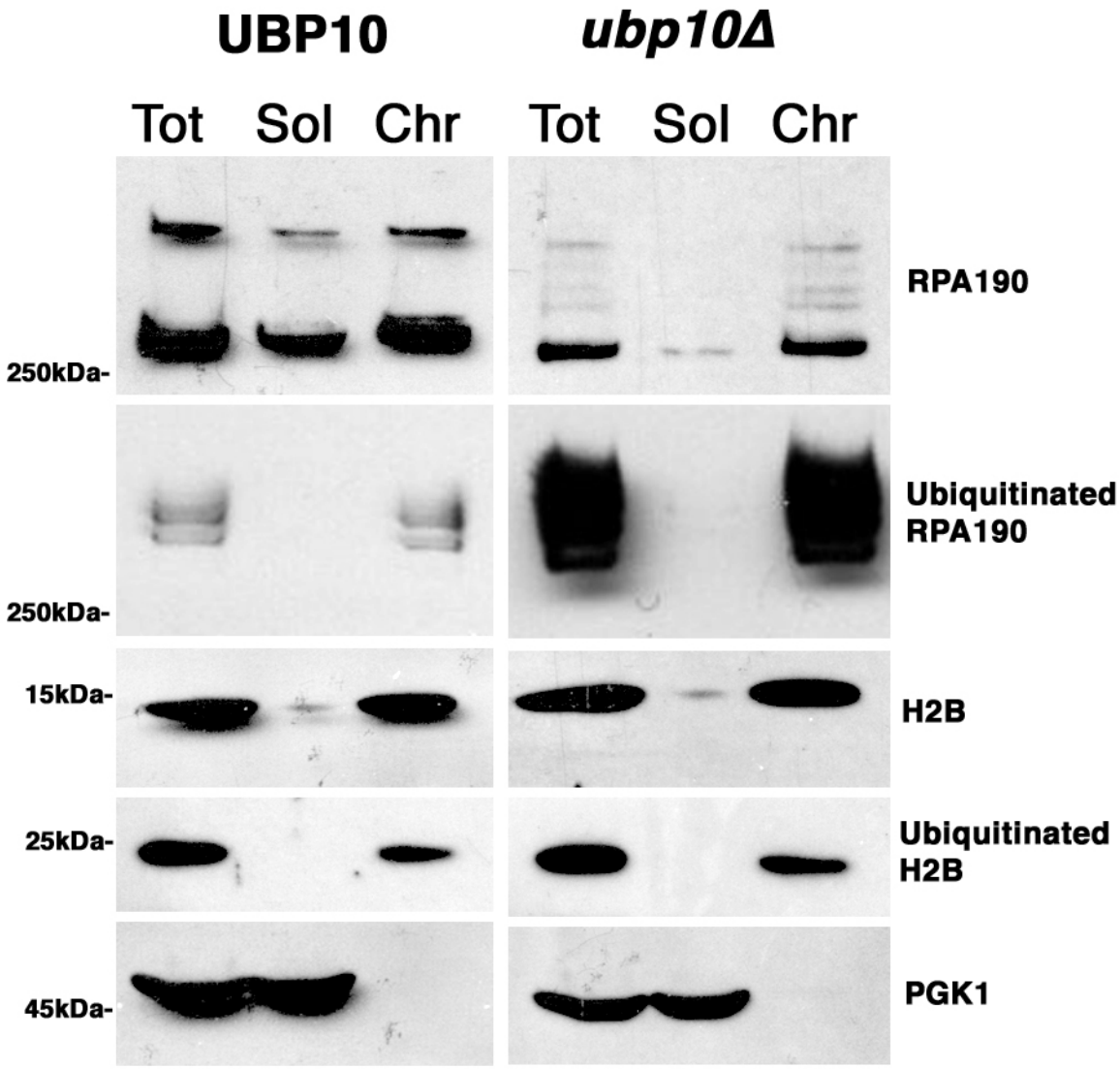

Figure 2.13 – Ubiquitinated Rpa190 is localized to chromatin. *UBP10* (wt) or *ubp10*Δ (Δ) cells were grown to log phase and then spheroplasted for 30 minutes. 40% of spheroplasted cells were removed, lysed in hypotonic solution containing detergent, and put on ice as the 'Total' (Tot) fraction. The remaining fraction was lysed by addition of a hypotonic solution and soluble (Sol) and chromatin (Chr) were separated by sucrose gradient. Ubiquitinated proteomes were then metal affinity purified from each fraction (total, soluble and chromatin). Levels of Rpa190-3HA (anti-HA), histone H2B (Anti-H2b) and PGK1 (Anti-PGK1) were determined by western analysis. RPA190, H2B and PGK1 indicate lysates (total protein) for each protein. Ubiquitinated RPA190 and Ubiquitinated H2B indicate eluate (ubiquitinated proteome) for each protein.

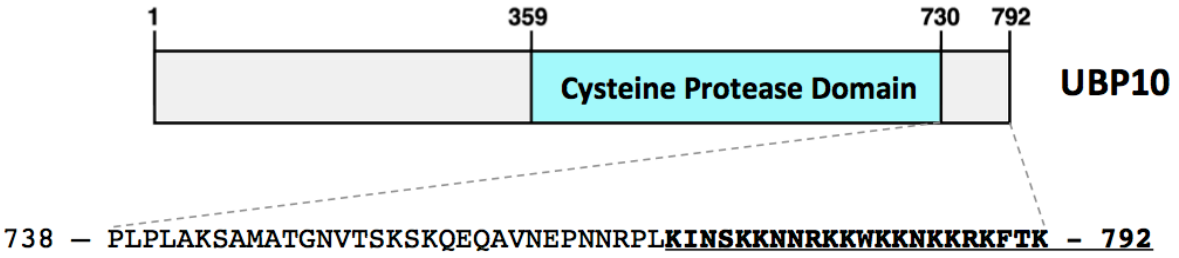

Figure 2.14 – Ubp10's C-terminal tail contains a short, basic amino acid stretch similar to other known nucleolar localization sequences. Top: Cartoon of Ubp10 with its only known domain, the cysteine protease domain. Bottom: Amino acid sequence in Ubp10's C-terminal tail which contains a predicted nucleolar localization sequence (**bold and underlined**).

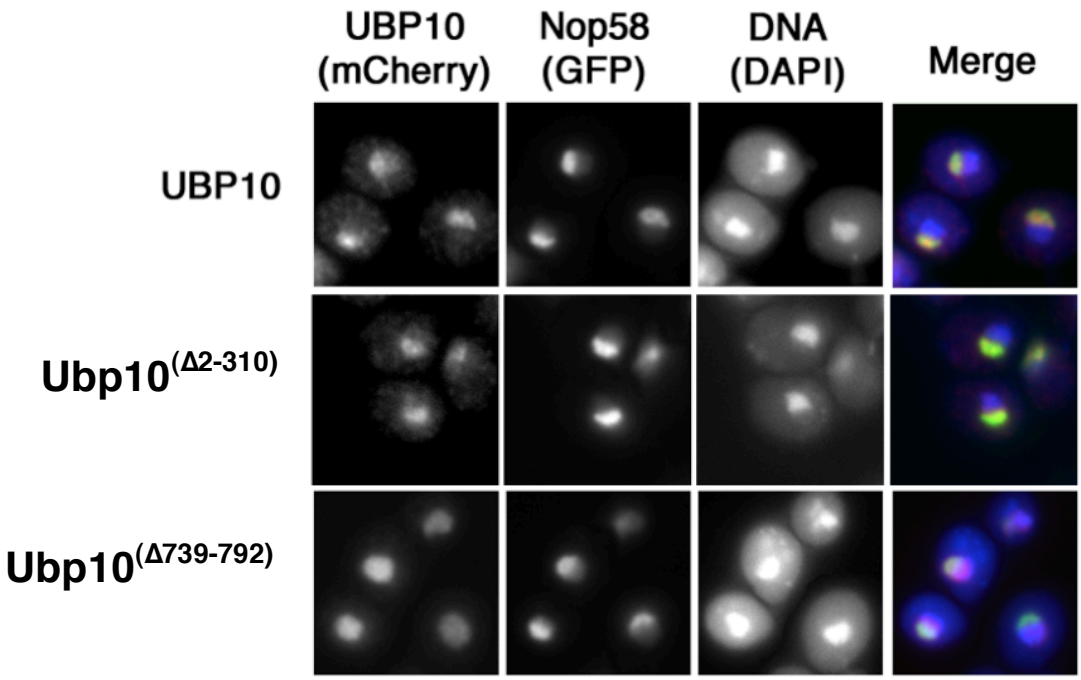

Figure 2.15 – Ubp10's nucleolar localization requires its carboxy terminus. Florescence microscopy of exponentially growing cells co-expressing Nop58-mCherry and either Ubp10-GFP, Ubp10$^{(\Delta 2\text{-}310)}$*-GFP,* or Ubp10$^{(\Delta 738\text{-}792)}$*-GFP.* Nop58-mCherry marks the nucleolus and DAPI staining marks the nucleus.

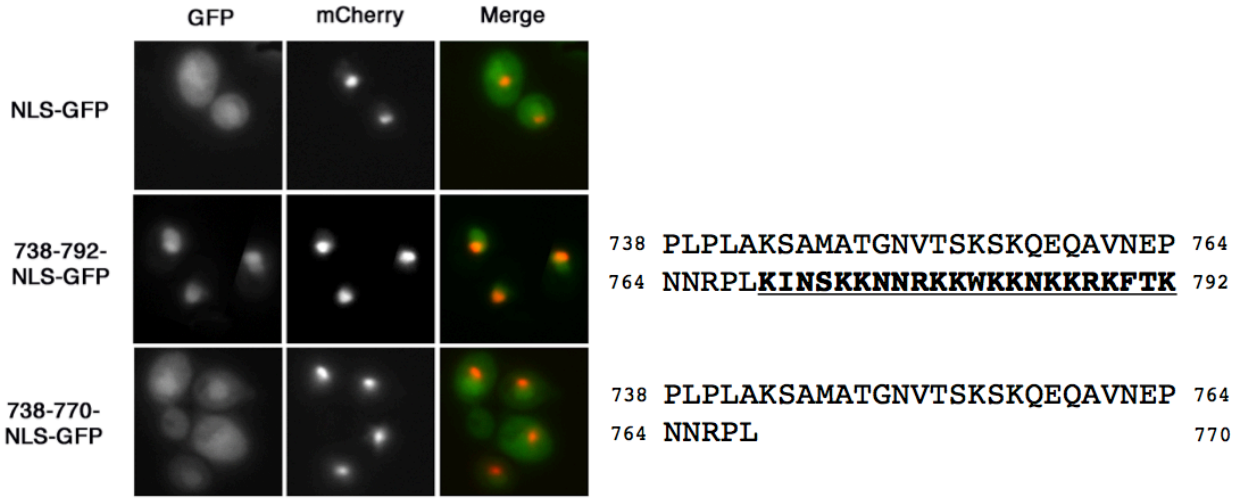

Figure 2.16 – Ubp10's C-terminal tail is sufficient for nucleolar localization. Florescence microscopy of exponentially growing cells co-expressing Nop58-mCherry and either NLS-GFP, Ubp10$^{(738\text{-}792)}$-*GFP*, or Ubp10$^{(738\text{-}770)}$-*GFP*. Nop58-mCherry marks the nucleolus and DAPI staining marks the nucleus. Peptide sequences used for Ubp10$^{(738\text{-}792)}$-*GFP* and Ubp10$^{(738\text{-}770)}$-*GFP* are noted to the right each construct.

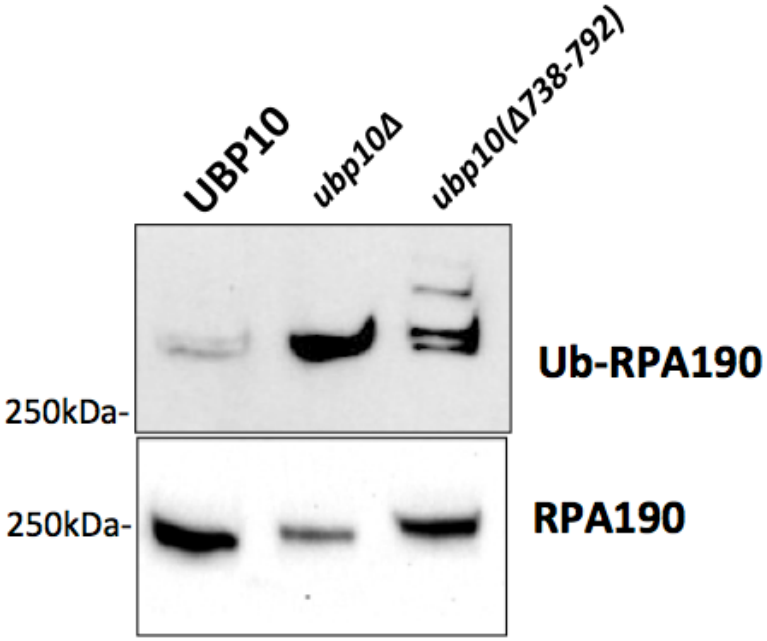

Figure 2.17 – Ubp10$^{(\Delta 738\text{-}792)}$ does not rescue ubiquitinated Rpa190 levels in a *ubp10*Δ. Ubiquitinated proteomes from *UBP10*, *ubp10*Δ, and *ubp10*$^{(\Delta 738\text{-}792)}$ were isolated using metal affinity purification. Levels of Rpa190 in lysates (total protein) and eluates (ubiquitinated Rpa190) were determined by western analysis using anti-HA antibodies. Top panel indicates lysates (total protein) and the bottom panel indicated eluates (ubiquitinated Rpa190). While ubp10$^{(\Delta 738\text{-}792)}$ mutants did not completely rescue ubiquitinated Rpa190, steady state levels of Rpa190 were partially rescued. This is likely due to ubp10$^{(\Delta 738\text{-}792)}$ still being nuclear localized.

	Lysine 410	Lysine 1376
Sites predicted to be modified	R'DLNDDLSK*LQKDK'	K'RLEEDNDEEQSHK*K'
Mutations used in plasmids	R'DLNDDLS**R**LQ**R**D**R**'	K'RLEEDNDEEQSH**RR**'T**R**Q

Table 2.1 – Predicted sites of ubiquitination in Rpa190. Predicted sites of ubiquitination on Rpa190 from Anti-GG enrichment and MS/MS. K* denotes ubiquitin modified peptide. K' or R' denotes trypsin digestion site. Second row shows the lysine to arginine mutations mutated in Rpa190 plasmids to confirm ubiquitination site. Local lysines were mutated to ensure compensation by ubiquitination of another local site did not occur.

CHAPTER THREE:

UBP10 USES INTRINSIC DISORDER TO INTERACT WITH RIBOSOMAL RNA PROCESSING PROTEINS

Ubp10 is predicted to contain intrinsically disordered regions

My previous chapters have demonstrated how the deubiquitinase Ubp10 interacts with a large network of proteins in the nucleolus and nucleus. To date, Ubp10 has been shown to deubiquitinate several different chromatin-associated proteins as well, including: histone H2B (Emre et al., 2005; Gardner et al., 2005), PCNA (Gallego-Sanchez et al., 2012; Lis and Romesberg, 2006), and now, Rpa190, the largest subunit of RNA Polymerase I (Richardson et al., 2012). Thus far, the mechanism of recruitment utilized by Ubp10 to interact with these many substrates is unknown.

DUBs typically possess a core catalytic domain essential for their deubiquitinating activity with variable length N- and C-terminal extensions that are thought to direct their function (26). Ubp10 has a large N-terminal region (residues 1-359), a DUB catalytic domain (residues 360-729), and a small C-terminal region (residues 730-792) (Fig. 3.1A). To gain insight into Ubp10's function, we analyzed Ubp10's domain composition and secondary structure characteristics using secondary structure, protein domain, and order/disorder prediction algorithms. The N- and C-terminal regions of Ubp10 contain no identifiable protein domains.

When I used different order/disorder prediction algorithms, we found that Ubp10 was predicted to contain high intrinsic disorder (≥85%) within its N- and C-terminal regions (Fig. 1*B*). The top panel in Figure 3.1B is the disorder prediction for Ubp10 by PONDR, which predicts disorder by comparing the sample protein sequence against a 'neural network' that was developed from curated disordered regions identified through missing electron densities in x-ray crystallography or from disordered regions characterized by nuclear magnetic resonance (NMR) structures (27). The middle panel is the disorder prediction from FoldIndex, which predicts disorder in local protein sequence by quantifying the sequence's net mean charge and net hydrophobicity (28). The bottom panel is the disorder prediction from IUPred, which predicts disorder by analyzing pairwise energies between local protein sequences and predicting the likelihood they will form globular structures (29). Interestingly, 5 of the 15 other yeast DUBs

(Ubp1, Ubp3, Ubp4, Ubp7, and Ubp13) also possess IDRs of at least 100 residues in length (Fig. 3.2), indicating that disorder is common among DUBs, as has been shown for E3s (14). However, the massive extent of Ubp10's disorder is unique among the yeast DUBs.

Protein disorder in regulating cellular function

How a protein functions has long been thought to be the direct result of its three-dimensional protein structure. Intrinsically disordered regions (IDR), or regions lacking three-dimensional structure, were thought to be limited within the proteome and act primarily as linkers for structured domain flexibility. However, the past 20 years has seen a dramatic growth in the number of proteins that are completely intrinsically disordered (IDPs) or contain large intrinsically disordered regions (IDRs) (Dunker et al., 2014). IDPs and IDRs have now been shown to play major roles in all aspects of cellular function (Iakoucheva et al., 2002; Namba, 2001; Wright and Dyson, 1999), and it has become apparent that IDRs grant functional advantages distinct from rigid order and are an important part of protein structure.

One key advantage for proteins with IDRs is that their flexibility allows them to more easily adopt multiple conformations. This enables these proteins to interact with multiple protein partners (Cumberworth et al., 2013) or interface with a single protein through multiple points of interaction (Disfani et al., 2012). Proteins with IDRs are able facilitate this through short linear motifs, such as SH3 (Kay et al., 2000). Studies on proteins with IDRs showcase them as chief 'hubs' within different subcellular compartments, using multiple linear motifs within an IDR to interact with a large 'network' of proteins or substrates (Cumberworth et al., 2013; Mosca et al., 2012; Schlessinger et al., 2011). As such, understanding how these intrinsically disordered proteins use multiple motifs to regulate a sub-cellular protein network is important for understanding cell function.

An excellent example of a cellular regulation where proteins often act as network hubs are the enzymes required for protein ubiquitination. Ubiquitin is a post-translational modification that is used to regulate protein degradation, localization and complex formation (Ciechanover, 2006), and is key for regulating nearly all intracellular functions. The conjugation of ubiquitin is catalyzed by a three enzyme cascade, where in a ubiquitin ligase is the final enzyme responsible for substrate targeting and recognition. This process is reversible as well, with the removal of

ubiquitination from substrates facilitated by deubiquitinating enzymes or DUBs (Reyes-Turcu et al., 2009). In this system, ~100 ubiquitin ligases and ~30 DUBS are responsible for regulating ~1000 ubiquitinated substrates at any given time and must be able target a diverse network of proteins in response to different signaling events. As such, it is not surprisingly that a large number of proteins required for ubiquitination have been predicted to contain intrinsically disordered regions (Bhowmick et al., 2013; Rosenbaum et al., 2011). However, little is understood about how IDRs function in ubiquitin ligases and DUBs.

Ubp10 contains two large intrinsically disordered regions

To determine whether Ubp10 was actually intrinsically disordered, I purified recombinant Ubp10 from *E. coli* for structural analysis. To verify that purified Ubp10 was functional, and thus maintaining its normal structure, we next confirmed its activity enzymatically. Recombinant Ubp10 (rUbp10) activity was first tested using an *in vitro* fluorescent DUB assay by Melissa Locke, in which rUbp10 is exposed the ubiquitin bound 7-amido-4-methylcoumarin (Ub-AMC). The florescent AMC molecule is inhibited as long as ubiquitin remains conjugated to it, and only if it the ubiquitin is removed does it then fluoresce. Recombinant Ubp10 was capable of deubiquitinating ubiquitin-conjugated AMC, which is indicated by a significant increase in fluorescent signal (Fig. 3.3). The increase in fluorescence could be inhibited by preincubation of Ubp10 with the DUB inhibitor N-ethylmaleimide (NEM), demonstrating that this increase in florescence was directly due to recombinant Ubp10's enzymatic function.

Next, Melissa Locke tested to see if recombinant Ubp10 was capable of deubiquitinating a natural substrate, ubiquitinated histone H2B. Ubiquitinated histone H2B was purified from yeast, and then exposed to rUbp10. Recombinant Ubp10 was also capable of deubiquitinating histone H2B *in vitro*, and this function could also by inhibited by preincubation of Ubp10 with NEM (Fig. 3.4). Both of these assays demonstrated that purified recombinant Ubp10, enzymatically active, and maintained normal structure sufficient to interact with natural substrates.

Having confirmed purified Ubp10 is functionally active, I collaborated with David Baker's lab at University of Washington to use circular dichroism to identify the α-helical, β-sheet and random coil secondary structure content of Ubp10. In the top graph in figure 3.5, representative

curves can be seen for proteins that are entirely α-helical, β-sheet or random coil. Recombinant Ubp10's spectrum (Fig. 3.5; black line) contains minima at 204 nm and 218 nm, indicative of the known alpha-helical structure in its DUB catalytic domain (Hu et al., 2002). However, when compared to the highly structured alpha-helical protein BSA (Fig. 3.5; gray line), Ubp10's spectra near 200 nm is shifted drastically downward. This is a characteristic of a protein with high degree of random coil (Greenfield, 2006).

Finally, Melissa Locke used limited proteolysis to directly assess Ubp10's intrinsic disorder. Limited proteolysis takes advantage of the greater number of exposed protease cleavage sites in IDRs versus highly structured regions (Fontana et al., 2004). Recombinant Ubp10 or BSA were exposed to trypsin over a time course of 45 minutes. As seen in Figure 3.6, Ubp10 was rapidly degraded with almost no visible full-length protein after 2 minutes of exposure to trypsin. This is in stark contrast to the highly structured protein BSA, which maintained the full-length protein throughout the 45 minute of trypsin digestion.

These data confirm the predictions that Ubp10 contains intrinsically disordered regions. However, it does not yet explain how intrinsic disorder plays a role in Ubp10's function. As discussed earlier in this chapter, proteins that are intrinsically disordered often contain mechanisms for transiently interacting with multiple different proteins (Uversky, 2015). We therefore went forward to identify if Ubp10 contained similar modes of protein interaction.

Ubp10 is predicted to contain binding modules within its intrinsic disorder

In Chapter 2, I demonstrated that Ubp10 was found to be enriched in the nucleolus, where it interacts with multiple different rRNA processing proteins, including those we've directly verified: Cbf5, Nop56, Nop58, Pwp2, Dhr2, and Utp22. While I've shown how Ubp10 is recruited to the nucleolus (Fig 2.15, 2.16), it does not explain why Ubp10 is able to interact with these rRNA processing proteins and whether or not they are required for deubiquitination of Rpa190. Current understanding of Ubp10's structure is only able to account for its interaction with Sir4. An earlier study found that the deletion of residues 94-250 in Ubp10 was sufficient to disrupt its interaction with Sir4 (Gardner et al., 2005), so I thought it likely that similar regions within Ubp10's intrinsic disorder might direct its interaction with the six rRNA processing proteins.

To identify if Ubp10 contained binding modules within its N- and C-terminal regions, I used an algorithm called Anchor, which predicts binding regions within protein intrinsic disorder. It operates on three principles: **(1)** a given residue is within disorder, **(2)** a residue is not predicted to make favorable contacts with other *in cis* local residues, and **(3)** a residue is able to make favorable contacts with an *in trans* globular interactor (Dosztanyi et al., 2009). The results from Anchor predicted twelve total binding modules throughout Ubp10's N- and C-terminal intrinsically disordered regions, ranging in length from 9-38 residues. These regions are shown in Figure 3.7, with the specific modules of binding shown below, and the sequences are listed in Table 3.1.

The binding modules identified by anchor presents a pattern of binding sites separated by linking interval regions. This pattern is similar to others seen in intrinsically disordered proteins that interact with multiple partners, such as yeast ubiquitin ligase San1 (Rosenbaum et al., 2011). San1 was previously shown to contain a similar pattern of binding modules separated by linking interval regions, and uses these sites to recognize exposed hydrophobic regions in misfolded proteins in order to ubiquitinate and target them for degradation. It therefore seemed very likely that Ubp10 was using these binding modules to facilitate protein interactions as well.

Binding modules in Ubp10's intrinsic disorder direct multiple protein interactions.

I next determined whether the predicted binding modules were required for Ubp10's protein interactions. With the aid of Melissa Locke, we assayed three representative proteins previously shown to interact with Ubp10 by the yeast 2-hybrid assay: the silencing protein Sir4 (Gardner et al., 2005; Kahana, 2001), the rRNA DEAD-box helicase Dhr2 (Richardson et al., 2012), and the rRNA processing factor Utp22 (Richardson et al., 2012). I first made short deletions in Ubp10 to remove the predicted binding modules or their separating intervals. Full-length Ubp10 and each deletion mutant of Ubp10 were probed for interaction with Dhr2, Sir4, and Utp22 using the Yeast 2-Hybrid assay.

The resulting Yeast 2-Hybrid (Fig 3.8) identified that Ubp10's predicted binding modules were necessary for its interaction with each protein (Dhr2, Sir4 and Utp22). The identified modules of Ubp10 were not only necessary for each protein interaction, but were unique between all three probed protein interactors. Ubp10 required residues 2-27 to interact with Dhr2, and loss

of these residues did not affect the interaction with Sir4 or Utp22. Likewise, Ubp10 required residues 109-122 and 123-141 to interact with Sir4, and loss of these residues had no effect on interaction with Dhr2 and Utp22. Finally, Ubp10 required residues 171-208 to interact with Utp22, and loss of these residues had no effect on interaction with Dhr2 and Sir4. The binding modules required for each protein interacter are shown in Table 3.2 Thus, each of the three representative Ubp10 interactions is defined by different binding modules within Ubp10's N-terminal IDR.

Having identified unique binding modules within Ubp10 that were required for each interaction, I wanted to determine whether these modules alone were sufficient for interaction with each protein. To test this, I probed for Yeast 2-Hybrid interactions using only the Ubp10 regions spanning residues 2-27, 109-141, or 171-208 to see if those modules alone were capable of interacting with Dhr2, Sir4, and Utp22, respectively. I found that each region of Ubp10 that was required to interact with each protein was also sufficient to drive that interaction by itself (Fig. 3.9). Residues 2-27 of Ubp10 was alone capable of interacting with Dhr2. Residues 109-141 of Ubp10 alone interacted with Sir4. Residues 171-208 of Ubp10 alone interacted with Utp22. Altogether, these results demonstrate that Ubp10 contains a series of binding modules that are both necessary and sufficient for interacting with each partner.

Ubp10 requires the Sir4-binding module for normal telomere silencing.

It was previously e established that Ubp10 is recruited to telomere-proximal regions by the silencing protein Sir4, and this facilitates telomere gene silencing through the deubiquitination of histone H2B (Emre et al., 2005; Gardner et al., 2005). The interaction between Ubp10 and Sir4 could be disrupted by deletion of residues 94-250 of Ubp10 and this reduced telomere gene silencing (Gardner et al., 2005; Kahana and Gottschling, 1999). Because I identified regions 109-122 and 123-141 of Ubp10 as important for Ubp10's interaction with Sir4, I thought it would be likely that deletion of these smaller regions would also lead to loss of silencing at telomeres equivalent to full deletion of *UBP10* (Gardner et al., 2005; Kahana and Gottschling, 1999). To examine telomere silencing, I used a yeast strain that contains the *URA3* gene at the telomere and allows for growth on selective media only when telomere gene silencing is disrupted (Singer et al., 1998). Ubp10 mutants deleted for each of the three identified

binding module regions (2-27, 109-141, and 171-208) were then tested for their ability to grow on plates lacking uracil.

My results confirmed our previous results showing that *ubp10*Δ cells have increased growth due to loss of silencing and that *sir4*Δ mutants show the greatest loss of silencing (Fig. 3.10). Only the Ubp10 mutant with residues 109-141 deleted resulted in loss of telomere gene silencing equivalent to the loss of silencing resulting from deletion of *UBP10* (*ubp10*Δ). These results demonstrate that the Ubp10 binding modules for Sir4 are not only required to coordinate the Ubp10-Sir4 interaction, but are required to direct its functional role in telomere gene silencing as well.

Discussion

In order for cells to function properly, they rely on proteins to be recruited to the correct subcellular locations and to identify appropriate enzymatic targets. Research suggests that intrinsically disordered proteins and protein regions are a common trait among proteins with a larger number of protein partners (Mosca et al., 2012; Uversky, 2015). Conversely, proteins with stable 3D structures tend to have a more limited number of protein partners with stronger interactions (Tompa et al., 2005). Such a case has been shown for protein ubiquitin ligases (Bhowmick et al., 2013; Rosenbaum et al., 2011). Ligases that have strict structure, or utilize complexes, were shown to have a more defined pool of protein targets. However, ubiquitin ligases that contained greater disorder instead had a much broader pool of protein substrates.

The data in this chapter now provides evidence suggesting that Ubp10 requires short amino acid sequences (<30) for several protein-protein interactions within the nucleolus. Earlier in this work, I demonstrated that Ubp10 is localized to the nucleolus and interacts *in-vivo* with several proteins required for rRNA synthesis. Here, I've shown that Ubp10 requires unique binding modules for interaction with two of those proteins, Dhr2 and Utp22. However, it is very likely that Ubp10 uses similar motifs to interact with other ribosomal processing proteins identified as interactors through the mass spectrometry screen. If Ubp10 does interact with several other ribosomal proteins through binding modules, it is possible that several motifs could be shared between those proteins (Ferreon et al., 2013; Tompa et al., 2005). Another possibility is that Ubp10 interacts with a distinct number of processing proteins, and that each binding

module is, in fact, unique to each interaction. However, it is yet unclear why Ubp10 interacts with these proteins, since it has been shown that it does not directly deubiquitinate them. Furthermore, because Rpa190/RNA Polymerase I ubiquitination seems dependent on Ubp10 being enzymatically active, it does not seem likely that Ubp10 is merely scaffolding proteins to direct their function.

One possibility could be that Ubp10 is recruited to the nucleolus as a quality control mechanism and senses protein recruitment and processing during ribosomal RNA synthesis. As discussed in the Chapter 1, RNA Polymerase I elongation is intimately connected with the processing of ribosomal RNA (Albert et al., 2012; Schneider, 2012; Turner et al., 2012). Failure to fold or process actively transcribed ribosomal RNA has been shown to lead to RNA Polymerase I pausing or arrest, and in some cases, early termination. Many of the proteins recruited to ribosomal RNA are essential for processing to proceed correctly (Henras et al., 2008). This places Ubp10 in a critical location to sense or respond to failure of ribosomal RNA processing, RNA Polymerase I pausing, or arresting. Given one of these mechanisms was unable to be mediated, Ubp10 would no longer deubiquitinate Rpa190 and this would lead to the poly-ubiquitination and extraction of RNA Polymerase I.

Much more work needs to be done in order to identify the mechanism responsible for initiating the ubiquitination of Rpa190. Several efforts are currently underway to do this, including inducing RNA Polymerase I pausing and arrest, as well as developing tools to deplete necessary processing proteins, such as Dhr2 and Utp22.

Acknowledgements

Melissa Locke was responsible the experimentation in Figure 3.3, 3.4, and 3.5, as well as for the construct design and experimentation in Figure 3.7.

Much of the data and text in this chapter is included in the following manuscript:
Reed, BJ, Locke, MN, Gardner, RG. A Conserved Deubiquitinating Enzyme Uses Intrinsically Disordered Regions to Scaffold Multiple Protein-Interaction Sites. *In Review.*

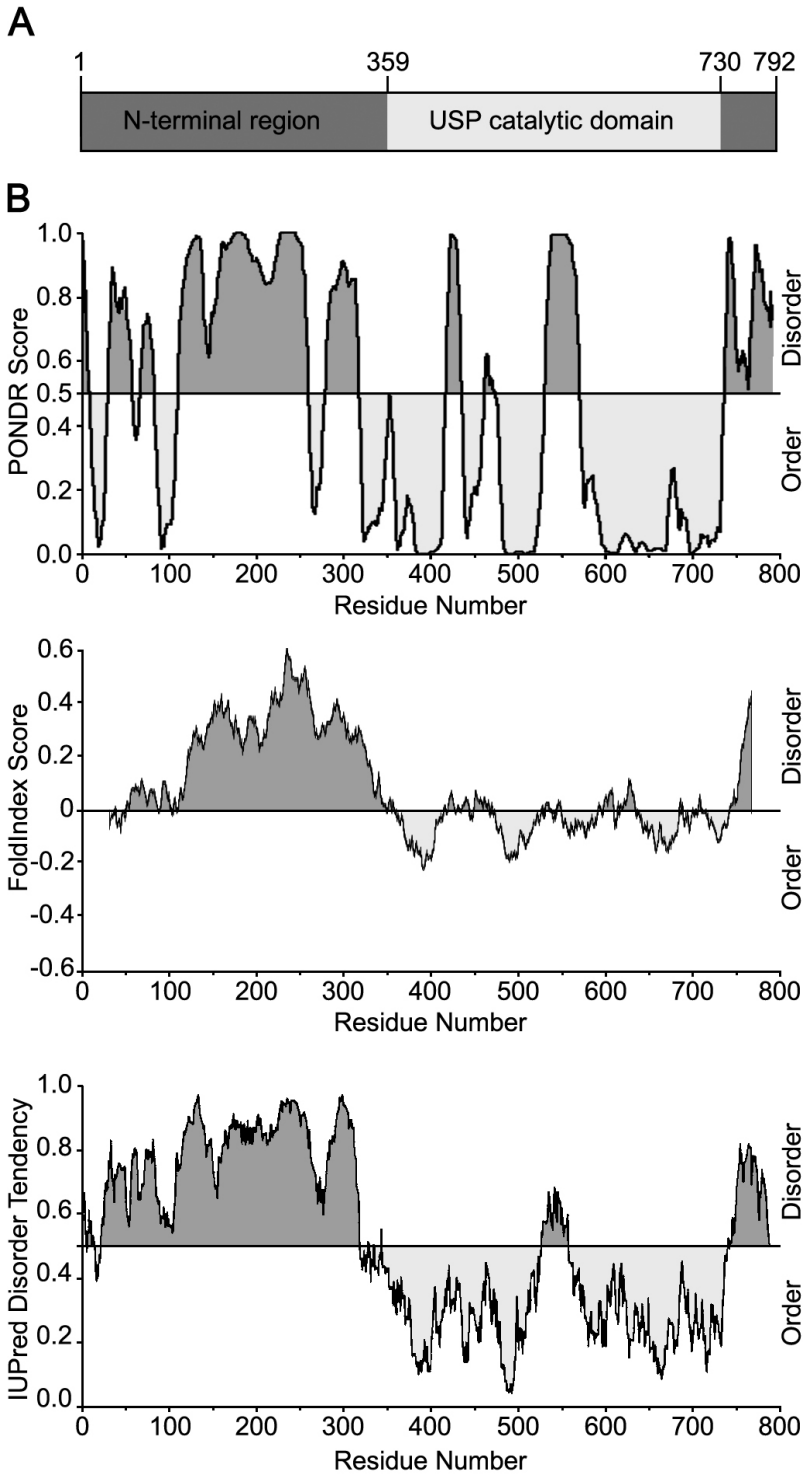

Figure 3.1 – Ubp10 is predicted to contain intrinsically disordered regions. *A,* A schematic representing overall topology of Ubp10. *B,* Disorder predictions of Ubp10. Top panel is PONDR (http://www.pondr.com/). Middle pandel is FoldIndex (http://bip.weizmann.ac.il/fldbin/findex). Bottom panel is IUPred (http://iupred.enzim.hu/index.html). Predicted disordered regions are dark gray and predicted ordered regions are light gray. Ubp10's catalytic domain is within 359-730.

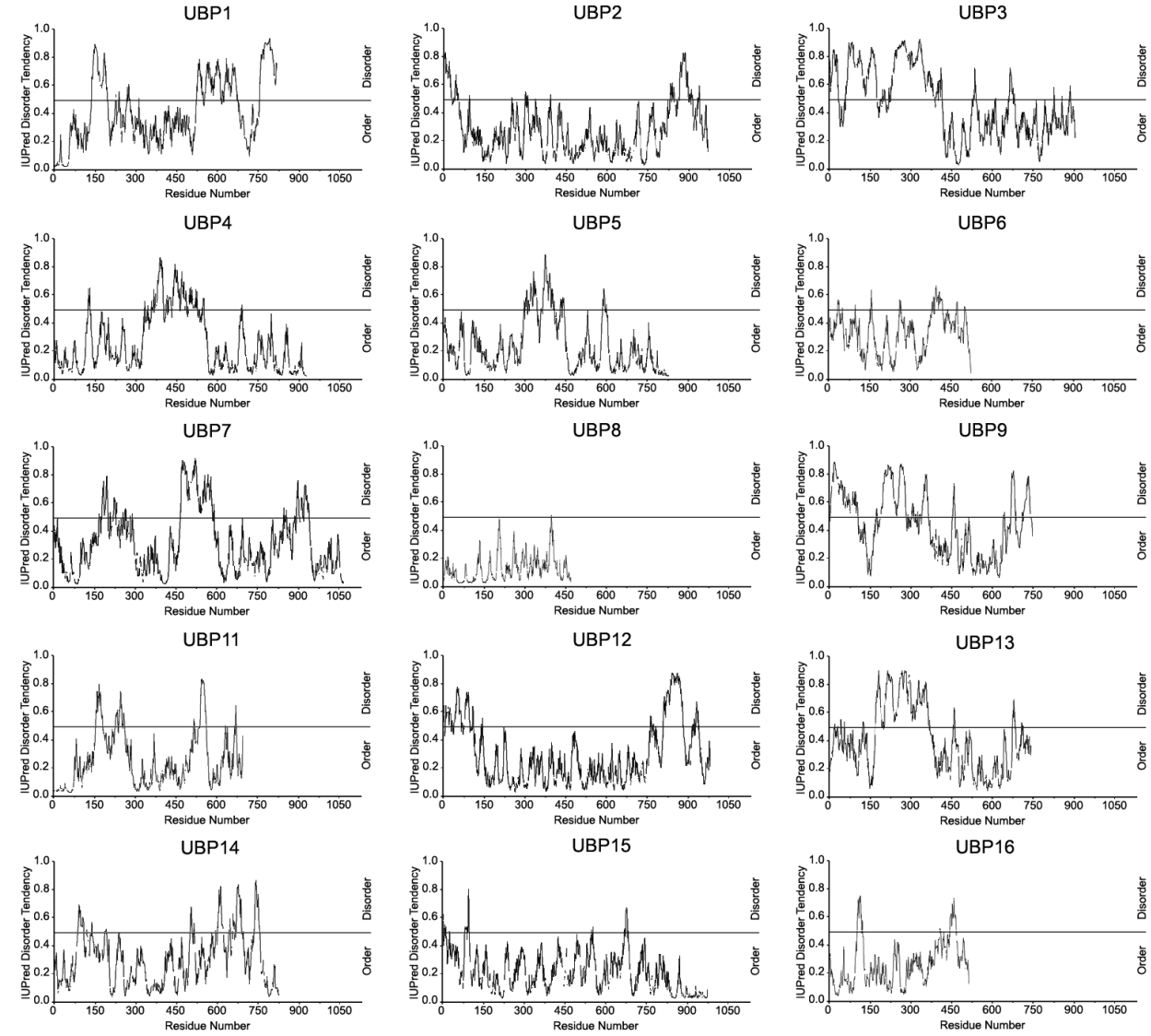

Figure 3.2 – Predicted intrinsic disorder of other yeast UBP deubiquitinases. IUPred (http://iupred.enzim.hu/index.html) intrinsic disorder predictions for all known yeast UBPs deubiquitinases.

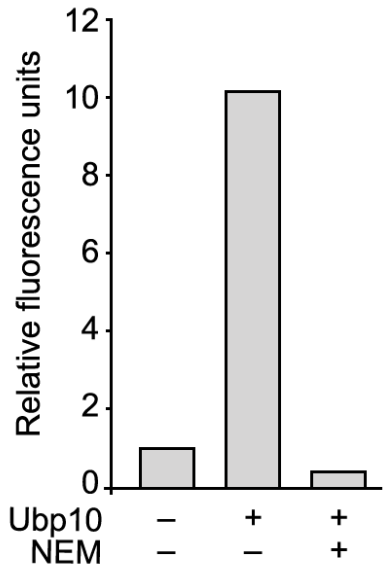

Figure 3.3 – Recombinant Ubp10 is an active DUB based on Ub-AMC assay. Ub-AMC was incubated alone, with Ubp10, or with Ubp10 + 10mM NEM for 40 minutes. Total florescence for each condition was plotted as Relative Florescence Units, which was calculated by normalizing each condition to the florescent signal of Ub-AMC alone.

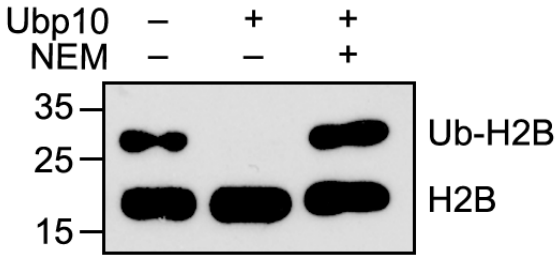

Figure 3.4 – Recombinant Ubp10 is able to deubiquitinate purified ubiquitinated H2b. Ubiquitinated histone H2B was purified from *S. cerevisiae* and incubated alone, with Ubp10, or with Ubp10 + 10mM NEM for 50 minutes. Proteins were separated by SDS-PAGE, transferred to nitrocellulose, and the Western blot was probed with anti-FLAG antibodies.

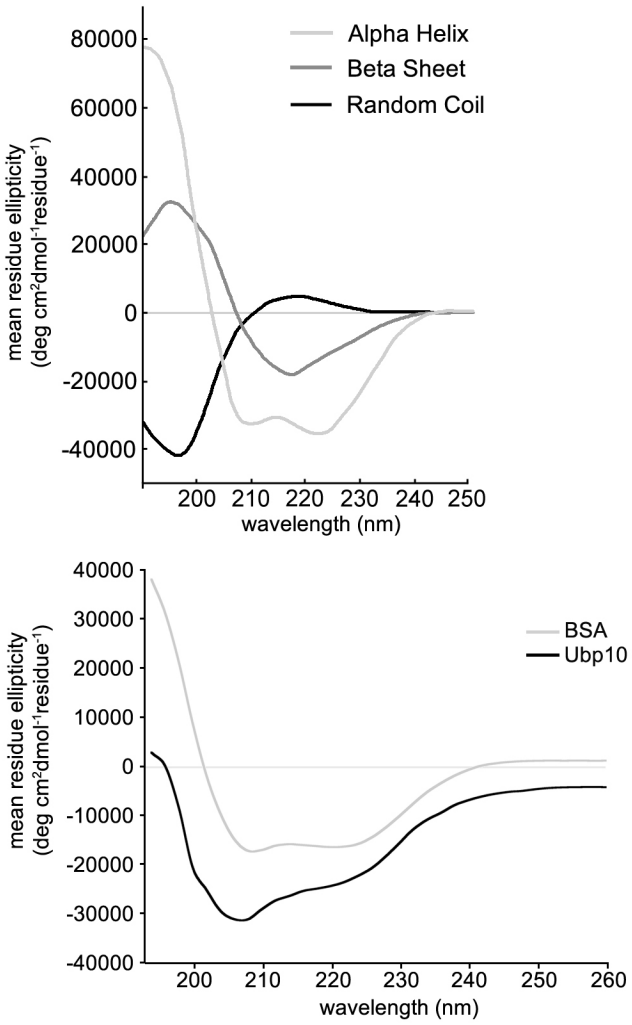

Figure 3.5 – Ubp10's secondary structure contains random coil. *Top*, Representative spectra for proteins that would be entirely α-helical (light gray), β-sheet (medium gray) or random coil (black). *Bottom,* CD spectra of Ubp10 (black) and BSA (gray) were recorded at 0.15 mg/ml for Ubp10 and 0.15 mg/ml for BSA in 50 mM NaCl and 15 mM Na2HPO4, pH 7.3 at 25C.

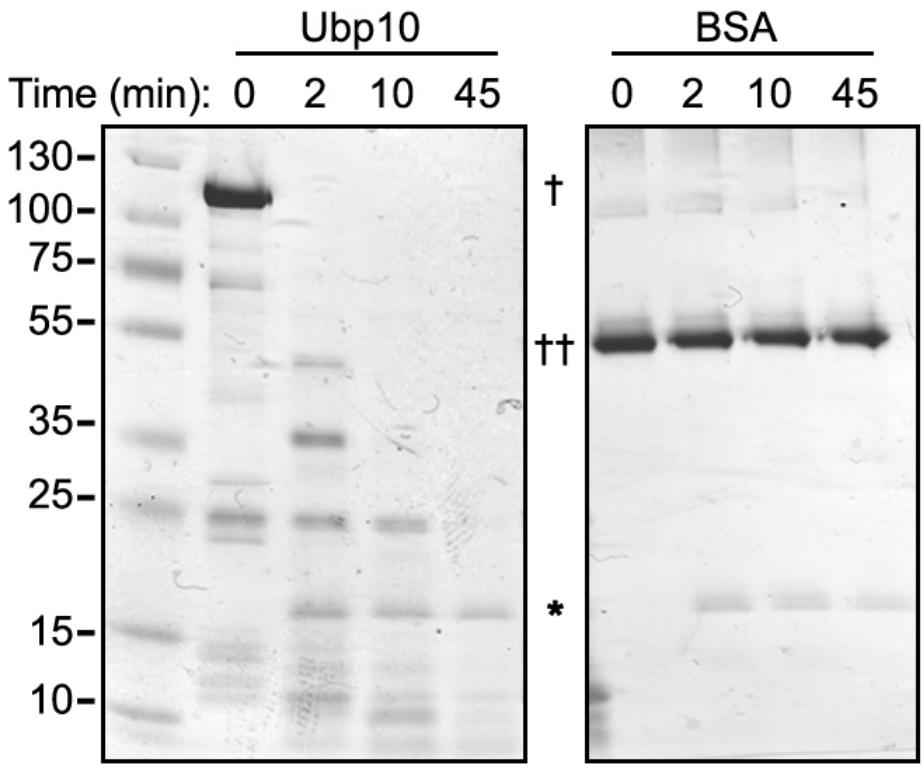

Figure 3.6 – Ubp10 is rapidly degraded when exposed to proteases. Purified Ubp10 or BSA was incubated with trypsin for the indicated times. Proteins were separated by SDS-PAGE and visualized by silver stain. The locations of trypsin (*), Ubp10 (†), and BSA (††) are marked.

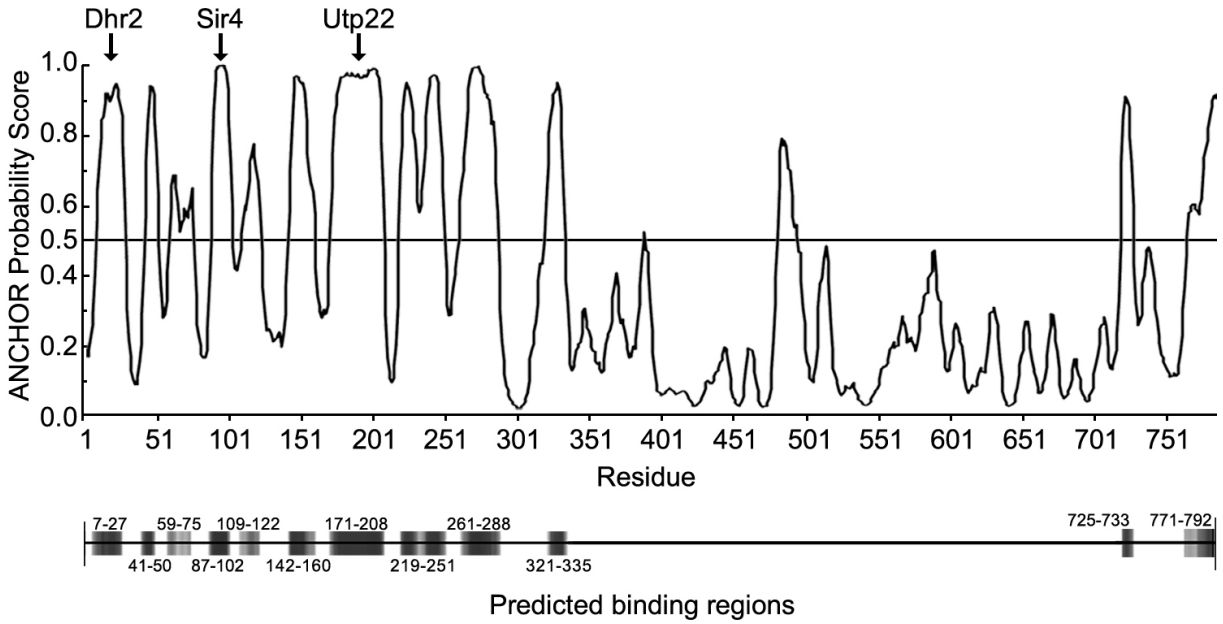

Figure 3.7 – Ubp10 contains a series of predicted binding modules. ANCHOR prediction of binding sites in Ubp10 (http://anchor.enzim.hu/). Arrows above the graph indicate which binding region is required for each protein interaction. Bars below the graph indicate the residues of Ubp10 that comprise each predicted binding module.

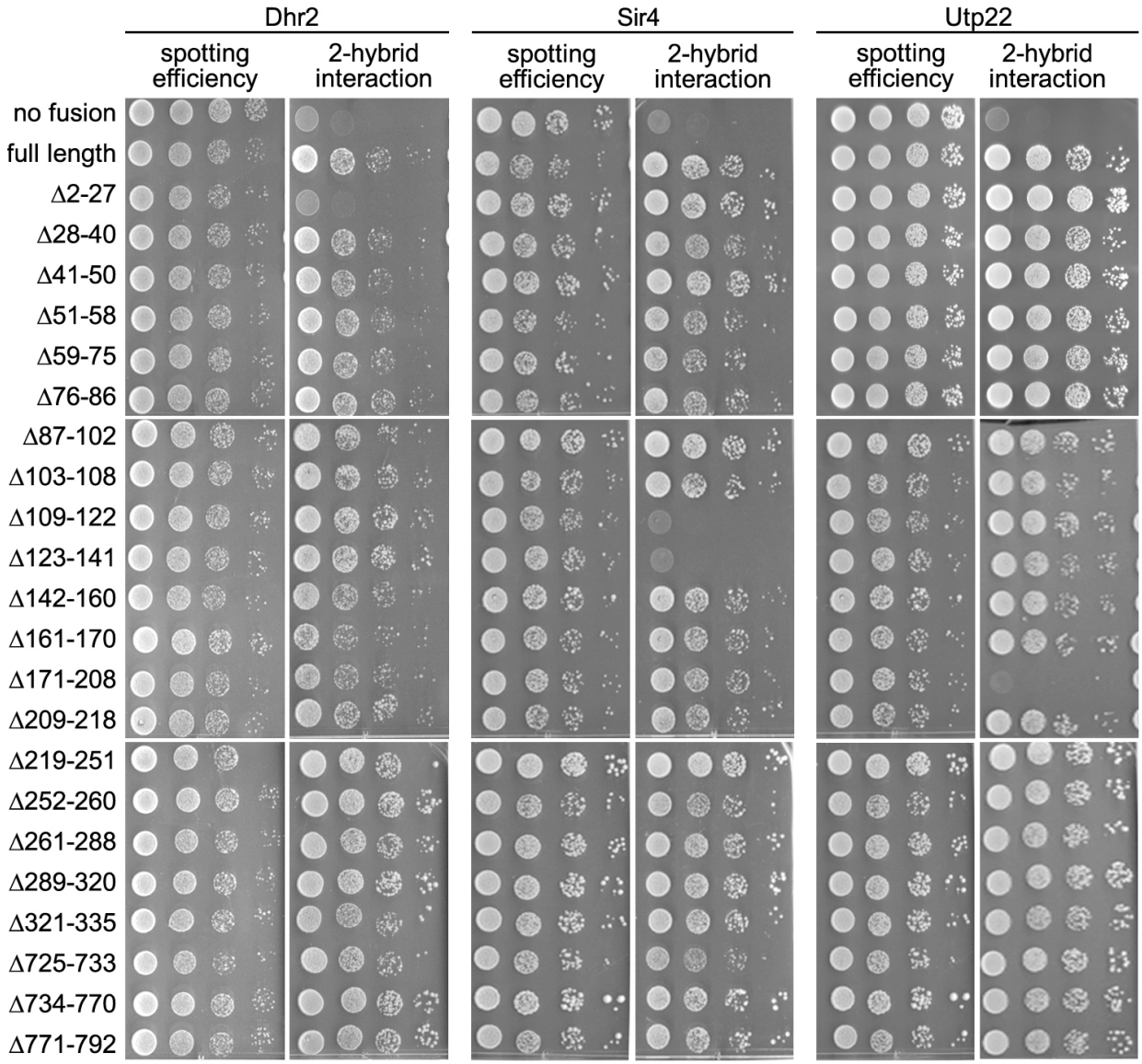

Figure 3.8 – Ubp10 contains unique, necessary binding modules for Dhr2, Sir4 and Utp22. Yeast 2-hybrid (Y2H) interaction assays in cells expressing the indicated Gal4 binding domain (GBD)-Ubp10 deletion variant (left) and Gal4 activation domain (GAD) fusion (top). Cells were spotted onto synthetic media with or without histidine to measure spotting efficiency and the Y2H interaction, respectively.

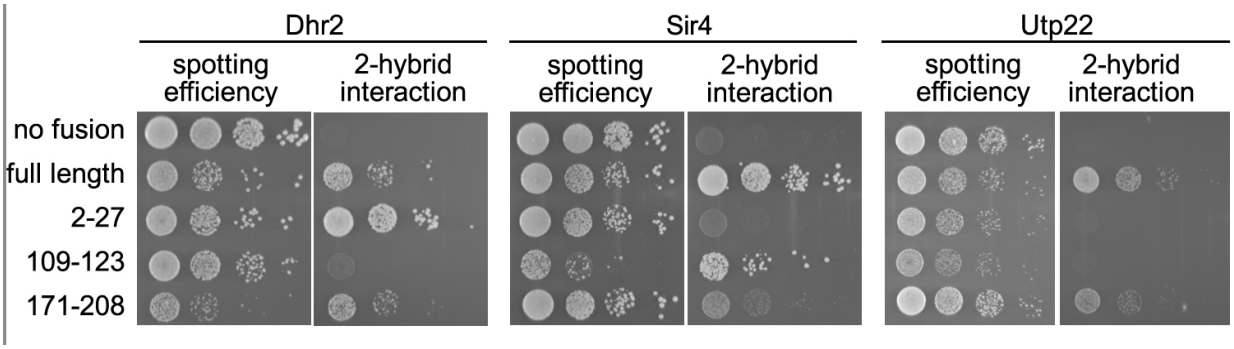

Figure 3.9 – Each unique binding module in Ubp10 are sufficient for interaction with Dhr2, Sir4 and Utp22. Cells expressing full-length GBD-Ubp10 or Ubp10 peptide sequence (left) and the indicated GAD fusion (top) were spotted onto synthetic media with or without histidine to measure spotting efficiency and the Y2H interaction, respectively.

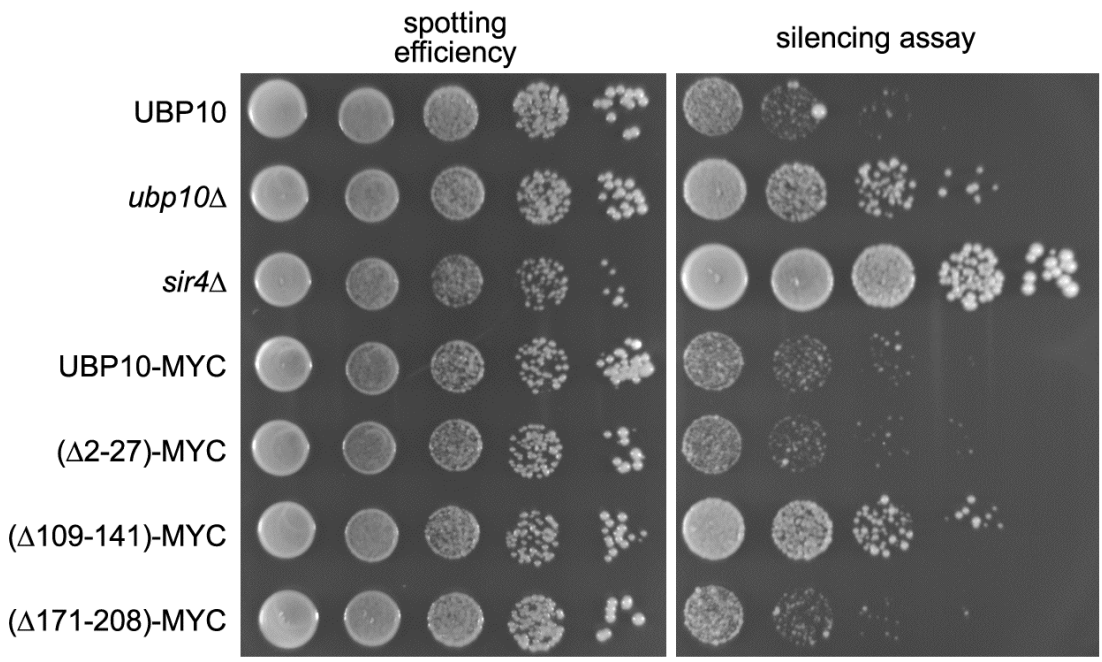

Figure 3.10 – Ubp10's binding region for Sir4 is required for its telomere chromatin silencing function. Yeast cells containing *URA3* near telomere VIIL (Gardner et al., 2005) and the indicated Ubp10 or Sir4 mutants (left) were spotted onto synthetic media with or without uracil to measure spotting efficiency and gene silencing.

Ubp10 - Anchor Sites

Seq #	*Start*	*Sequence*	*Finish*	*Length*
1	7	IKPLVDRILSNPLQFNAAMI	27	20
2	41	NSSYIVIGK	50	9
3	59	AIAATAESKQIKENNL	75	16
4	87	PKSMAEALLLYTSKN	102	15
5	109	TGAKKSAELSTEL	122	13
6	142	EGEIFHEARDYVEPRKAS	160	18
7	171	GEDIGEDIGEDIGEDIGEDIGEDIGENLGSPLATIDD	208	37
8	219	ELSTSISSDDEIEDDEDEDDMDYDSSAMEKEL	251	32
9	261	KISEGEKKSLYQDLMENSTVEVNRYEP	288	27
10	321	PVTISNLSNFYQFN	335	14
11	725	AYYLLYTR	733	8
12	771	KINSKKNNRKKWKKNKKRKFT	792	21

Table 3.1 – Predicted Anchor binding modules within Ubp10's intrinsic Disorder. Peptide sequences identified by Anchor (http://anchor.enzim.hu/) to be predicted binding modules. Columns from left to right: *Seq #*: Binding module number, *Start*: location for first amino acid of identified peptide in Ubp10's sequence, *Sequence:* Identified peptide sequence, *Finish:* location for last amino acid of identified peptide in Ubp10's sequence, *Length*, Peptide length for each binding module.

Interactor	Ubp10 sequence	Sequence location
Dhr2	IKPLVDRILSNPLQFNAAMI	2-27
Sir4	TGAKKSAELSTEL	109-122
Sir4	STEPPSSSSEDDKVGKEEEE	123-141
Utp22	GEDIGEDIGEDIGEDIGEDIGEDIGENLGSPLATIDD	171-208

Table 3.2 – Identified binding modules necessary and sufficient for Ubp10's interaction with Dhr2, Sir4 and Utp22. Protein interactors and their associated Ubp10 binding modules. From left to right: Identified protein interactor, its Ubp10 binding module, and that modules location within Ubp10's sequence.

CHAPTER FOUR:

USP36 IS AN INTRINSICALLY DISORDERED MAMMALIAN DEUBIQUITINASE WITH CONSERVED FUNCTION OF UBP10

Predicted human and *Drosophilia* orthologs of Ubp10

Ubp10 has two predicted orthologs: human DUB USP36 and *Drosophilia* DUB scrawny. USP36 was shown to localize to the nucleolus by a short, basic nucleolar localization signal similar to Ubp10. Recruitment of USP36 is required to regulate nucleolar structure, and more recently, USP36 was shown to deubiquitinate RPA194 to slow its rate of turnover (Endo et al., 2009a; Endo et al., 2009b; Peltonen et al., 2014). Scrawny has been shown to be required to regulate histone H2B ubiquitination and chromatin silencing during *Drosophilia* growth and development (Buszczak et al., 2009), but it has not been implicated in regulating RPA194 turnover.

The identification of both USP36 and scrawny as potential orthologs is based on cellular functions; Ubp10 contains very little sequence identity to either protein outside of its catalytic domain. Global amino acid sequence identity predicts that, while USP36 and scrawny share 26% identity, and 50% similarity (LALIGN, global alignment), Ubp10 only shares 26% identity in catalytic domain between either USP36 or scrawny. Comparisons of their domain structure suggests why this might be the case (Fig 3.1*A,* Fig 4.1*A*, Fig 4.2*A*). While USP36 and scrawny are similar in size and domain composition, Ubp10 looks much different; Ubp10 is roughly 300 amino acids shorter, and with its cysteine protease domain C-terminal, as opposed to USP36/scrawny's N-terminal protease domain.

USP36 and scrawny are predicted to contain intrinsically disordered regions.

One characteristic that all three proteins share, however, is a very similar degree of intrinsic protein disorder. USP36 and scrawny both contain a short N-terminal and a long C-terminal that flank their cysteine protease domain (Fig. 4.1A and Fig 4.2A, respectively), both of which contain no known domains that might explain regulation of their action. When probed with the three independent disorder algorithms (Figure 4.2B: PONDR, FoldIndex and IUPred, top to bottom) USP36's N- and C-terminal regions were consistently predicted to contain ≥87%

intrinsic disorder, very similar to Ubp10's ≥85% (Fig 4.1B). Similarly, scrawny's N- and C-terminal regions consistently predicted to contain ≥75% intrinsic disorder, similar to Ubp10 and USP36. All three deubiquitinases are predicted to contain a highly structured cysteine protease domain, with entirely intrinsically disordered N- and C-terminal arms. Having shown the importance of Ubp10's intrinsic disorder for both its function and maintaining protein-protein interactions, I thought it very likely that the conserved intrinsic disorder between these deubiquitinases was responsible for their conserved function as well.

USP36 is able to compliment Ubp10 in yeast.

In order to test whether that the intrinsic disorder in USP36 was functionally conserved from Ubp10, I first wanted to demonstrate USP36 was capable of complimenting Ubp10 in *ubp10*Δ yeast. If USP36 can be recruited to deubiquitinate the same targets as Ubp10 in yeast it supports our hypothesis that it is functionally conserved. Because RNA polymerase I stability and histone H2B deubiquitination are fundamental to eukaryotes, as well as acted on by Ubp10, I examined whether expression of USP36 from the *UBP10* promoter could restore deubiquitination of yeast Rpa190 and histone H2B in *ubp10*Δ cells. In both cases, I found that expression of USP36 in *ubp10*Δ cells result in decreased ubiquitination of Rpa190 (Fig4.3) and histone H2B (Fig. 4.5), confirming the conservation of function for USP36 in the deubiquitination of these substrates. Cells deleted for *UBP10* have a slow growth phenotype due to reduced levels of Rpa190 that result from increased degradation. Consistent with its ability to rescue the deubiquitination of Rpa190, expression of USP36 rescued the slow growth of *ubp10*Δ cells (Fig. 4.4). On the other hand, expression of USP36 did not rescue the telomere gene silencing defect of *ubp10*Δ cells (Fig. 4.6). This result is consistent with the fact that human cells do not have a homolog of Sir4 and use a different mechanism for gene silencing (Blasco, 2007). It may also explain why rescue of H2B deubiquitination by expression of USP36 in *ubp10*Δ cells was partial (Fig. 4.5). Although Ubp10 deubiquitinates histone H2B in silent regions, it also does so throughout the genome in active regions (Gardner et al., 2005; Schulze et al., 2011). Thus, while the silencing defect could not be rescued by expression of USP36, the active region function for histone H2B deubiquitination could.

USP36 contains a conserved binding module for yeast DHR2

Having established that USP36 shares conserved function and predicted order/disorder with Ubp10, it seemed likely that USP36 would also contain conserved binding modules as well. I probed USP36's protein structure with Anchor and found that there were 17 predicted binding modules ranging from 10-51 residues in length (Fig. 4.7, Table 4.1). USP36 has known roles in ribosome biosynthesis and nucleolar structure (Endo et al., 2009a; Endo et al., 2009b; Peltonen et al., 2014), so I thought it possible that it may interact with nucleolar interactors of Ubp10 as well. I used the Yeast 2-Hybrid assay to examine interactions between human USP36 and yeast Dhr2, Utp22, and Sir4. I found that USP36 interacted with Dhr2, though it did not interact with Utp22 or Sir4 (Fig. 4.8).

A lack of interaction with Sir4 is expected, since human cells do not possess a homolog of Sir4. We could not find a human homolog of Utp22 by sequence identity. Utp22 is thought to play dual roles in yeast, both regulating tRNA export as well as ribosome processing (Eswara et al.). Structural studies have identified a protein with similar structure to Utp22 in mammals that only plays a role in tRNA export (Lin et al.), thus the lack of interaction between USP36 and yeast Utp22 is not surprising. There is a human homolog of Dhr2, DHX33, that was found to interact with USP36 in a global proteomic study of DUB interactions in human cells (Sowa et al., 2009). These results lend confidence to the conservation of interaction between USP36 and yeast Dhr2 in the Yeast 2-Hybrid.

To identify whether USP36 contained a binding module for Dhr2 similar to Ubp10, I created truncations of USP36 to identify which regions of its N- and C-terminal IDRs were required for interaction. As a first start, I deleted the entire N- or C-terminal IDRs of USP36. Only deletion of the N-terminal IDR disrupted the interaction with Dhr2 (Fig 4.9). This region contains two predicted binding modules: residues 27-40 and 49-63. I then made USP36 mutants containing deletions of both of these regions and tested their interaction with Dhr2 by Yeast 2-Hybrid. I found that deletion of residues 49-63 disrupted the interaction with Dhr2 (Fig. 4.10). Together, these results demonstrate that USP36 contains a conserved binding module for Dhr2.

Discussion

Here, I present evidence for the conservation of function and intrinsic disorder between the yeast deubiquitinase Ubp10 and the mammalian deubiquitinase USP36. While USP36 is capable of rescuing *ubp10*Δ phenotypes and has been suggested to be an ortholog of Ubp10 (Buszczak et al., 2009; Richardson et al., 2012), both proteins only share 26% identity within their catalytic cores, and less than 8% identity within their N- and C-terminal regions. Instead, both share a very similar profile of intrinsically disordered regions surrounding their catalytic domain. Within this intrinsic disorder, both proteins are predicted to contain a series of protein binding modules. As both proteins lack a high degree of identity, their shared secondary structure and binding modules are most likely what impart their conserved cellular function (Rost, 2002). This seems to be the case for Ubp10, which requires these unique binding modules, or linear motifs, to coordinate its enzymatic activity. Loss of Ubp10's intrinsically disordered regions results in an increase in ubiquitination of both Rpa190 and histone H2B (data not shown). I directly demonstrated the functional requirement of Ubp10's specific binding modules as well, as loss of the Sir4 binding module leads to impaired chromatin silencing at the telomere.

The conservation of both function and intrinsic disorder between Ubp10 and USP36 in the absence of sequence identity can likely be explained by the ability of linear motifs to be added, removed, or relocated without loss of deubiquitinating function (Disfani et al., 2012; Mészáros et al., 2012). Similarly, mutations in these motifs, or surrounding intrinsic disorder, would be allowed given they maintained interaction with their associated partner, and the flexibility of intrinsic disorder. This would explain why Ubp10's sequence looks so different from USP36. Genetic rearrangements that move both the cysteine protease domain or binding motifs would be allowed, as long as protein interactions and deubiquitinase function are maintained (Mosca et al., 2012). As a result, we find that Ubp10's C-terminal catalytic domain has relocated itself to USP36's amino terminal, and proteins that look very different, but still maintains the same function. Given the evolutionary distance between yeast, and both fruit fly and humans, it is possible that the lengths of each intrinsically disordered arm changed due to loss and/or gain of species-specific binding modules (such as loss of the Sir4-binding region from yeast Ubp10 to human USP36). These linear motifs give great flexibility to changes in the sequence identity of a intrinsically disordered protein, than a highly structured one, giving

different advantages in evolution for intrinsically disordered proteins than proteins with strict 3D structure (Marsh and Teichmann, 2014; Mosca et al., 2012; Schlessinger et al., 2011).

Our results demonstrate the powerful ability to utilize different predictive software in conjunction with molecular biology to identify the structural and functional capabilities of intrinsically disordered proteins. Current methods for studying intrinsically disordered proteins are still lacking (Uversky, 2013). Here, we were able to predict and confirm intrinsic disorder in two evolutionarily conserved proteins that look drastically different by identify and domain composition alone. Identification of these proteins provide new opportunities to understand how intrinsically disordered proteins utilize linear motifs to coordinate protein-protein interactions.

Acknowledgements

Much of the data and text in this chapter is included in the following manuscript:
Reed, BJ, Locke, MN, Gardner, RG. A Conserved Deubiquitinating Enzyme Uses Intrinsically Disordered Regions to Scaffold Multiple Protein-Interaction Sites. *In Review*

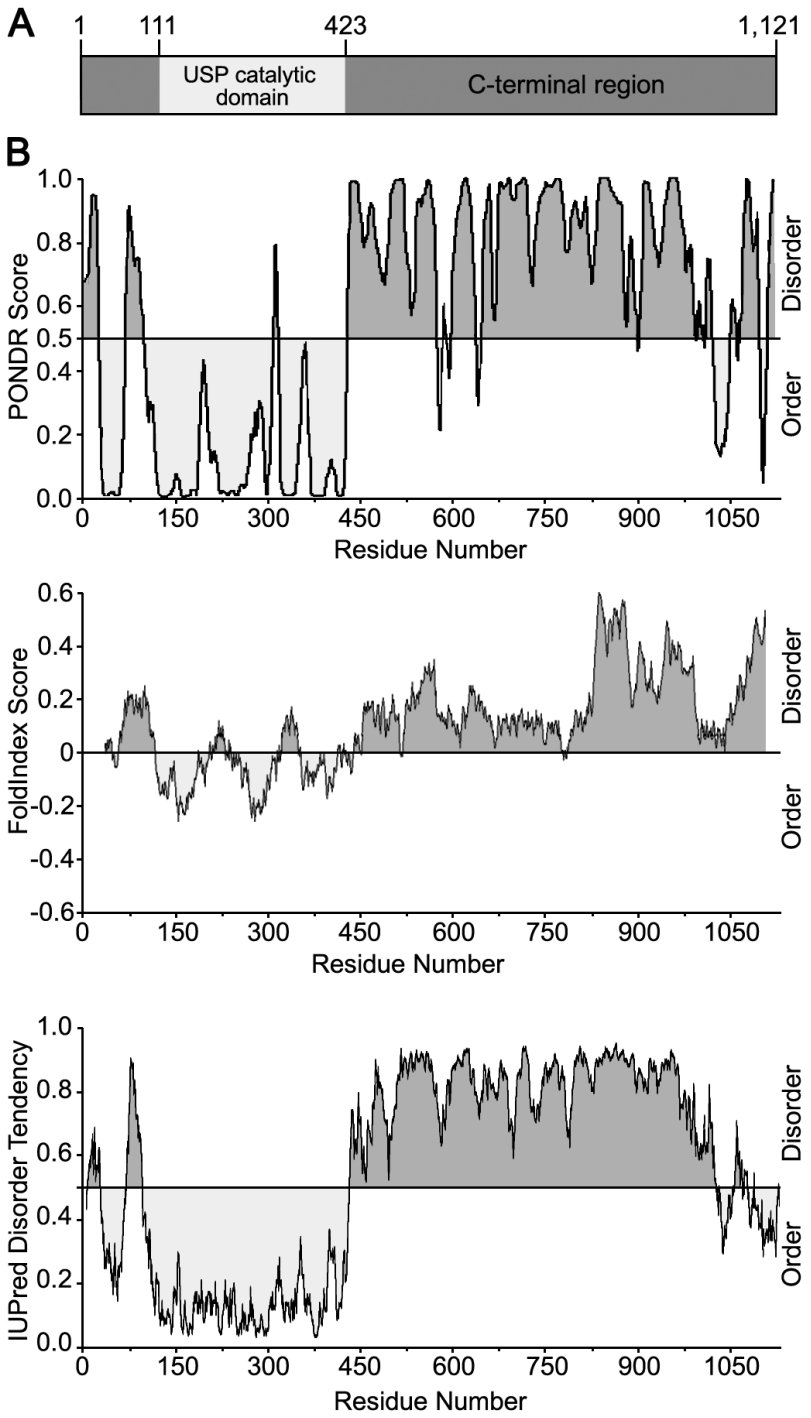

Figure 4.1 – Human USP36 is predicted to be intrinsically disordered. *A,* A schematic representing overall topology of USP36. *B,* Disorder predictions of USP36. Top panel is PONDR (http://www.pondr.com/). Middle panel is FoldIndex (http://bip.weizmann.ac.il/fldbin/findex). Bottom panel is IUPred (http://iupred.enzim.hu/index.html). Predicted disordered regions are dark gray and predicted ordered regions are light gray. USP10's catalytic domain is within 111-423.

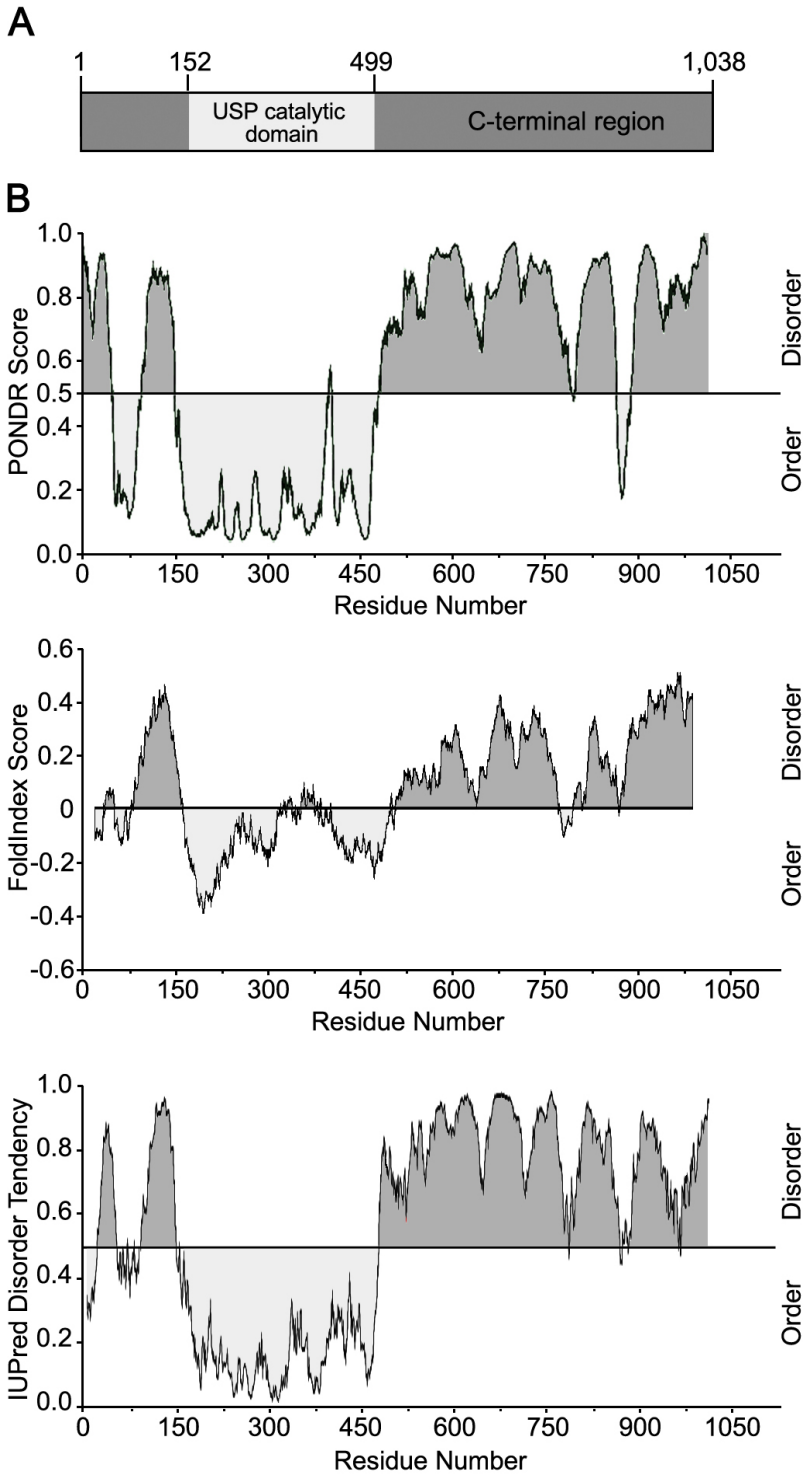

Figure 4.2 – *Drosophilia* scrawny is predicted to be intrinsically disordered. *A,* A schematic representing overall topology of scrawny. *B,* Disorder predictions of scrawny. Top panel is PONDR (http://www.pondr.com/). Middle panel is FoldIndex (http://bip.weizmann.ac.il/fldbin/findex). Bottom panel is IUPred (http://iupred.enzim.hu/index.html). Predicted disordered regions are dark gray and predicted ordered regions are light gray. USP10's catalytic domain is within 152-499.

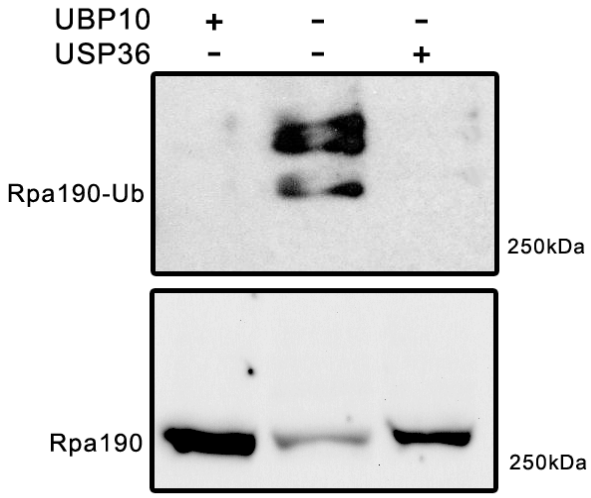

Figure 4.3 – USP36 rescues Rpa190 ubiquitination and steady state in *ubp10*Δ yeast. Ubiquitinated proteomes from UBP10, *ubp10*Δ, and *ubp10*Δ*/USP36* cells were isolated using metal affinity purification. Levels of Rpa190 in lysates (total protein) and eluates (ubiquitinated Rpa190) were determined by western analysis using anti-HA antibodies. Top panel indicates lysates (total protein) and the bottom panel indicated eluates (ubiquitinated Rpa190).

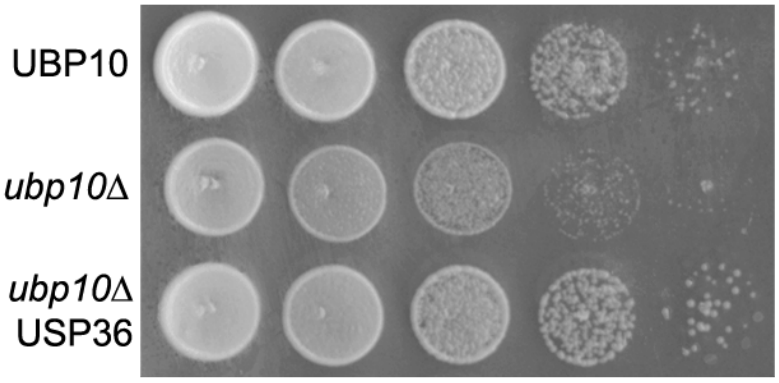

Figure 4.4 – USP36 rescues slow growth in *ubp10*Δ yeast. UBP10 (wt), *ubp10*Δ *(*Δ*)* or *ubp10*Δ*/USP36* cells were spotted at ten-fold serial dilutions onto rich media and incubated for 3 days at 30°C.

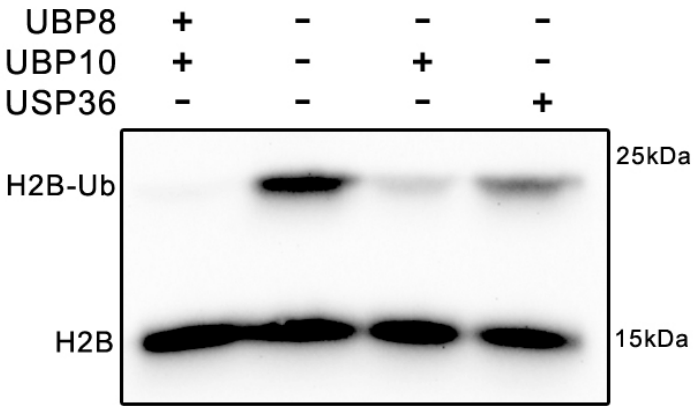

Figure 4.5 – USP36 rescues ubiquitinated histone H2B levels in *ubp10Δ/ubp8Δ* yeast.
UBP10, *ubp8Δ/ubp10Δ*, *ubp8Δ,* and *ubp8Δ/ubp10Δ*/*USP36* cells were lysed in SUMEB, proteins separated by SDS-PAGE, transferred to nitrocellulose, and Western blots probed with anti-FLAG antibodies.

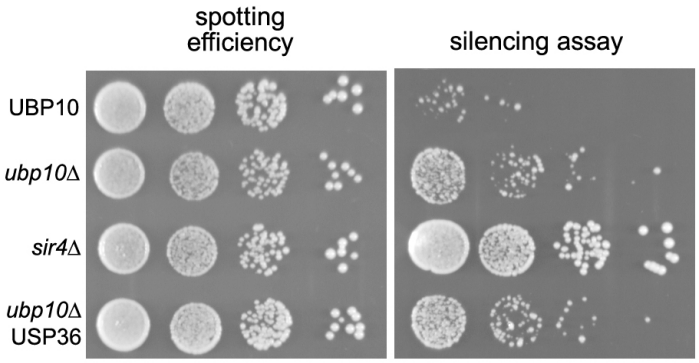

Figure 4.6 – USP36 does not rescue Ubp10's chromatin silencing function in yeast. *UBP10*, *ubp10*Δ*, sir4*Δ*, ubp10*/*UBP10,* and *ubp10*Δ/*USP36* cells expressing *URA3* near telomere VIIL (Gardner et al., 2005) were spotted onto synthetic media with or without uracil to measure spotting efficiency.

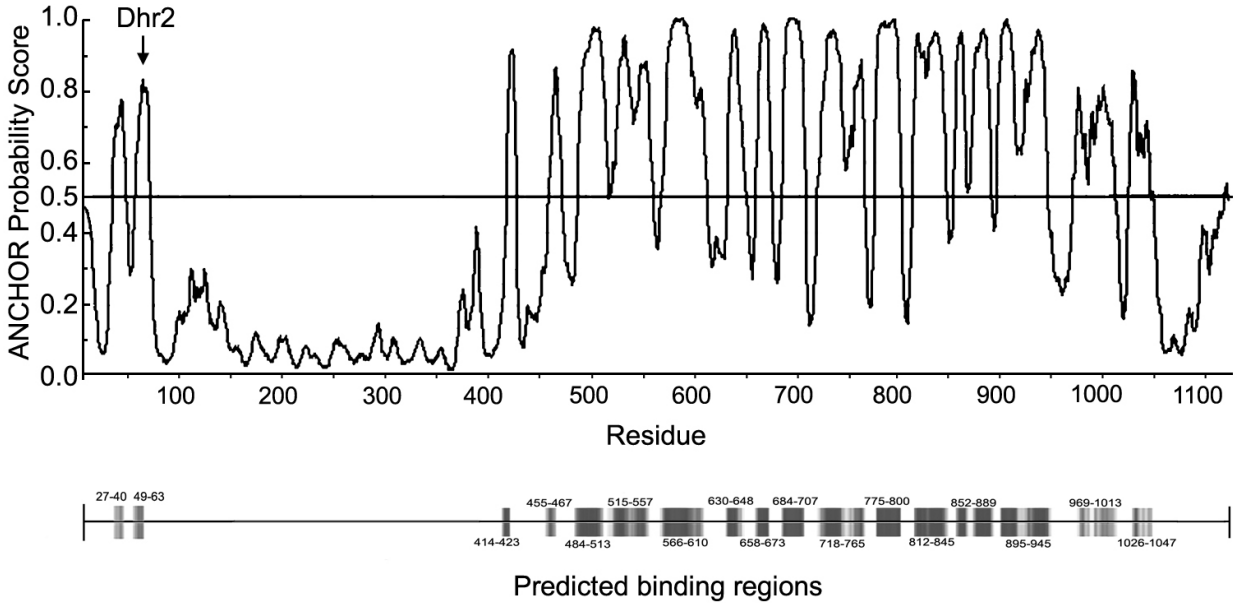

Figure 4.7 – USP36 is predicted to contain a series of binding modules within intrinsic disorder. ANCHOR prediction of binding sites in USP36 (http://anchor.enzim.hu/). Bars below the graph indicate the residues of USP36 associated with each binding module.

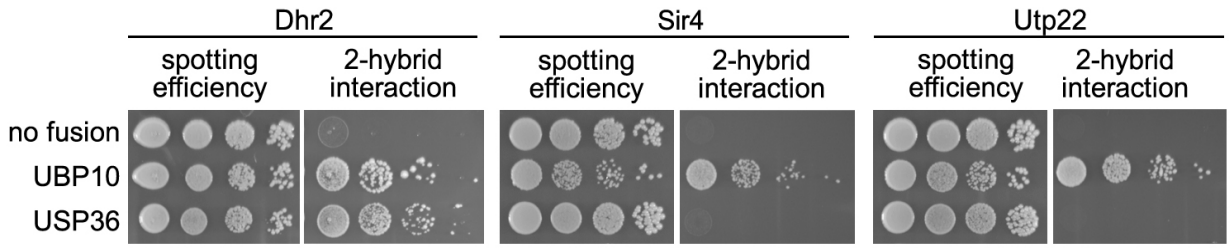

Figure 4.8 – USP36 interacts with yeast Dhr2, but not with Sir4 or Utp22. Y2H interaction assays in cells expressing the indicated GBD-USP36 deletion (left) and GAD fusion (top) were spotted onto synthetic media with or without histidine to measure spotting efficiency and the Y2H interaction, respectively.

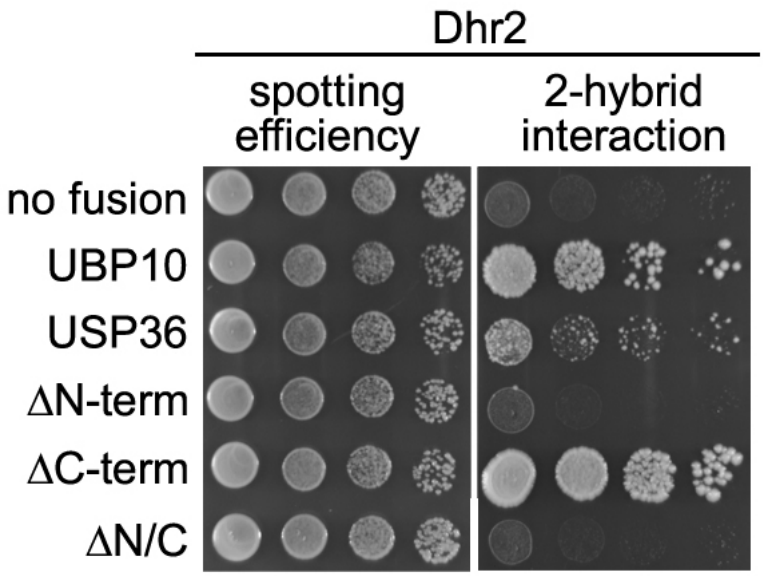

Figure 4.9 – The N-terminal intrinsically disordered region of USP36 is required for it to interact with Dhr2. Y2H interaction assays in cells expressing the indicated GBD-USP36 deletion (left) and GAD fusion (top) were spotted onto synthetic media with or without histidine to measure spotting efficiency and the Y2H interaction, respectively.

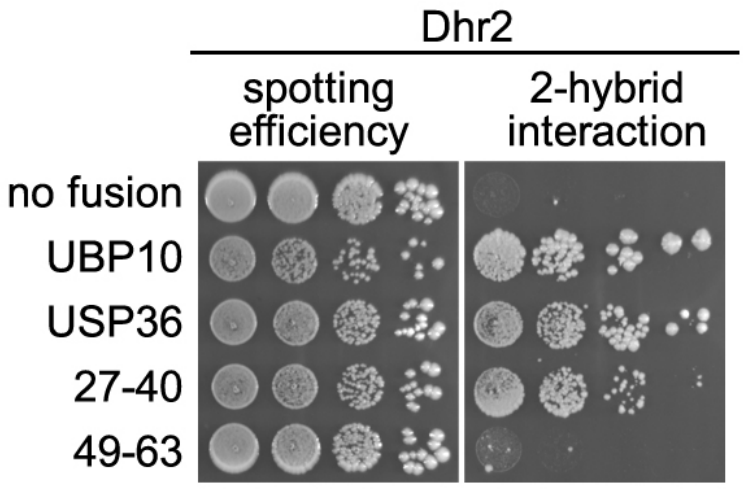

Figure 4.10 – USP36 requires a unique, predicted binding module to interact with Dhr2. Y2H interaction assays in cells expressing the indicated GBD-USP36 deletion (left) and GAD fusion (top) were spotted onto synthetic media with or without histidine to measure spotting efficiency and the Y2H interaction, respectively.

Usp36 - Anchor Sites

Seq #	*Start*	*Sequence*	*Finish*	*Length*
1	27	LLASSAKKVLLQK	40	13
2	49	FSYQLEALKSKYVL	63	14
3	414	QAYVLFYLR	423	9
4	455	KNIGNGIISSPL	467	12
5	484	EIGVPISRNGSTLGLKSQNGCIPPKLPSG	513	29
6	515	SPKLSQTPTHMPTILDDPGKKVKKPAPPQHFSPRTAQGLPGT	557	42
7	566	SQRQGSWDSRDVVLSTSPKLLATATANGHGLKGNDESAGLDRRG	610	44
8	630	PRSGAAHLCDSQETNCST	648	18
9	658	ADSKTVKLKSPVLSN	673	15
10	684	PPAKKLALSAKKASTLWRATGND	707	23
11	718	LTHPMKTSHPVVASTWPVHRARAVSPAPQSSSRLQPPFSPHPTLLSS	765	47
12	775	RSCSSISTALPQVNEDLVSLPHQLP	800	25
13	812	RKKTFVGEPQRLGSETRLPQHIREATAAPHGKR	845	33
14	852	PEDTAASALQEGQTQRQPGSPMYRREGQAQLPAVRRQ	889	37
15	895	QVNGQQVGCVTDGHHASSRKRRRKGAEGLGEEGGLHQDPLRHSCSPMGDG	945	50
16	969	VEEDGHLKCPRSAKPQDAVVPESSSCAPSANGWCPGDRMGLSQA	1013	44
17	1026	VQELLKYSSDKAYGRKVLTWD	1047	21

Table 4.1 – Anchor predicted binding modules within USP36's intrinsic disorder. Peptide sequences identified by Anchor (http://anchor.enzim.hu/) to be predicted binding modules. Columns from left to right: *Seq #*: Binding module number, *Start*: location for first amino acid of identified peptide in USP36's sequence, *Sequence:* Identified peptide sequence, *Finish:* location for last amino acid of identified peptide in USP36's sequence, *Length*, Peptide length for each binding module.

CHAPTER FIVE:

CONCLUSIONS

When I first started this work, I had set out to identify new mechanisms for regulating RNA Polymerase I during rRNA transcription. There was an identifiable gap in our understanding of ribosome biogenesis, which was that while there was so much known about the regulators of induction for ribosomal RNA synthesis, much information was incomplete about the quality control mechanisms that mediated failure of RNA Polymerase I. Work over the past several years has developed this substantially, by identifying several internal and external proteins which mediate RNA Polymerase I elongation. These proteins allow RNA Polymerase I to overcome minor kinetic barriers. However, none of these mechanisms are sufficient to mediate major failures, which may require extraction of RNA Polymerase I from the chromatin.

Overall, the research in this dissertation has introduced a new mechanism of regulation for how RNA Polymerase I levels are controlled post-translationally. In understanding how RNA Polymerase I functions, this provides a mechanism for how failed RNA Polymerase I may be extracted from the chromatin. Having demonstrated that ubiquitination occurs on chromatin, is not required for function, and leads to the destruction, it seems very likely that this ubiquitination event is use to regulate a quality control event, or failure, of RNA Polymerase I. Given that similar events have been observed for ubiquitination or RNA Polymerase II, this seems very likely.

Particularly more abstract, but more fascinating, is the importance of proteins networks that regulate ubiquitination of RNA Polymerase I. As discussed earlier, the landscape associated with ribosomal RNA synthesis is made up of over 200 required proteins. When this stoichiometry is off, it leads to failures in ribosomal synthesis. In the case of some proteins, such as RPL5 (Dai and Lu, 2004) and RPL11(Bhat et al., 2004; Zhang et al., 2003) in mammals, incorrect stoichiometry can signal a major cellular failure and trigger cell death. As such, the nucleolus is filled with an incredibly complex cellular network that must precisely work together in order to successfully function.

This is why the identification of both yeast Ubp10 and human USP36 as conserved, intrinsically disordered proteins is so interesting. While research into intrinsic protein disorder is still in its youth, a consistency that has arise out of the research is that these disordered proteins

are capable of interacting with a much broader number of proteins than proteins with stricter structure (Uversky, 2015). In fact, some research suggests that intrinsically disordered proteins exist as 'hubs' within a greater protein network: working to coordinate, sense, or scaffold (Mosca et al., 2012). As both Ubp10 and USP36 have been found to exist within one of the most complex protein networks, what role is theirs within this 'network hub'? RNA Polymerase I elongation and ribosomal RNA processing have been suggested to be directly interconnected, so it seems very likely that both Ubp10 and USP36 are working to monitor that both the polymerase and ribosomal processing is proceeding functionally, together. Confirmation of this hypothesis does require more work and is currently under investigation within the Gardner lab.

A final interesting conjecture that has arisen from this work is the identification of two proteins, both yeast Ubp10 and human USP36, who have such similar functions with such different sequence identities. In many cases such as this, their conservation of function could be ascribed to their shared rigid structure. I would argue that their shared intrinsic disorder grants them the same conservation of function. It has now been shown in several informatics studies that conservation of intrinsic disorder is no easy task (Marsh and Teichmann, 2014; Mosca et al., 2012). Proteins with conserved intrinsic disorder must evolve without disrupting disorder while still maintaining functional motifs and protein interactions. These requirements are understandably different from those imposed on proteins with rigid structure. What does this mean for our understanding of protein identity? Much of our work on sequence identity has been based off proteins with identifiable structure. Even in the case presented here, the conserved binding module Ubp10 and Usp36 share for Dhr2 are drastically varied in sequence identity. These points highlight the importance of better understanding how intrinsically disordered proteins function in comparison to structured proteins, and how that difference in function changes their course for evolution.

Final Remarks

This research begun as a journey to identify mechanisms that regulated RNA Polymerase I function. However, it evolved into learning about the importance of intrinsic disorder, and understanding how intrinsic disorder may regulate or function within a larger protein network. In the beginning I could not have anticipated that change in perspective or where the work would lead. However, it has reminded me that many times in trying understanding the unknown we

may find something that, at the time, makes no sense. My experiences during this project now lead me to understand that it is important to always be open to new discoveries, and new experiences, because those lead to the most interesting places. I encourage everyone else to stay determined, stay excited, and do the same.

REFERENCES

Albert, B., Perez-Fernandez, J., Leger-Silvestre, I., and Gadal, O. (2012). Regulation of ribosomal RNA production by RNA polymerase I: does elongation come first? Genet Res Int *2012*, 276948.

Amerik, A.Y., and Hochstrasser, M. (2004). Mechanism and function of deubiquitinating enzymes. Biochim Biophys Acta *1695*, 189-207.

Anindya, R., Aygun, O., and Svejstrup, J.Q. (2007). Damage-induced ubiquitylation of human RNA polymerase II by the ubiquitin ligase Nedd4, but not Cockayne syndrome proteins or BRCA1. Mol Cell *28*, 386-397.

Baek, K.H. (2003). Conjugation and deconjugation of ubiquitin regulating the destiny of proteins. Exp Mol Med *35*, 1-7.

Beckouet, F., Labarre-Mariotte, S., Albert, B., Imazawa, Y., Werner, M., Gadal, O., Nogi, Y., and Thuriaux, P. (2008). Two RNA polymerase I subunits control the binding and release of Rrn3 during transcription. Mol Cell Biol *28*, 1596-1605.

Bedwell, G.J., Appling, F.D., Anderson, S.J., and Schneider, D.A. (2012). Efficient transcription by RNA polymerase I using recombinant core factor. Gene *492*, 94-99.

Bernstein, K.A., Gallagher, J.E.G., Mitchell, B.M., Granneman, S., and Baserga, S.J. (2004). The Small-Subunit Processome Is a Ribosome Assembly Intermediate. Eukaryotic Cell *3*, 1619-1626.

Bhat, K.P., Itahana, K., Jin, A., and Zhang, Y. (2004). Essential role of ribosomal protein L11 in mediating growth inhibition-induced p53 activation. EMBO J *23*, 2402-2412.

Bhowmick, P., Pancsa, R., Guharoy, M., and Tompa, P. (2013). Functional Diversity and Structural Disorder in the Human Ubiquitination Pathway. PLoS ONE *8*, e65443.

Blasco, M.A. (2007). The epigenetic regulation of mammalian telomeres. Nat Rev Genet *8*, 299-309.

Buszczak, M., Paterno, S., and Spradling, A.C. (2009). Drosophila stem cells share a common requirement for the histone H2B ubiquitin protease scrawny. Science *323*, 248-251.

Choe, S.Y., Schultz, M.C., and Reeder, R.H. (1992). In vitro definition of the yeast RNA polymerase I promoter. Nucleic Acids Res *20*, 279-285.

Ciechanover, A. (2006). The ubiquitin proteolytic system: from a vague idea, through basic mechanisms, and onto human diseases and drug targeting. Neurology *66*, S7-19.

Colley, A., Beggs, J.D., Tollervey, D., and Lafontaine, D.L.J. (2000). Dhr1p, a Putative DEAH-Box RNA Helicase, Is Associated with the Box C+D snoRNP U3. Molecular and Cellular Biology *20*, 7238-7246.

Cumberworth, A., Lamour, G., Babu, M.M., and Gsponer, J.r. (2013). Promiscuity as a functional trait: intrinsically disordered regions as central players of interactomes. Biochemical Journal *454*, 361-369.

Dai, M.S., and Lu, H. (2004). Inhibition of MDM2-mediated p53 ubiquitination and degradation by ribosomal protein L5. J Biol Chem *279*, 44475-44482.

Dang, L.C., Melandri, F.D., and Stein, R.L. (1998). Kinetic and Mechanistic Studies on the Hydrolysis of Ubiquitin C-Terminal 7-Amido-4-Methylcoumarin by Deubiquitinating Enzymes. Biochemistry *37*, 1868-1879.

Disfani, F.M., Hsu, W.L., Mizianty, M.J., Oldfield, C.J., Xue, B., Dunker, A.K., Uversky, V.N., and Kurgan, L. (2012). MoRFpred, a computational tool for sequence-based prediction and characterization of short disorder-to-order transitioning binding regions in proteins. Bioinformatics *28*, i75-83.

Dosztanyi, Z., Csizmok, V., Tompa, P., and Simon, I. (2005). IUPred: web server for the prediction of intrinsically unstructured regions of proteins based on estimated energy content. Bioinformatics *21*, 3433-3434.

Dosztanyi, Z., Meszaros, B., and Simon, I. (2009). ANCHOR: web server for predicting protein binding regions in disordered proteins. Bioinformatics *25*, 2745-2746.

Dragon, F., Gallagher, J.E., Compagnone-Post, P.A., Mitchell, B.M., Porwancher, K.A., Wehner, K.A., Wormsley, S., Settlage, R.E., Shabanowitz, J., Osheim, Y.*, et al.* (2002). A large nucleolar U3 ribonucleoprotein required for 18S ribosomal RNA biogenesis. Nature *417*, 967-970.

Drygin, D., Rice, W.G., and Grummt, I. (2010). The RNA Polymerase I Transcription Machinery: An Emerging Target for the Treatment of Cancer. Annual Review of Pharmacology and Toxicology *50*, 131-156.

Dunker, A.K., Bondos, S.E., Huang, F., and Oldfield, C.J. (2014). Intrinsically disordered proteins and multicellular organisms. Semin Cell Dev Biol.

Emmerich, C.H., Schmukle, A.C., and Walczak, H. (2011). The emerging role of linear ubiquitination in cell signaling. Sci Signal *4*, re5.

Emmott, E., and Hiscox, J.A. (2009). Nucleolar targeting: the hub of the matter, Vol 10.

Emre, N.C., Ingvarsdottir, K., Wyce, A., Wood, A., Krogan, N.J., Henry, K.W., Li, K., Marmorstein, R., Greenblatt, J.F., Shilatifard, A., and Berger, S.L. (2005). Maintenance of low histone ubiquitiylation by Ubp10p correlates with telomere-proximal Sir2 association and gene silencing. Molecular Cell *17*, 585-594.

Endo, A., Kitamura, N., and Komada, M. (2009a). Nucleophosmin/B23 regulates ubiquitin dynamics in nucleoli by recruiting deubiquitylating enzyme USP36. J Biol Chem *284*, 27918-27923.

Endo, A., Matsumoto, M., Inada, T., Yamamoto, A., Nakayama, K.I., Kitamura, N., and Komada, M. (2009b). Nucleolar structure and function are regulated by the deubiquitylating enzyme USP36. J Cell Sci *122*, 678-686.

Esser, C., Alberti, S., and Hohfeld, J. (2004). Cooperation of molecular chaperones with the ubiquitin/proteasome system. Biochim Biophys Acta *1695*, 171-188.

Eswara, M.B.K., Clayton, A., and Mangroo, D. Utp22p acts in concert with Utp8p to channel aminoacyl-tRNA from the nucleolus to the nuclear tRNA export receptor Los1p but not Msn5p. Biochemistry and Cell Biology *90*, 731-749.

Feklistov, A. (2013). RNA polymerase: in search of promoters. Annals of the New York Academy of Sciences *1293*, 25-32.

Feng, Q., Wang, H., Ng, H.H., Erdjument-Bromage, H., Tempst, P., Struhl, K., and Zhang, Y. (2002). Methylation of H3-lysine 79 is mediated by a new family of HMTases without a SET domain. Curr Biol *12*, 1052-1058.

Ferreon, A.C.M., Ferreon, J.C., Wright, P.E., and Deniz, A.A. (2013). Modulation of allostery by protein intrinsic disorder. Nature *498*, 390-394.

Finley, D., Ozkaynak, E., and Varshavsky, A. (1987). The yeast polyubiquitin gene is essential for resistance to high temperatures, starvation, and other stresses. Cell *48*, 1035-1046.

Fontana, A., de Laureto, P.P., Spolaore, B., Frare, E., Picotti, P., and Zambonin, M. (2004). Probing protein structure by limited proteolysis. Acta Biochim Pol *51*, 299-321.

Fredrickson, E.K., and Gardner, R.G. (2012). Selective destruction of abnormal proteins by ubiquitin-mediated protein quality control degradation. Semin Cell Dev Biol *23*, 530-537.

Gallagher, J.E., Dunbar, D.A., Granneman, S., Mitchell, B.M., Osheim, Y., Beyer, A.L., and Baserga, S.J. (2004). RNA polymerase I transcription and pre-rRNA processing are linked by specific SSU processome components. Genes Dev *18*, 2506-2517.

Gallego-Sanchez, A., Andres, S., Conde, F., San-Segundo, P.A., and Bueno, A. (2012). Reversal of PCNA Ubiquitylation by Ubp10 in *Saccharomyces cerevisiae*. PLoS Genet *8*, e1002826.

Ganley, A.R.D., and Kobayashi, T. (2014). Ribosomal DNA and cellular senescence: new evidence supporting the connection between rDNA and aging, Vol 14.

Gardner, R.G., Nelson, Z.W., and Gottschling, D.E. (2005). Ubp10/Dot4p regulates the persistence of ubiquitinated histone H2B: distinct roles in telomeric silencing and general chromatin. Mol Cell Biol *25*, 6123-6139.

Graifer, D., and Karpova, G. (2014). Roles of ribosomal proteins in the functioning of translational machinery of eukaryotes. Biochimie *109*, 1-17.

Grandi, P., Rybin, V., Bassler, J., Petfalski, E., Strauss, D., Marzioch, M., Schafer, T., Kuster, B., Tschochner, H., Tollervey, D*., et al.* (2002). 90S pre-ribosomes include the 35S pre-rRNA, the U3 snoRNP, and 40S subunit processing factors but predominantly lack 60S synthesis factors. Mol Cell *10*, 105-115.

Greenfield, N.J. (2006). Using circular dichroism spectra to estimate protein secondary structure. Nat Protoc *1*, 2876-2890.

Guthrie, C., and Fink, G.R. (1991). Guide to yeast genetics and molecular biology. Methods Enzymol *194*, 1-863.

Ha, C.W., and Huh, W.-K. (2010). Rapamycin increases rDNA stability by enhancing association of Sir2 with rDNA in Saccharomyces cerevisiae. Nucleic Acids Research *39*, 1336-1350.

Ha, C.W., Sung, M.-K., and Huh, W.-K. (2012). Nsi1 plays a significant role in the silencing of ribosomal DNA in Saccharomyces cerevisiae. Nucleic Acids Research *40*, 4892-4903.

Harreman, M., Taschner, M., Sigurdsson, S., Anindya, R., Reid, J., Somesh, B., Kong, S.E., Banks, C.A., Conaway, R.C., Conaway, J.W., and Svejstrup, J.Q. (2009). Distinct ubiquitin ligases act sequentially for RNA polymerase II polyubiquitylation. Proc Natl Acad Sci U S A.

Henras, A.K., Soudet, J., Gerus, M., Lebaron, S., Caizergues-Ferrer, M., Mougin, A., and Henry, Y. (2008). The post-transcriptional steps of eukaryotic ribosome biogenesis. Cell Mol Life Sci *65*, 2334-2359.

Hochstrasser, M. (1996). Ubiquitin-dependent protein degradation. Annu Rev Genet *30*, 405-439.

Hoppe, S., Bierhoff, H., Cado, I., Weber, A., Tiebe, M., Grummt, I., and Voit, R. (2009). AMP-activated protein kinase adapts rRNA synthesis to cellular energy supply. Proceedings of the National Academy of Sciences *106*, 17781-17786.

Hu, M., Li, P., Li, M., Li, W., Yao, T., Wu, J., Gu, W., Cohen, R., and Shi, Y. (2002). Crystal structure of a UBP-family deubiquitinating enzyme in isolation and in complex with ubiquitin aldehyde. Cell *111*, 1041-1054.

Huibregtse, J.M., Yang, J.C., and Beaudenon, S.L. (1997). The large subunit of RNA polymerase II is a substrate of the Rsp5 ubiquitin-protein ligase. Proc Natl Acad Sci U S A *94*, 3656-3661.

Iakoucheva, L.M., Brown, C.J., Lawson, J.D., Obradovi*ƒ*á, Z., and Dunker, A.K. (2002). Intrinsic Disorder in Cell-signaling and Cancer-associated Proteins. Journal of Molecular Biology *323*, 573-584.

Kahana, A. (2001). The deubiquitinating enzyme Dot4p is involved in regulating nutrient uptake. Biochem Biophys Res Commun *282*, 916-920.

Kahana, A., and Gottschling, D.E. (1999). DOT4 links silencing and cell growth in Saccharomyces cerevisiae. Mol Cell Biol *19*, 6608-6620.

Kay, B.K., Williamson, M.P., and Sudol, M. (2000). The importance of being proline: the interaction of proline-rich motifs in signaling proteins with their cognate domains. The FASEB Journal *14*, 231-241.

Keener, J., Josaitis, C.A., Dodd, J.A., and Nomura, M. (1998). Reconstitution of yeast RNA polymerase I transcription in vitro from purified components. TATA-binding protein is not required for basal transcription. J Biol Chem *273*, 33795-33802.

Keogh, M.-C., Kurdistani, S.K., Morris, S.A., Ahn, S.H., Podolny, V., Collins, S.R., Schuldiner, M., Chin, K., Punna, T., Thompson, N.J.*, et al.* Cotranscriptional Set2 Methylation of Histone H3 Lysine 36 Recruits a Repressive Rpd3 Complex. Cell *123*, 593-605.

Keys, D.A., Lee, B.S., Dodd, J.A., Nguyen, T.T., Vu, L., Fantino, E., Burson, L.M., Nogi, Y., and Nomura, M. (1996). Multiprotein transcription factor UAF interacts with the upstream element of the yeast RNA polymerase I promoter and forms a stable preinitiation complex. Genes Dev *10*, 887-903.

Kirisako, T., Kamei, K., Murata, S., Kato, M., Fukumoto, H., Kanie, M., Sano, S., Tokunaga, F., Tanaka, K., and Iwai, K. (2006). A ubiquitin ligase complex assembles linear polyubiquitin chains. EMBO J *25*, 4877-4887.

Kraft, C., Deplazes, A., Sohrmann, M., and Peter, M. (2008). Mature ribosomes are selectively degraded upon starvation by an autophagy pathway requiring the Ubp3p/Bre5p ubiquitin protease. Nat Cell Biol *10*, 602-610.

Kressler, D., Hurt, E., and BaŒ≤ler, J. (2010). Driving ribosome assembly. Biochimica et Biophysica Acta (BBA) - Molecular Cell Research *1803*, 673-683.

Kuhn, C.D., Geiger, S.R., Baumli, S., Gartmann, M., Gerber, J., Jennebach, S., Mielke, T., Tschochner, H., Beckmann, R., and Cramer, P. (2007). Functional architecture of RNA polymerase I. Cell *131*, 1260-1272.

Kulkens, T., Riggs, D.L., Heck, J.D., Planta, R.J., and Nomura, M. (1991). The yeast RNA polymerase I promoter: ribosomal DNA sequences involved in transcription initiation and complex formation in vitro. Nucleic Acids Res *19*, 5363-5370.

Lacombe, T., Garcia-Gomez, J.J., de la Cruz, J., Roser, D., Hurt, E., Linder, P., and Kressler, D. (2009). Linear ubiquitin fusion to Rps31 and its subsequent cleavage are required for the efficient production and functional integrity of 40S ribosomal subunits. Mol Microbiol *72*, 69-84.

Lempiainen, H., and Shore, D. (2009). Growth control and ribosome biogenesis. Curr Opin Cell Biol *21*, 855-863.

Lin, J., Lu, J., Feng, Y., Sun, M., and Ye, K. An RNA-Binding Complex Involved in Ribosome Biogenesis Contains a Protein with Homology to tRNA CCA-Adding Enzyme. PLoS Biology *11*, e1001669.

Lis, E.T., and Romesberg, F.E. (2006). Role of Doa1 in the Saccharomyces cerevisiae DNA damage response. Mol Cell Biol *26*, 4122-4133.

Marsh, J.A., and Teichmann, S.A. (2014). Parallel dynamics and evolution: Protein conformational fluctuations and assembly reflect evolutionary changes in sequence and structure. BioEssays *36*, 209-218.

Mayer, C., Zhao, J., Yuan, X., and Grummt, I. (2004). mTOR-dependent activation of the transcription factor TIF-IA links rRNA synthesis to nutrient availability. Genes & Development *18*, 423-434.

Memet, S., Gouy, M., Marck, C., Sentenac, A., and Buhler, J.M. (1988). RPA190, the gene coding for the largest subunit of yeast RNA polymerase A. J Biol Chem *263*, 2830-2839.

Mészáros, B., Dosztányi, Z., and Simon, I. (2012). Disordered Binding Regions and Linear Motifs‚ÄîBridging the Gap between Two Models of Molecular Recognition. PLoS ONE *7*, e46829.

Michaelis, J., and Treutlein, B. (2013). Single-Molecule Studies of RNA Polymerases. Chemical Reviews *113*, 8377-8399.

Mogk, A., and Bukau, B. (2004). Molecular chaperones: structure of a protein disaggregase. Curr Biol *14*, R78-80.

Moore, M.J., and Proudfoot, N.J. (2009). Pre-mRNA Processing Reaches Back toTranscription and Ahead to Translation. Cell *136*, 688-700.

Mosca, R., Pache, R.A., and Aloy, P. (2012). The Role of Structural Disorder in the Rewiring of Protein Interactions through Evolution. Molecular & Cellular Proteomics *11*.

Namba, K. (2001). Roles of partly unfolded conformations in macromolecular self-assembly. Genes to Cells *6*, 1-12.

Neuman-Silberberg, F.S., Bhattacharya, S., and Broach, J.R. (1995). Nutrient availability and the RAS/cyclic AMP pathway both induce expression of ribosomal protein genes in Saccharomyces cerevisiae but by different mechanisms. Molecular and Cellular Biology *15*, 3187-3196.

Oliver, S. (1992). The molecular and cellular biology of the yeast saccharomyces: Genome dynamics, protein synthesis and energetics. . Yeast *8*.

Osley, M.A. (2004). H2B ubiquitylation: the end is in sight. Biochim Biophys Acta *1677*, 74-78.

Ozkaynak, E., Finley, D., Solomon, M.J., and Varshavsky, A. (1987). The yeast ubiquitin genes: a family of natural gene fusions. EMBO J *6*, 1429-1439.

Peltonen, K., Colis, L., Liu, H., Trivedi, R., Moubarek, M.S., Moore, H.M., Bai, B., Rudek, M.A., Bieberich, C.J., and Laiho, M. (2014). A Targeting Modality for Destruction of RNA Polymerase I that Possesses Anticancer Activity. Cancer Cell *25*, 77-90.

Perez-Fernandez, J., Roman, A., De Las Rivas, J., Bustelo, X.R., and Dosil, M. (2007). The 90S preribosome is a multimodular structure that is assembled through a hierarchical mechanism. Mol Cell Biol *27*, 5414-5429.

Philippi, A., Steinbauer, R., Reiter, A., Fath, S., Leger-Silvestre, I., Milkereit, P., Griesenbeck, J., and Tschochner, H. (2010a). TOR-dependent reduction in the expression level of Rrn3p lowers the activity of the yeast RNA Pol I machinery, but does not account for the strong inhibition of rRNA production. Nucleic Acids Res *38*, 5315-5326.

Philippi, A., Steinbauer, R., Reiter, A., Fath, S., Leger-Silvestre, I., Milkereit, P., Griesenbeck, J., and Tschochner, H. (2010b). TOR-dependent reduction in the expression level of Rrn3p lowers the activity of the yeast RNA Pol I machinery, but does not account for the strong inhibition of rRNA production. Nucleic Acids Research *38*, 5315-5326.

Prescott, E.M., Osheim, Y.N., Jones, H.S., Alen, C.M., Roan, J.G., Reeder, R.H., Beyer, A.L., and Proudfoot, N.J. (2004). Transcriptional termination by RNA polymerase I requires the small subunit Rpa12p. Proc Natl Acad Sci U S A *101*, 6068-6073.

Prilusky, J., Felder, C.E., Zeev-Ben-Mordehai, T., Rydberg, E.H., Man, O., Beckmann, J.S., Silman, I., and Sussman, J.L. (2005). FoldIndex: a simple tool to predict whether a given protein sequence is intrinsically unfolded. Bioinformatics *21*, 3435-3438.

Ra≈°ka, I., Shaw, P.J., and Cmarko, D.a. (2006). Structure and function of the nucleolus in the spotlight. Current Opinion in Cell Biology *18*, 325-334.

Ramakrishnan, V. (2014). The Ribosome Emerges from a Black Box. Cell *159*, 979-984.

Raska, I., Shaw, P.J., and Cmarko, D. (2006). Structure and function of the nucleolus in the spotlight. Current Opinion in Cell Biology *18*, 325-334.

Reid, J., and Svejstrup, J.Q. (2004). DNA damage-induced Def1-RNA polymerase II interaction and Def1 requirement for polymerase ubiquitylation in vitro. J Biol Chem *279*, 29875-29878.

Reyes-Turcu, F.E., Ventii, K.H., and Wilkinson, K.D. (2009). Regulation and cellular roles of ubiquitin-specific deubiquitinating enzymes. Annu Rev Biochem *78*, 363-397.

Ribar, B., Prakash, L., and Prakash, S. (2006). Requirement of ELC1 for RNA polymerase II polyubiquitylation and degradation in response to DNA damage in Saccharomyces cerevisiae. Mol Cell Biol *26*, 3999-4005.

Ribar, B., Prakash, L., and Prakash, S. (2007). ELA1 and CUL3 are required along with ELC1 for RNA polymerase II polyubiquitylation and degradation in DNA-damaged yeast cells. Mol Cell Biol *27*, 3211-3216.

Richardson, L.A., Reed, B.J., Charette, J.M., Freed, E.F., Fredrickson, E.K., Locke, M.N., Baserga, S.J., and Gardner, R.G. (2012). A conserved deubiquitinating enzyme controls cell growth by regulating RNA polymerase I stability. Cell Rep *2*, 372-385.

Romero, P., Obradovic, Z., Li, X., Garner, E.C., Brown, C.J., and Dunker, A.K. (2001). Sequence complexity of disordered protein. Proteins *42*, 38-48.

Rosenbaum, J.C., Fredrickson, E.K., Oeser, M.L., Garrett-Engele, C.M., Locke, M.N., Richardson, L.A., Nelson, Z.W., Hetrick, E.D., Milac, T.I., Gottschling, D.E., and Gardner, R.G. (2011). Disorder targets misorder in nuclear quality control degradation: a disordered ubiquitin ligase directly recognizes its misfolded substrates. Mol Cell *41*, 93-106.

Rost, B. (2002). Enzyme Function Less Conserved than Anticipated. Journal of Molecular Biology *318*, 595-608.

Ruggero, D., and Pandolfi, P.P. (2003). Does the ribosome translate cancer? Nat Rev Cancer *3*, 179-192.

Rumpf, S., and Jentsch, S. (2006). Functional division of substrate processing cofactors of the ubiquitin-selective Cdc48 chaperone. Mol Cell *21*, 261-269.

Russell, J., and Zomerdijk, J.C. (2006). The RNA polymerase I transcription machinery. Biochem Soc Symp, 203-216.

Schlessinger, A., Schaefer, C., Vicedo, E., Schmidberger, M., Punta, M., and Rost, B. (2011). Protein disorder -- a breakthrough invention of evolution? Current Opinion in Structural Biology *21*, 412-418.

Schneider, D.A. (2012). RNA polymerase I activity is regulated at multiple steps in the transcription cycle: recent insights into factors that influence transcription elongation. Gene *493*, 176-184.

Schultz, M.C., Reeder, R.H., and Hahn, S. (1992). Variants of the TATA-binding protein can distinguish subsets of RNA polymerase I, II, and III promoters. Cell *69*, 697-702.

Schulze, J.M., Hentrich, T., Nakanishi, S., Gupta, A., Emberly, E., Shilatifard, A., and Kobor, M.S. (2011). Splitting the task: Ubp8 and Ubp10 deubiquitinate different cellular pools of H2BK123. Genes Dev *25*, 2242-2247.

Shou, W., Sakamoto, K.M., Keener, J., Morimoto, K.W., Traverso, E.E., Azzam, R., Hoppe, G.J., Feldman, R.M.R., DeModena, J., Moazed, D.*, et al.* (2001). Net1 Stimulates RNA Polymerase I Transcription and Regulates Nucleolar Structure Independently of Controlling Mitotic Exit. Molecular Cell *8*, 45-55.

Singer, M.S., Kahana, A., Wolf, A.J., Meisinger, L.L., Peterson, S.E., Goggin, C., Mahowald, M., and Gottschling, D.E. (1998). Identification of High-Copy Disruptors of Telomeric Silencing in Saccharomyces cerevisiae. Genetics *150*, 613-632.

Somesh, B.P., Reid, J., Liu, W.F., Sogaard, T.M., Erdjument-Bromage, H., Tempst, P., and Svejstrup, J.Q. (2005). Multiple mechanisms confining RNA polymerase II ubiquitylation to polymerases undergoing transcriptional arrest. Cell *121*, 913-923.

Sowa, M.E., Bennett, E.J., Gygi, S.P., and Harper, J.W. (2009). Defining the human deubiquitinating enzyme interaction landscape. Cell *138*, 389-403.

Strahl, B.D., Ohba, R., Cook, R.G., and Allis, C.D. (1999). Methylation of histone H3 at lysine 4 is highly conserved and correlates with transcriptionally active nuclei in Tetrahymena. Proc Natl Acad Sci U S A *96*, 14967-14972.

Straight, A.F., Shou, W., Dowd, G.J., Turck, C.W., Deshaies, R.J., Johnson, A.D., and Moazed, D. (1999). Net1, a Sir2-Associated Nucleolar Protein Required for rDNA Silencing and Nucleolar Integrity. Cell *97*, 245-256.

Thrower, J.S., Hoffman, L., Rechsteiner, M., and Pickart, C.M. (2000). Recognition of the polyubiquitin proteolytic signal. EMBO J *19*, 94-102.

Tompa, P., Sz√°sz, C., and Buday, L.s. (2005). Structural disorder throws new light on moonlighting. Trends in Biochemical Sciences *30*, 484-489.

Tsang, C.K., Bertram, P.G., Ai, W., Drenan, R., and Zheng, X.F.S. (2003). Chromatin-mediated regulation of nucleolar structure and RNA Pol I localization by TOR, Vol 22.

Turner, A.J., Knox, A.A., and Watkins, N.J. (2012). Nucleolar disruption leads to the spatial separation of key 18S rRNA processing factors. RNA Biol *9*, 175-186.

Udeshi, N.D., Svinkina, T., Mertins, P., Kuhn, E., Mani, D.R., Qiao, J.W., and Carr, S.A. (2013). Refined Preparation and Use of Anti-diglycine Remnant (K-Œμ-GG) Antibody Enables Routine Quantification of 10,000s of Ubiquitination Sites in Single Proteomics Experiments. Molecular & Cellular Proteomics *12*, 825-831.

Uversky, V.N. (2013). A decade and a half of protein intrinsic disorder: Biology still waits for physics. Protein Science *22*, 693-724.

Uversky, V.N. (2015). Functional roles of transiently and intrinsically disordered regions within proteins. FEBS J.

van der Gulik, P., and Speijer, D. (2015). How Amino Acids and Peptides Shaped the RNA World. Life *5*, 230-246.

Vannini, A., and Cramer, P. (2012). Conservation between the RNA Polymerase I, II, and III Transcription Initiation Machineries. Molecular Cell *45*, 439-446.

Varshavsky, A. (2006). The early history of the ubiquitin field. Protein Sci *15*, 647-654.

Verma, R., Oania, R., Fang, R., Smith, G.T., and Deshaies, R.J. (2011). Cdc48/p97 mediates UV-dependent turnover of RNA Pol II. Mol Cell *41*, 82-92.

Vu, L., Siddiqi, I., Lee, B.S., Josaitis, C.A., and Nomura, M. (1999). RNA polymerase switch in transcription of yeast rDNA: role of transcription factor UAF (upstream activation factor) in silencing rDNA transcription by RNA polymerase II. Proc Natl Acad Sci U S A *96*, 4390-4395.

Warner, J.R. (1999). The economics of ribosome biosynthesis in yeast. Trends Biochem Sci *24*, 437-440.

Wickner, S., Maurizi, M.R., and Gottesman, S. (1999). Posttranslational quality control: folding, refolding, and degrading proteins. Science *286*, 1888-1893.

Wilson, M.D., Harreman, M., and Svejstrup, J.Q. (2013). Ubiquitylation and degradation of elongating RNA polymerase II: The last resort. Biochim Biophys Acta *1829*, 151-157.

Woolford, J.L., and Baserga, S.J. (2013). Ribosome Biogenesis in the Yeast Saccharomyces cerevisiae. Genetics *195*, 643-681.

Wright, P.E., and Dyson, H.J. (1999). Intrinsically unstructured proteins: re-assessing the protein structure-function paradigm. Journal of Molecular Biology *293*, 321-331.

Wu, J., Zhang, N., Hayes, A., Panoutsopoulou, K., and Oliver, S.G. (2004). Global analysis of nutrient control of gene expression in Saccharomyces cerevisiae during growth and starvation. Proc Natl Acad Sci U S A *101*, 3148-3153.

Yamamoto, R.T., Nogi, Y., Dodd, J.A., and Nomura, M. (1996). RRN3 gene of Saccharomyces cerevisiae encodes an essential RNA polymerase I transcription factor which interacts with the polymerase independently of DNA template. Embo J *15*, 3964-3973.

Young, K.H. (1998). Yeast two-hybrid: so many interactions, (in) so little time. Biology of Reproduction *58*, 302-311.

Zhang, L., Lin, J., and Ye, K. Structural and functional analysis of the U3 snoRNA binding protein Rrp9. RNA *19*, 701-711.

Zhang, Y., Wolf, G.W., Bhat, K., Jin, A., Allio, T., Burkhart, W.A., and Xiong, Y. (2003). Ribosomal protein L11 negatively regulates oncoprotein MDM2 and mediates a p53-dependent ribosomal-stress checkpoint pathway. Mol Cell Biol *23*, 8902-8912.

APPENDIX I - METHODS

Yeast strains and plasmids–Yeast strains and plasmids used in this study are listed in Appendix II. Standard yeast growth media and yeast genetic methods were employed (Guthrie and Fink, 1991). Standard cloning methods were used to construct each plasmid. The relevant portion of each plasmid was sequenced to verify the fusions. Plasmid sequences, oligonucleotide sequences, and cloning details will be provided upon request.

Expression and purification of Ubp10–We used the vector GST-TEV-UBP10 (gift from Erik Zimmerman and Ning Zheng) for expression of Ubp10. Vectors were transformed into T7 express cells (NEB). Transformed cells were grown in Luria broth (LB) plus ampicillin (100µg/ml final concentration) to an optical density at 600nm (OD_{600}) of ~0.8. Protein expression was induced by addition of 250µM IPTG and 100µM $ZnCl_2$ (final concentrations) for 16 hours at 16˚C. Cells were harvested and lysed with a microfluidizer in a buffer containing 200mM NaCl, 20mM Tris-HCl pH 8.0, 1 mM PMSF, 5 mM DTT. Soluble extract was applied to a GST resin (GE healthcare). Ubp10 or USP36 were cleaved from the resin with recombinant TEV protease, then concentrated using an Amicon Ultracel concentrator (cutoff ≥50 kDa).

Deubiquitination assay–To assay *in vitro* deubiquitinating activity of recombinantly purified Ubp10, we used a ubiquitin conjugated 7-amido-4-methylcoumarin florescence (Ub-AMC) assay (Dang et al., 1998). Ub-AMC Assay Buffer (50mM HEPES pH 7.5, 0.5mM EDTA, 1mM DTT) was aliquoted (100µl/well) to ½ white AreaPlate (Perkin Elmer) 96 well plate. Recombinant Ubp10 was added either directly to wells in triplicate, or pre-incubated with N-ethylmaleimide (NEM, Sigma) for 5 minutes at room temperature and then added in triplicate. Ubiquitin-AMC (Lifesensors) was added to each mixture and immediately measured with at excitation 346nm, emission 442nm at 30˚C for 40 minutes.

Histone H2B deubiquitination assay–To assay deubiquitination of histone H2B *in vitro*, we prepared whole cell yeast lysates from a 50ml culture of cells that expressed FLAG-tagged H2B grown in rich media at 30˚C to a density of 1.5 x 10^7 cells/ml. Cells were harvested by centrifugation and lysed in 1mL lysis buffer (200mM NaCl, 20mM Tris pH 8.0, 1 mM PMSF, 10 mM NEM) by vortexing with glass beads. The isolated cell lysate was combined with 800 µL lysis buffer wash of the beads. The combined lysate and wash were clarified by centrifugation for 5 minutes at 13,000 x g. histone H2B was immunopurified by combining the clarified lysate

with 30µl anti-Flag M2 affinity resin (Sigma). After mixing 16 hours at 4˚C, the resin was washed 3x with 1 mL lysis buffer, and resuspended in 30µl deubiquitation assay buffer (100mM Tris-HCl pH 8.0, 1mM EDTA, 5% glycerol). 10µl of resin slurry was incubated with purified recombinant Ubp10 for 50 minutes at 37˚C. Proteins were eluted in SUMEB (1% SDS, 8 M Urea, 10 mM MOPS, pH 6.8, 10 mM EDTA, 0.01% bromophenol blue) by incubating for 10 minutes at 65˚C and separated by SDS-PAGE. Western analysis using anti-FLAG antibodies revealed the extent of histone H2B deubiquitination.

Limited proteolysis–Proteolysis of Ubp10 or BSA was carried out by trypsin digestion at 25˚C in digestion buffer (50 mM NaCl and 15 mM Na_2HPO_4, pH 7.3). The enzyme to substrate ratio was 1:50. Proteolysis was stopped by adding SUMEB and boiling for 10 min. Digestion was examined by SDS-PAGE followed by silver staining.

Circular dichroism–Far-UV Circular Dichroisim (CD) spectra of recombinantly purified Ubp10 or commercial BSA were obtained on an Aviv 62DS CD spectrometer. Spectra were recorded at 25˚C with a 1mm optical cuvette from 260 to 190 nm. An average of three runs was obtained by sampling every 2 nm with a 30 second averaging time. Each protein was resuspended in CD buffer (50mM NaCl, 15mM Na_2HPO_4, pH7.3). Protein concentrations were between 5 and 10 mM. We subtracted the background CD buffer spectrum from each protein spectrum.

Yeast 2-Hybrid (Y2H) assay–Y2H assays were performed as previously described (Rosenbaum et al., 2011). Cells expressing fusions of the Gal4 binding domain (GBD) with Ubp10 or USP36 containing the indicated mutations and the appropriate fusions to the Gal4 activation domain (GAD) were spotted onto selective (media minus histidine) and nonselective media (media plus histidine) to assess interactions and spotting efficiency, respectively. All interaction tests were performed in duplicate using two independent isolates. Growth plates were scanned on an Epson Perfection V350 Photo scanner. Images were cropped and processed using the Mac version of Photoshop CS (Adobe Inc.).

In vivo Western analyses–Western analyses of lysates generated from *in vivo* cultures were performed as previously described (Richardson et al., 2012). Cultures were grown to a cell density of ~$0.7x10^7$ cells/ml. Cells were lysed by 20 minutes of bead beating at 4˚C in SUMEB with 10mM PMSF. Proteins were separated on 6% SDS-PAGE gels for Rpa190 or 10% SDS-PAGE gels for histone H2B, transferred to nitrocellulose, and visualized by Western analyses

using anti-Rpa190 antibodies (generous gift from David Schneider) or anti-FLAG antibodies (Sigma).

Ubiquitin affinity pulldown–Purification of ubiquitinated proteins from yeast was performed as previously described (Richardson et al., 2012). Cells expressing 8His-ubiquitin were grown in 50mL rich media to a density of $0.7x10^7$ cells/ml. Harvested cells were lysed by 20 minutes of bead beating at 4˚C in 1mL lysis buffer (8M Urea, 0.05% SDS, 50mM Tris pH 8.0 with 1 mM PMSF and 10 mM NEM). Lysates were clarified by centrifugation, and incubated with 40µl slurry TALON resin (Novagen) overnight at 4˚C. The resin was washed 3x with 1mL lysis buffer (8M Urea, 0.05% SDS, 50mM Tris pH 8.0, 1mM PMSF, 10mM NEM). Ubiquitinated proteins were eluted from the column by addition of 40µl SUMEB. Proteins in the lysate and eluate were separated on 6% SDS-PAGE gels and examined by Western analyses.

Microscopy–Cells were grown in 5 ml cultures to a density of $0.7x10^7$ cells/ml. Harvested cells were fixed with 4% paraformaldehyde in 0.1 M sorbitol for 15 min, washed once with wash buffer (1.2 M sorbitol, 0.4 M KPO4), stained with DAPI for 5 min in wash buffer plus 2% Triton X-100 and washed two times in wash buffer. Cells were imaged on a Nikon Eclipse 90i with a 1003 objective (DIC N2 N.A. 1.4), filters for green (ET470/403, T495LP, ET525/50 m) or red (ET560/403, T585LP, ET630/75 m) fluorescence, and a Photometrics Cool Snap HQ2 cooled CCD camera with NIS-Elements acquisition software. All images were processed using Photoshop CS (Adobe Systems Inc.).

Formaldehyde Crosslinking Coimmunoprecipitation–Crosslinking experiments were conducted similar to those previously described (Rosenbaum et al., 2011). Cells were grown in 500 ml cultures to a density of $1.8 3 107 cells/ml. Formaldehyde was added to a final concen- tration of 1% (v/v), and cultures incubated for 5 min at 30□ C. Crosslinking was quenched with glycine added to a final concentration of 125 mM. Harvested cells were lysed in SUME buffer (8 M Urea, 1% SDS, 10 mM MOPS [pH 6.8], 10 mM EDTA) and lysates were diluted 1:5 in IP buffer (15 mM Na2HPO4, 150 mM NaCl, 2% Triton X-100, 0.1% SDS, 0.5% deoxycholate, 10 mM EDTA). Lysates were incubated with 1:1,000 mouse anti-HA antibody (Nova- gen) preconjugated to 1.25 mg/ml Protein A Dynabeads (Invitrogen) for 16 hr at 4□C. Beads were washed three times with IP buffer and proteins were eluted by incubation at 65□C for 10 min in 50 ml SUMEB (SUME + 0.01% bromophenol blue).

Mass Spectrometry and Data Analysis–Samples analyzed by MS/MS were run 1 cm into an 8%–16% SDS-PAGE gel and gel slices excised. Proteins in the gel slices were digested with trypsin (see Extended Experimental Procedures). The digestion products were desalted and dried by vacuum centrifugation. Dried peptide mixtures were resuspended in 7 ml of 0.1% formic acid and 5 ml was analyzed by LC/ESI MS/MS using either an LTQ-FT or LTQ-OrbiTrap mass spectrometer (ThermoElectron). Complete MS/MS methods are in the Extended Experi- mental Procedures. The protein database search algorithm X!Tandem (Craig and Beavis, 2004) was used to identify peptides from the Saccharomyces Genome Database (http://www.yeastgenome.org). Peptide false discovery rates were measured using Peptide Prophet (Keller et al., 2002), and results were stored and analyzed in the Computational Proteomics Analysis System (Rauch et al., 2006). To apply different levels of stringency, peptides were filtered using Peptide Prophet scores of R0.35 (10% error rate), R0.65 (5% error rate), and R0.85 (2% error rate). The data obtained after each of these filters are in Tables S1 and S2. For Tables S1 and S2, we used the data that was filtered using a Peptide Prophet score R0.35. Distributions for the case and control replicates were compared using an unpaired Student's t test (with the replicate groups having equal sample size and unequal vari- ance). Two tailed p values are reported.

Nondenaturing Coimmunoprecipitation–Cells were grown in 10 ml cultures to a density of $0.7x10^7$ cells/ml. Harvested cells were lysed in IP buffer. Lysates were diluted 1:5 in IP buffer and incubated for 16 hr at 4°C with 1:1,000 mouse anti-HSV antibody (Novagen) bound to 1.25 mg/ml Protein A Dynabeads (Invitrogen). Beads were washed three times in IP buffer. Proteins were eluted by incubation at 65°C for 10 min in SUMEB (SUME + 0.01% bromophenol blue). Proteins were sepa- rated on 8% SDS-PAGE gels, transferred to nitrocellulose, and visualized with anti-HSV (Novagen) or anti-HA (Sigma) antibodies.

Purification of Ubiquitinated Rpa190 from Yeast–Cells expressing 8His-ubiquitin and Rpa190-3HA were grown in 1 L cultures to a density of $0.7x10^7$ cells/ml. Harvested cells were lysed at 4□C in lysis buffer (20 mM Tris [pH 8.0], 200 mM NaCl with 1 mM PMSF and 10 mM NEM). The supernatant was removed and sonicated 4x3 20 s (duty cycle 60 and output 2). Lysates were clarified by centrifugation, and incubated with TALON resin (Novagen) for 4 hr at 4°C. The resin was washed 33 with wash buffer (20 mM Tris [pH 8.0], 200 mM NaCl, 1 mM PMSF, 10 mM NEM, 7.5 mM imidazole). Ubiquitinated proteins were eluted from the column by addition of 10 mM EDTA to the wash buffer. Anti-HA antibodies conjugated to Protein G Dynabeads

(Dynal) were added to the ubiquitinated protein eluate and incubated overnight at 4□C. The beads were washed once in lysis buffer, and twice in IP wash buffer (100 mM Tris, 1 mM EDTA, 5% Glycerol, 1 mM DTT, 1 mM PMSF). The beads containing ubiquitinated Rpa190 were resus- pended in IP wash buffer 2 and stored on ice.

In Vitro Rpa190 DUB Assay–Purified Ubp10 or vehicle was added to purified ubiquitinated Rpa190 and incubated for two hours at 37°C in reaction buffer (100 mM Tris, 1 mM EDTA, 5% Glycerol, 1 mM DTT, 1 mM PMSF). SUMEB was added to the samples, which were subsequently incubated at 65°C for 10 min. Proteins were separated on a 4%–12% Tris-Glycine gradient gel, transferred to nitro- cellulose, and Rpa190-3HA visualized with anti-HA (Sigma) antibodies.

Northern Blot Analyses–Northern blot analyses were performed similarly to previously described (Pestov et al., 2008). Cultures were grown at 17°C in glucose medium for 72 hr for genetic depletion of the tagged protein. Cultures were grown, kept in log phase by frequent dilution with fresh media, to a final density of 0.53 – 0.87 3 107 cells/ml and harvested by centrifugation. Total RNA was extracted by the acid phenol method (Collart and Oliviero, 1994). RNA was resuspended in formamide loading dye and 3 mg was loaded per lane. Pre-RNAs were separated on an agarose-formaldehyde gel and transferred to a Hybond XL membrane. Methylene blue staining was used to detect the mature 18S and 25S rRNAs. Oligonucleotide probes used to detect pre-rRNAs are: b 50GCT CTT TGC TCT TGC C, c 50CCT CTG GGC CCC GAT TGC TCG AA, and e 50GGC CAG CAA TTT CAA GT.

Cycloheximide-Chase Degradation Assays–Cycloheximide-chase degradation assays were performed similar to previ- ously described (Gardner et al., 2005a). Cultures were grown to a cell density of 1 3 107 cells/ml. Cycloheximide was added to a final concentration of 50 mg/ml and the cells were further incubated at 25° C, 30° C, 33° C, or 38° C for 0–3 hr. In some cases, rapamycin was added (200 nM final concentration) or glucose or tryptophan was removed from the media 2 hr prior to cyclohex- imide addition. Cells were lysed at the appropriate time point in 200 ml SUMEB with 10 mM PMSF. Proteins were separated on 8% SDS-PAGE gels, trans- ferred to nitrocellulose, and Rpa190-3HA visualized with anti-HA (Sigma) antibodies.

Image processing–Western blots were scanned using an Epson Perfection V350 Photo scanner at 300 dpi. All images were processed with a Mac iMac or Pro computer (Apple) using Photoshop CS (Adobe).

APPENDIX II – STRAINS AND PLASMIDS

YEAST STRAINS

Strain Name	*Genotype*	Reference
BY4741	met15Δo, his3Δ1, ura3Δ0, leu2Δ2	Brachmann et al., 1998
PJ-4a	*MAT* ***a****, trp1-Δ1, leu2-3,112, ura3-52, his3-200, gal4Δ, gal80Δ, GAL2-ADE2, LYS2::GAL1-HIS3, met2::GAL7-lacZ*	James et al., 1996
RGY311	RGY379 *ubp10Δ::KanMX::ubp10(C371S)-MT6::URA3*	Gardner et al, 2005
RGY312	RGY379 *ubp10Δ::KanMX::ubp10Δ(94-250)-MT6::URA3*	Gardner et al, 2005
RGY313	RGY379 *ubp10Δ::KanMX::UBP10-MT6::URA3*	Gardner et al, 2005
RGY375	*HMLa, Mata, HMRa, cdc7-1, bar1, trp1-289, ura3-52, leu2-3,112, his6 HTAI-FLAG-HTB1*	Gardner et al, 2005
RGY376	RGY375 *sir2Δ::LEU2*	Gardner et al, 2005
RGY377	RGY375 *sir3Δ::LEU2*	Gardner et al, 2005
RGY378	RGY375 *sir4Δ::LEU2*	Gardner et al, 2005
RGY379	RGY375 *ubp10Δ::KanMX*	Gardner et al, 2005
RGY1221	BY4741 *trp1Δ::LEU2*	
RGY4595	RGY1221 *ubp10Δ::NatMX*	Richardson, et al 2012
RGY4625	RGY1221 *NOP56-3HA::KanMX*	Richardson, et al 2012
RGY4626	RGY1221 *NOP58-3HA::KanMX*	Richardson, et al 2012
RGY4627	RGY1221 *PWP2-3HA::KanMX*	Richardson, et al 2012
RGY4653	*RPA190-3HA::KanMX, all ubiquitin genes 8XHistidine tagged*	Richardson, et al 2012
RGY4668	RGY4595 *ubp10Δ::NatMX, UBP10-3HSV::TRP1*	Richardson, et al 2012
RGY4671	RGY1221 *CBF5-3HA::KanMX*	Richardson, et al 2012
RGY4696	RGY4625 *NOP56-3HA::KanMX, ubp10Δ::NatMX*	Richardson, et al 2012
RGY4697	RGY4626 *NOP58-3HA::KanMX, ubp10Δ::NatMX*	Richardson, et al 2012
RGY4698	RGY4627 *PWP2-3HA::KanMX, ubp10Δ::NatMX*	Richardson, et al 2012
RGY4709	RGY4671 *CBF5-3HA::KanMX, ubp10Δ::NatMX*	Richardson, et al 2012
RGY4728	RGY4653 *ubp10Δ::NatMX*	Richardson, et al 2012
RGY4742	RGY1221 *RPA190-3HA::KanMX*	Richardson, et al 2012
RGY4750	RGY4742 *ubp10Δ::NatMX*	Richardson, et al 2012
RGY4803	RGY4750 *UBP10-3HSV::TRP1*	Richardson, et al 2012
RGY5045	RGY4750 P^{UBP10}*-USP36::URA3 (2μ plasmid)*	Richardson, et al 2012
RGY5114	PJ-4a *GAD::LEU2 (2μ plasmid) GBD-UBP10*^{C371S}*::TRP1 (YEp)*	Richardson, et al 2012
RGY5115	PJ-4a *GAD-DHR2::LEU2 (2μ plasmid) GBD-UBP10*^{C371S}*::TRP1 (YEp)*	Richardson, et al 2012
RGY5116	PJ-4a *GAD-UTP22::LEU2 (2μ plasmid) GBD-UBP10*^{C371S}*::TRP1 (YEp)*	Richardson, et al 2012
RGY5117	PJ-4a *GAD-SIR4(612-1358)::LEU2 (2μ plasmid) GBD-UBP10*^{C371S}*::TRP1 (YEp)*	Richardson, et al 2012
RGY5118	RGY4742 *RPA190-3HA::TRP1 (2μ plasmid)*	Richardson, et al 2012
RGY5119	RGY4750 *RPA190-3HA::TRP1 (2μ plasmid)*	Richardson, et al 2012

RGY5285	*RPA190-3HA::KanMX, all ubiquitin genes 8 X Histidine tagged, ubp10Δ, P^{UBP10}-USP36::URA3 (2μ plasmid)*	Richardson, et al 2012
PJ69-4A	MATa *his3Δ200 ura3-52 trp1-901 leo2-3,122 met2*::P_{GAL7}-*lacZ lys2*::P_{GAL1}-*HIS3 ade2*::P_{GAL2}-*ADE2 gal4Δ gal80Δ*	
RGY799	MATa *ade2Δ:hisG met15Δ0 his3Δ200 ura3Δ0 trp1Δ63 lys2Δ0 leu2Δ0 TEL-VIIL::*P_{ADH4}-*URA3*	
RGY800	RGY799 *ubp10Δ::NatMX*	
RGY801	RGY799 *sir4Δ*::*KanMX*	
RGY5453	RGY800 *ubp10Δ*::*NatMX::ubp10-3HSV*	
RGY5487	RGY800 *ubp10Δ::NatMX*::*ubp10(Δ2-27)-3HSV*	
RGY5454	RGY800 *ubp10Δ*::*NatMX::ubp10(Δ109-122)-3HSV*	
RGY5455	RGY800 *ubp10Δ*:: *NatMX::ubp10(Δ123-141)-3HSV*	
UCC6389	*MATa ade2Δ::hisG met15Δ0 his3Δ200 ura3Δ0 trp1Δ63 lys2Δ0 leu2Δ0 HTA1-FLAG-HTB1*	
UCC6390	UCC6389 *ubp10Δ::NatMX*	
UCC6393	UCC6389 *ubp10Δ::NatMX ubp8Δ::KanMX*	
RGY4468	UCC6393 *ubp8Δ::KanMX ubp10Δ::NatMX::USP36*	
RGY4546	*MATa met15Δ0 his3Δ0 ura3Δ0 leu2Δ0 rpal40aΔ::8HIS-Rpl40a rps31::8H-rps31 ubi4Δ::8H-ubi-8H-ubi-8H-ubi-8H-ubi-8H-ubi*	
RGY4728	RGY4546 *ubp10Δ::NatMX*	
RGY7945	RGY4728 *ubp10Δ::NatMX::USP36*	

PLASMIDS

Plasmid	Relevent genes	Reference
pRG67	*trp1Δ::LEU2*	
pRG116	*LEU2 2μ pACT-GW-attR*	
pRG616	*URA3 INT $ubp10^{C371S}$-MT6*	Gardner et al, 2005
pRG617	*URA3 INT $ubp10^{\Delta 94\text{-}250}$-MT6*	Gardner et al, 2005
pRG637	*URA3 INT STR4/DOT4-6Myc*	Gardner et al, 2005
pRG898	*TRP1 YEp Gal4BD-$UBP10^{C371S}$*	Richardson et al, 2012
pRG1332	*LEU2 2μ Gal4AD-$Sir4^{(612\text{-}1358)}$*	Richardson et al, 2012
pRG1337	*NatMX INT NOP58-dsRed*	Richardson et al, 2012
pRG1738	*TRP1 INT UBP10-3HSV*	Richardson et al, 2012
pRG2490	*LEU2 2μ pACT-GW-t-DHR2*	Richardson et al, 2012
pRG3410	*URA3 INT SIR4-GFP*	Richardson et al, 2012
pRG3232	*TRP1 2μ RPA190-3HA*	Richardson et al, 2012
pRG3351	*LEU2 2μ pACT-GW-t-UTP10*	Richardson et al, 2012
pRG3352	*LEU2 2μ pACT-GW-t-UTP22*	Richardson et al, 2012
pRG3421	*URA3 2μ P^{UBP10}-USP36*	Richardson et al, 2012
pRG2747	P_{COOL}-*GST-TEV-UBP10*	
pRG118	P_{ADH1}-*GBD* (empty vector), *TRP1*	
pRG898	P_{ADH1}-*GBD-UBP10(C371S)*, *TRP1*	
pRG1332	P_{ADH1}-*GAD-SIR4(612-1358), LEU2*	
pRG2490	P_{ADH1}-*GAD-DHR2, LEU2*	

pRG3352	P_{ADH1}-*GAD-UTP22, LEU2*
pRG4201	P_{ADH1}-*GBD-USP36, TRP1*